Identification of novel candidate genes involved in individual antidepressant treatment response

Dissertation

an der Fakultät für Biologie

der Ludwig-Maximilians-Universität München

Vorgelegt von

Christiana Labermaier

München, September 2014

Dissertation eingereicht am: 18.09.2014

Mündliche Prüfung am: 06.02.2015

1. Gutachter: PD Dr. Mathias V. Schmidt

2. Gutachter: Prof. Dr. Benedikt Grothe

3. Gutachter: Prof. Dr. Gisela Grupe

4. Gutachter: Prof. Dr. Angelika Böttger

5. Gutachter: PD. Dr. Mario Wullimann

6. Gutachter: PD. Dr. Martin Heß

„Wenn du ein Schiff bauen willst, dann trommle nicht Männer zusammen, um Holz zu beschaffen und Arbeit einzuteilen, sondern lehre die Männer die Sehnsucht nach dem weiten endlosen Meer!“

Antoine de Saint-Exupéry (1900 -1944)

Table of Contents

List of Abbreviations

5-HT	serotonin
a.U.	arbitrary units
AAV	adeno-associated virus
ACTH	adrenocorticotropic hormone
Acvr1c	activinA receptor type 1c
ANOVA	analysis of variance
AVP	arginine vasopressin
BDNF	brain-derived neurotrophic factor
BrdU	5-bromo-2-deoxyuridine
BW	body weight
C1ql2	complement component 1, q subcomponent-like 2
CA1	cornu ammonis region 1
CA2	cornu ammonis region 2
CA3	cornu ammonis region 3
cDNA	complementary deoxyribonucleic acid
CI	confidence interval
CNS	central nervous system
CRH	corticotropin-releasing hormone
CRHR1	corticotropin-releasing hormone receptor type 1
cRNA	complementary RNA
CTCF	CCCTC-binding factor
Cxcl12	C-X-C motif chemokine 12
CYP2D6	cytochromeP450 2D6
DaLi	dark-light box test
Dex	dexamethasone

DG	dentate gyrus
DNA	desoxyribonucleic acid
ec	entorhinal cortex
ECT	electroconvulsive seizure therapy
EDTA	ethylenediaminetetraacetic acid
FST	forced swim test
GENDEP	Genome-Based Therapeutic Drugs for Depression
GFAP	glial fibrillary acidic protein
GWAS	genome-wide association study
HC	hippocampus
HDRS	Hamilton Rating Scale for Depression
HMG	high mobility group
HPA axis	hypothalamic-pituitary-adrenal axis
HPLC	high performance liquid chromatography
i.p.	intraperitoneal injection
Il-16	interleukin-16
IL-6	interleukin-6
ISH	*in situ* hybridization
KD	knockdown
MAO	monoamine oxidase
MAOI	monoamine oxidase inhibitor
Map2	microtubule-associated protein 2
MARS	Munich Antidepressant Response Signature
MDD	major depressive disorder
mf	mossy fibers
mRNA	messenger RNA
NDRI	norepinephrine and dopamine reuptake inhibitor

NE	norepinephrine
NERI	norepinephrine reuptake inhibitor
NIH	novelty induced hypophagia test
NMDA	N-Methyl-D-aspartate
NSPCs	neurogenic neural stem/progenitor cells
OE	overexpression
OF	open field test
PBMC	peripheral blood mononuclear cells
PCR	polymerase chain reaction
PEDF	pigment epithelium-derived factor
PVC	polyvinyl chloride
qRT-PCR	quantitative reverse transcription PCR
RIA	radioimmunoassay
RIN	RNA integrity number
RNA	ribonucleic acid
Sc	Schaffer collaterals
SGZ	subgranular zone
shRNA	short-hairpin RNA
SNP	single nucleotide polymorphism
SNRI	serotonin-norepinephrine reuptake inhibitor
Sox11	SRY-box containing gene 11
Sry	sex-determining region Y
SSRI	serotonin reuptake inhibitor
STAR*D	Sequenced Treatment Alternative to Relieve Depression
Stat3	signal transducer and activator of transcription 3
SVZ	subventricular zone
TCA	tricyclic antidepressant drug

TGFα	transforming growth factor alpha
TGFβ	transforming growth factor beta
TrkB	neurotrophic tyrosine kinase receptor
Tubb3	tubulin, beta 3 class III
UTP	uridine triphosphate
Vim	vimentine
WHO	World Health Organization

Abstract

The search for novel candidate genes determining antidepressant treatment response received a lot of attention within the last decade. In times of genome wide association studies, a lot of effort was done to detect key target gene that are involved in antidepressant treatment outcome. However, the search for such central target genes that modulate antidepressant treatment outcome was rather disappointing. In the current thesis, we established a novel unbiased experimental approach to investigate individual antidepressant response in mice and furthermore tried to link these findings to the clinical situation. In a translational approach, we were able to identify novel target genes that are modulated after chronic antidepressant treatment. In a second step, we also investigated early antidepressant response within this approach, which is in line with the human early response following antidepressant treatment. Here, our main focus was placed on the analysis of a gene expression profile in the peripheral blood, which allowed us to integrate our findings with the human data set. This integration enabled us to predict antidepressant response within a subset of patient. Even more, we could find commonly regulated transcription factors in both species which may play a role in antidepressant response. Additionally, to these interesting findings we also investigated novel candidate genes that were regulated after chronic paroxetine treatment. One of the detected genes was Sox11, which was found to be upregulated after subchronic as well as chronic antidepressant treatment. We could show that Sox11 is mainly regulated in a time dependant manner via SSRIs. After various manipulations of Sox11, we could also demonstrate that Sox11 plays a crucial role in anxiety-related behavior and is thus a very promising candidate for further anxiety-related studies.

Zusammenfassung

In den letzten Jahren wurden eine Reihe an Studien veröffentlicht deren Ziel es war, neue Kandidatengene mit einer potentiellen Rolle im Behandlungserfolg von Antidepressiva zu detektieren. In Zeiten von genomweiten Assoziationsstudien wurde die Suche nach Genen die einen Behandlungserfolg vorhersagen könnten, immer populärer. Trotz all der Bemühungen in den letzten Jahren, waren diese Studien jedoch überwiegend enttäuschend. In der vorliegenden Arbeit haben wir in einem neuen, unvoreingenommenen, experimentellen Ansatz versucht, individuelle Antidepressiva Responsivität in Mäusen zu modulieren. Darüber hinaus haben wir diese präklinischen Befunde mit Ergebnissen aus humanen Studien integriert. Durch diesen translationalen Ansatz waren wir in der Lage, neue Kandidatengene zu identifizieren, welche nach einer chronischen Antidepressivagabe reguliert werden. Neben der chronischen Verabreichungsdauer waren wir auch an einem subchronischen Verabreichungszeitpunkt interessiert. Dieser Zeitpunkt war für uns von großem Interesse, da auch in klinischen Studien Untergruppen von sogenannten frühen Respondern identifiziert werden konnten. Deshalb untersuchten wir im peripheren Blut das Genexpressionsprofil in den Respondersubgruppen und verglichen diese mit den Humandaten. Durch diesen Ansatz war es möglich Responsivität in Humandaten vorherzusagen. Des Weiteren wurden neue Kandidatengene untersucht, welche durch Verabreichung von Antidepressiva reguliert werden. Eines dieser Gene ist Sox11, welches nach subchronischer und chronischer Antidepressivagabe, primär durch Serotonin-Wiederaufnahmehemmer, reguliert wird. Nach genetischer Manipulation von Sox11 konnten wir zeigen, dass es eine zentrale Rolle in angstbezogenem Verhalten spielt. Dies macht Sox11 zu einem sehr vielversprechenden neuen Kandidaten für Studien die sich mit Angsterkrankungen befassen.

1 Introduction

1.1 Depression

"Mental pain is less dramatic than physical pain, but it is more common and also more hard to bear. The frequent attempt to conceal mental pain increases the burden: it is easier to say "My tooth is aching" than to say "My heart is broken." (C.S. Lewis, The Problem of Pain).

Major depressive disorder (MDD) is one of the most common mental disorders. It is a very complex and multifactorial psychiatric disease, which affects up to 20% of the general population (Kessler et al., 2005). Furthermore, unipolar depressive disorders place an immense burden on society and the World Health Organization (WHO) ranked depression as the fourth leading cause of disability (Murray and Lopez, 1996; Rubinow, 2006). Depression is different from normal sadness. It is a recurring, severe mental disorder with a high complexity of symptoms, as depressed mood, avolition, sleep or psychomotoric disturbances, anhedonia, dysregulation of metabolism, endocrine and inflammatory parameters, impaired cognitive performance and finally may also lead to suicide (reviewed in (Villanueva, 2013; Pae and Patkar, 2013; Nestler et al., 2002a)). Additionally, bipolar disorders (episodes of major depression and mania) and anxiety are two diseases that most frequently overlap diagnostically with depression (Flint and Kendler, 2014). Specifically, various studies could demonstrate that about 60% of the depressed patients report one or more anxiety disorders throughout their lives (reviewed in (Flint and Kendler, 2014)).

Despite tremendous efforts over the past decades to understand the molecular underpinnings of depression, the neuropathology of depression remains largely unknown. Various hypotheses have nevertheless been postulated to explain depression and the treatment of depression.

Monoamine theory of depression

In the 1960s, monoamine oxidase inhibitors (MAOIs) were found to effectively treat depressive disorders. As their pharmacological mechanism of action comprises the inhibition of monoamine reuptake, namely serotonin (5-HT) and norepinephrine (NE), Schildkraut and colleagues introduced the monoamine hypothesis of depression, in which a deficiency of monoamines is responsible for depression (Schildkraut, 1965). Although

this hypothesis is nearly 50 years old, today's antidepressants are still designed to acutely increase monoamine transmission by either inhibiting the degradation or the neuronal reuptake of monoamines (reviewed in (Krishnan and Nestler, 2008)). However, the validity of the monoamine hypothesis and whether an imbalance of monoamines in fact underlies depression has been frequently questioned. MAOIs and serotonin reuptake inhibitors (SSRIs) produce immediate effects on monoamine transmission, whereas their effects on the improvement of depressive symptoms require weeks of treatment (Krishnan and Nestler, 2008). The monoamine hypothesis of depression still underlies the first-line therapy for treating depressed patients, however the delayed onset of action as well as the low remission rates of antidepressants (Trivedi et al., 2006) have encouraged scientists to search for alternative explanations.

Dysfunction of the neuroendocrine and immune system in depression

Another well-established model of depression comprises the dysfunction of the hypothalamic-pituitary-adrenal (HPA) axis in depressed patients (Holsboer, 2000). Acute as well as chronic physical and psychological stressors are potential activators of the HPA axis (Keeney et al., 2006). Stress-related inputs converge in the paraventricular nucleus of the hypothalamus, where neurons synthesize corticotropin-releasing hormone (CRH), arginine vasopressin (AVP) and other neuropeptides. This in turn stimulates the synthesis and release of adrenocorticotropic hormone (ACTH) from the anterior pituitary. ACTH subsequently activates the synthesis and the release of glucocorticoids (cortisol in humans and corticosterone in rodents) from the adrenal cortex. This synthesis and release leads to hormonal, autonomic and behavioral effects, which allow the system to adapt to an acute challenge (e.g. effects on metabolism). Therefore, it can be stated that the HPA axis is a key component of the stress response and thus an important regulator of various higher brain structures including the amygdala and hippocampus (Nestler et al., 2002a; Holsboer, 2001). The release of glucocorticoids is essential as they are responsible for the regulation of the HPA axis via a negative feedback loop (Nestler et al., 2002a). Healthy individuals can adapt to these changes, whereas depressed patients fail to adapt (de Kloet et al., 2005). It has been suggested that the sustained increase in glucocorticoid levels (e.g. after severe stress or trauma) may damage the hippocampus, specifically the neurons within the cornu ammonis region 3 (CA3), to facilitate dysregulation of the feedback system, whereby the negative feedback loop becomes a positive feedback loop. This positive feedback loop consequently promotes greater increase in circulating glucocorticoids and thus more damage (Holsboer, 2000). To

support this theory, clinical studies have challenged the neuroendocrine system, to demonstrate that a subset of depressed patients show disturbed HPA axis regulation. Moreover, post-mortem studies could demonstrate that an elevation of neuropeptides, such as CRH and AVP, is common in a subset of patients (reviewed in (de Kloet et al., 2005)).

Cytokines, hormonal mediators of the immune response, are also a crucial part of the neuroendocrine system and accordingly play an important role in mood disorders (Schiepers et al., 2005; Raison et al., 2006; Miller et al., 2009). As afore mentioned, elevated levels of glucocorticoids is a characteristic feature of depression in a subset of depressed patients. Normally, glucocorticoids promote potent anti-inflammatory effects. Depressed patients show high levels of circulating proinflammatory cytokines, such as interleukin-6 (IL-6) and tumor necrosis factor alpha (Villanueva, 2013; Dunn, 2000; Dunn, 2006) to offset the elevated levels of glucocorticoids. Proinflammatory cytokines not only contribute to the innate immune response and inflammation, but they also have relevant neuroendocrine and metabolic effects, including neurotransmitter metabolism and neural plasticity (Villanueva, 2013). Preclinical studies have shown that administration of Il-6 induces depressive-like behavior in rodents and furthermore neutralizes the antidepressant effects of fluoxetine (Sukoff Rizzo et al., 2012). This has been supported by a clinical study in which people were treated with interferon alpha and consequently developed depression (Shelton and Miller, 2010). Furthermore, post-mortem brain studies have shown that different cytokines and genes involved in apoptotic processes are upregulated in depressed patients (Shelton et al., 2011). Interestingly, cytokines also stimulate the HPA axis and activate the secretion of growth hormone (Leonard, 2000), all endocrine processes associated with depression (Villanueva, 2013). Nevertheless, results have been inconsistent when investigating serum cytokine concentrations in depressed patients, suggesting that immune activation only accounts for a small subset of patients (Krishnan and Nestler, 2008).

Neurogenesis and depression

Adult neurogenesis has drawn a lot of attention in neuroscience within the last years. It has been shown that the adult mammalian brain is still able to remove existing glia cells and neurons as well as establish novel neural circuits (Villanueva, 2013). Adult hippocampal neurogenesis describes the process by which neuronal progenitor cells of the hippocampal subgranular zone (SGZ) and the subventricular zone (SVZ) of the lateral

ventricles divide mitotically to form new neurons that differentiate and integrate into the dentate gyrus (DG) or the olfactory system (reviewed in (Krishnan and Nestler, 2008)). Gould and colleagues were the first to suggest a potential role of SGZ neurogenesis in mood regulation. They clearly demonstrated that corticosteroid administration results in the suppression of cell division in the SGZ (Gould et al., 1992). Subsequent animal studies effectively demonstrated that a variety of chronic stress paradigms, commonly used as a preclinical model of depression, lead to a reduction in cell proliferation (Mirescu and Gould, 2006). However, studies investigating the effects of acute stress are not completely in line with those examining chronic stress. Acute foot shock, for example, was shown to reduce cell proliferation in male rats, whereas acute restrained stress had no influence on cell proliferation (reviewed in (Zhao et al., 2008)). In contrast to these findings, the regulation of cell survival after stress is not completely understood (Zhao et al., 2008). Increased glucocorticoid levels are considered the central mechanism underlying stress-induced suppression of cell proliferation in the SGZ. This hypothesis could be supported by two main findings. First, corticosterone administration decreases cell proliferation, and secondly adrenalectomy increases SGZ neurogenesis (Zhao et al., 2008; Mirescu and Gould, 2006). In contrast to stress, antidepressant administration is able to increase cell proliferation in the SGZ (Warner-Schmidt and Duman, 2006; Duman, 2004). Furthermore, antidepressants are able to reverse the stress-mediated decrease in cell proliferation (Warner-Schmidt and Duman, 2006). However the most interesting aspect is that the time course of antidepressant-induced changes correspond with the time delay for mood-elevating effects in humans (Miller et al., 2007). When administering antidepressants 1 to 5 days, no effect on cell proliferation can be found. Nevertheless, after 7 to 14 days of antidepressant treatment, an increased rate of neuronal proliferation can be detected. Extending the antidepressant treatment up to 4 weeks, produces a significant increase in the cell survival rate (Malberg et al., 2000; de Foubert et al., 2004). To strengthen the hypothesis that neurogenesis is involved in antidepressant treatment outcome Santarelli and colleagues combined hippocampal irradiation with chronic fluoxetine treatment in mice to show that fluoxetine treatment was ineffective in hippocampal-irradiated mice (Santarelli et al., 2003). To date, cell proliferation studies have not been very conclusive in human analyses. However, imaging studies could reveal that a decrease in hippocampal volume as well as in other forebrain regions is present in a subset of depressed patients, and thus supports the theory of neurotrophic factors, neurogenesis and depression (Krishnan and Nestler, 2008).

Depression - influence of genetic and environmental factors

Increasing evidence demonstrates that depression is highly influenced by genetic factors (Ising and Holsboer, 2006; Lesch, 2004), and is indeed a highly heritable disorder (up to 38%) (Kendler et al., 2006). However, the search for specific relevant genes has been very disappointing so far (Nestler et al., 2002a). As depression is a very complex psychiatric disorder, it is hard to find one common gene responsible for the development of depression. It is more likely that many genes are involved in the development of the disorder (Burmeister, 1999). Alternatively, variations of genes may contribute to depression in every affected family. More and more studies demonstrate that single nucleotide polymorphisms (SNPs), genetic variations in one single gene, are capable of contributing to either a stress-resilient or stress-vulnerable phenotype, which consequently determines the chance of developing depressive disorders. Binder and colleagues could demonstrate that different SNP variations in the human corticotropin releasing hormone receptor type 1 (CRHR1) gene, a gene that is highly involved in HPA axis regulation, modulate individual stress susceptibility and lead to a higher risk of developing psychiatric disorders such as depression (Binder and Nemeroff, 2010; Ressler et al., 2010). However, individual vulnerability to depression is only partly driven by genetic factors. More and more studies demonstrate that environmental factors, namely stress or trauma, are also important key players in the development of depression (Nestler et al., 2002a). Depression is often referred to as a stress-related disorder. Evidence show that severe stress, including early trauma or chronic stress during adulthood, leads to an increased risk of developing depression (Nestler et al., 2002a; Heim and Nemeroff, 2001; Heim et al., 2008). In summary, these findings indicate that stress, per se, is not sufficient to cause depressive episodes. It rather seems likely that an interplay between genetic risk factors and environmental factors underlies the etiology of depression.

Depression and the glutamate system

Glutamate was first recognized as a neurotransmitter in the 1980s and it is now known as the major excitatory neurotransmitter in the central nervous system (CNS) (Orrego and Villanueva, 1993). Glutamate mediates fast excitatory transmission (Sanacora et al., 2012), and the majority of brain neurons and synapses are glutaminergic in nature (Pessoa, 2008). Furthermore, glutamate synaptic transmission is a key player in mediating cognitive and emotional processes (Pessoa, 2008). In the 1990s, Trullas and Skolnick shed new light on the role of the glutamate system in depressive disorders. They

could demonstrate that a *N*-Methyl-D-aspartate (NMDA) receptor antagonist exert antidepressant-like effects (Trullas and Skolnick, 1990). Subsequent animal models revealed that different types of environmental stressors enhance glutamate release and transmission in limbic and cortical brain regions. These molecular changes result in structural alterations, e.g. dendritic remodeling and reduction of synapses, which in turn further alter synaptic transmission (Sanacora et al., 2012). To additionally strengthen the role of glutamate in depressive disorders, clinical studies provide evidence that glutamate transmission is abnormal in depressed patients (Sanacora et al., 2012). In fact, increased glutamate levels are found in the patients' plasma (Sanacora et al., 2012). Furthermore, studies have shown that antidepressant treatment is able to reduce the higher plasma glutamate levels in depressed patients (Altamura et al., 1995; Maes et al., 1998). Frey and colleagues could show in one study with a mixed set of patients (bipolar and unipolar depression) that glutamate levels were decreased in central spinal fluid (Frye et al., 2007). A postmortem brain tissue study of the frontal cortex of depressed patients stated an increase in glutamate levels (Hashimoto et al., 2007).

Despite no clear unifying hypothesis of depression nor a comprehensive understanding of the underlying pathophysiological mechanisms of depression, effective treatment strategies are nonetheless already available.

1.2 Antidepressant drugs

During the mid-1950s two precursors of the main contemporary classes of antidepressants were discovered, iproniazid for MAOIs (Crane, 1956) and imipramine for tricyclic antidepressant drugs (TCAs) (Kuhn, 1957; Kuhn, 1989). This discovery subsequently led to the development of a large number of antidepressant compounds (Papakostas et al., 2007). Within the following decades, other classes of antidepressants, for example SSRIs and serotonin-norepinephrine reuptake inhibitor (SNRIs) were discovered and are nowadays commonly prescribed to treat depressive disorders (Papakostas et al., 2007). These antidepressants are in general effective but far from ideal, as their therapeutic effects presents a delayed onset, taking several weeks to exert their full clinical effects and are often accompanied by unwanted side-effects, such as body weight gain or fatigue (reviewed in (Flint and Kendler, 2014)). While many patients respond well to the currently available antidepressants, a significant number of patients neither show an adequate response to the treatment nor complete symptom relief, and often the patients relapse (Trivedi et al., 2006). In 2007, the Sequenced Treatment

Alternatives to Relieve Depression study (STAR*D) revealed that only one-third of patients on citalopram monotherapy remitted and the remaining two-thirds of patients failed to remit. In follow-up studies, other antidepressant monotherapies were prescribed to these patients (Trivedi et al., 2006). Based on this study and similar studies, it became clear, that treatment strategies are largely based on a trial and error principle (Fabbri et al., 2013) and that the longer the patients are treated, the less chance they have to remit (Trivedi et al., 2006). To-date, commonly prescribed antidepressants are mainly acting on monoamine transmission. Their main aim is to increase the concentration of monoamines on the one hand, by blocking reuptake or inhibiting monoaminergic neurotransmitter metabolism, or on the other hand, by blocking receptors downstream of monoaminergic signal transduction (Delgado, 2004). For example, SSRIs, SNRIs, norepinephrine reuptake inhibitors (NERIs) as well as norepinephrine and dopamine reuptake inhibitors (NDRIs) all fall within this category (Wong and Licinio, 2004; Yadid et al., 2000). Collectively, these antidepressant drugs are not completely selective for a single neurotransmitter and thereby potentially increase the side-effects (Lucki and O'Leary, 2004). Regardless, SSRIs are still used for first-line antidepressant therapy (Nemeroff, 2007). MAOIs as well as TCAs are used for second-line antidepressant therapy. TCAs mainly block the NE transporter and some also block the 5-HT transporter, which ultimately lead to higher levels of 5-HT and NE in the synaptic cleft, features, which underlie their antidepressant effects. MOAI can block an enzyme called monoamine oxidase (MAO), which degrades 5-HT and NE in the synaptic cleft and the presynaptic cell. Blocking the MAO leads to a lower degradation of the monoamines and is thus leading to higher concentrations of the neurotransmitters (Bortolato et al., 2008) (Figure 1).

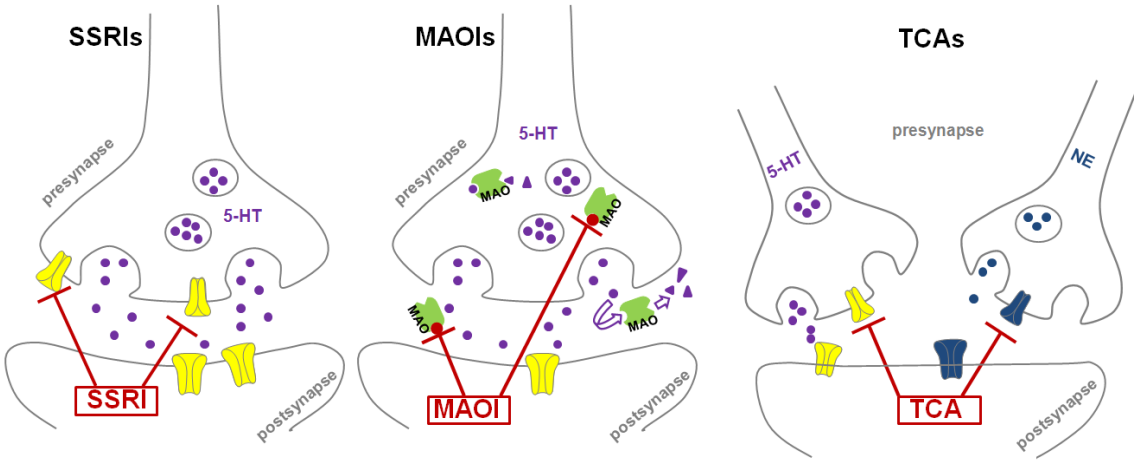

Figure 1: Work mechanisms of different antidepressant classes. The main aim of SSRIs is to increase the concentration of 5-HT (indicated in purple) by blocking the presynaptic 5-HT receptors (indicated in yellow) and thus blocking the reuptake of the neurotransmitters. 5-HT is longer available in the synaptic cleft and therefore exert its antidepressant effect. MAOIs can block an enzyme called MAO, which degrades 5-HT and NE in the synaptic cleft and the presynaptic cell. While blocking the MAO the degradation of the monoamines is prevented and thus leading to higher concentrations of the neurotransmitters (in this figure only 5-HT is represented as a neurotransmitter). TCAs mainly block the NE transporter and some also the 5-HT transporter, which is then leading to higher levels of 5-HT and NE in the synaptic cleft, both features that can lead to antidepressant effects.

During the past years, advances in antidepressant treatment approaches were made when old antidepressants were "made-over" to novel classes of antidepressants, presenting improved treatment efficacy. For example, desvenlaflaxine, an active metabolite of venlaflaxine, was "made-over" into its own antidepressant. Desvenlaflaxine is less metabolized by cytochrome P450 2D6 (CYP2D6) compared to venlaflaxine and thereby demonstrates more stable plasma levels (Beyer and Stahl, 2010). The next generation of antidepressants are targeting novel structures, namely receptors, and range from low-molecular-weight compounds that are acting on the HPA axis (like R121919, a CRHR1 antagonists) to neurokinin receptor antagonists (Beyer and Stahl, 2010). For instance, CRHR1 antagonist (R121919) treatment could significantly reduce depression and anxiety scores in depressed patients (Zobel et al., 2000). Although the exploration trials of CRHR1 antagonists were very promising, more recently in follow-up studies, these drugs have not been successful (reviewed in (Holsboer, 2014)).

Despite advances in novel antidepressant drug design, 40% of the patients do not present an adequate response to the first medication prescribed. Even more concerning, 30% of all patients with MDD do not respond to any intervention (Baghai et al., 2006). For these patients, it is typical to alternate between different classes of antidepressants, different concentrations and to combine different antidepressant drugs. Another novel approach for

treatment-resistant patients is the use of ketamine, a NMDA receptor antagonist. Clinical studies have demonstrated that, an acute injection of ketamine has rapid antidepressant effects without the unpleasant time-delay. Nevertheless, ketamine produces strong side effects and is therefore not suitable as a standard antidepressant therapy (Li et al., 2010). Electroconvulsive seizure therapy (ECT) is another therapeutic application that is used for treatment-resistant patients, in which generalized epileptic seizures are provoked by electrical stimulation of the brain (Frey et al., 2001).

There are many possibilities to treat depression, however the clinical response to the treatment is not always satisfying.

1.3 Depression and the hippocampus

Neuroimaging technologies as well as neuropathological and lesion studies enabled in vivo characterization of anatomical and physiological correlates of mood disorders (Drevets, 2000; Czéh et al., 2001). These results as well as post-mortem studies shed new light on brain regions that are of major interest in mood disorders. It has been shown that brain regions involved in the regulation of mood and emotion, reward processing, attention, motivation, stress response as well as social cognition are altered in depressed patients (Phillips et al., 2003). The limbic-cortical-striatal-pallidal-thalamic circuit is formed by the connection between the orbital and medial prefrontal cortex, amygdala, hippocampus (HC), ventromedial striatum, mediodorsal and midline thalamic nuclei as well as the ventral pallidum (Öngür et al., 2003). Although various brain regions are important for a comprehensive understanding of depressive disorders, the hippocampal formation is one of the most studied brain regions in depressed patients (Videbech and Ravnkilde, 2004). It is involved in learning and memory (Fanselow, 2000), and is one of the few brain regions where adult neurogenesis occurs (Braun and Jessberger, 2014).

The HC is a bilaminar grey-matter structure, which receives input from the amygdala, the claustrum, the septal complex and the supramammillary area, the hypothalamus, the thalamus and the brain stem. In turn, it projects to the septal nuclei, the thalamus, the mamillary, striatum as well as the amygdaloid complexes among others (Rosene and Van Hoesen, 1977). The laminae that form the HC complex consist of the DG and the cornu ammonis, which can be divided further into three regions, cornu ammonis region 1-3 (CA1 - CA3), based on their pyramidal neuronal morphology and sensitivity to anoxia (Freund and Buzsaki, 1996; Lucas and Strangeways, 1963). The DG receives the principle

afferent input from the entorhinal cortex (ec) and then transmits the signal to the CA3 neurons via the mossy fibers. The CA1 subregion represents the last station of the intrahippocampal trisynaptic loop and is mainly targeted via the pyramidal cells of the CA3, the Schaffer collaterals (Sc). The principle hippocampal output is formed by the CA1 pathway via the subiculum, which projects to the ec formation, among others (Freund and Buzsaki, 1996).

Extensive preclinical as well as clinical research have shown that the mnemonic and neuroplasticity function of the hippocampus is highly sensitive to stress, specifically elevated cortisol/corticosterone levels, which are often altered in depressed patients (Videbech and Ravnkilde, 2004; Checkley, 1996). Various studies have demonstrated that both physiological and psychosocial stress lead to adaptive changes in the hippocampus, e.g. reduction of neurogenesis in the DG. Indeed, the adult mammalian brain contains substantial numbers of neurogenic neural stem/progenitor cells (NSPCs) that retain the ability to generate new neurons throughout life, which is also known as adult neurogenesis (reviewed in (Braun and Jessberger, 2014)). However, adult neurogenesis is limited to two brain areas, namely the SGZ of the hippocampal DG and the SVZ lining the lateral ventricles (Braun and Jessberger, 2014). NSPCs reside in the SGZ of the adult DG and give rise to granular cell neurons via multiple steps. NSPCs, known as type 1 cells, extend a radial process through the granular cell layer into the molecular layer and can then be activated to generate proliferating type 2 non-radial NSPCs. These type 2 cells give rise to neuroblasts, which begin to branch out upon neuronal differentiation. Immature neurons migrate into the granular cell layer and over a 3-week period, newborn granule cell neurons form large dendritic arbor into the molecular layer as well as into the hilus, which then targets cells in the hilus and CA3 region (reviewed in (Braun and Jessberger, 2014)) (Figure 2). After migrating into the dentate granular layer the neurons become dentate granular cells and are thus integrated into existing circuits and begin to receive functional input (Zhao et al., 2008).

The reduction in neurogenesis has been hypothesized to be linked to depressive episodes and has been shown to be restored following antidepressant treatment (see chapter 1). In line with this theory, clinical studies have shown a significant reduction in hippocampal volume in depressed patients compared to healthy controls (Krishnan and Nestler, 2008). Additionally, studies have demonstrated that antidepressants increase neurogenesis whereas chronic stress leads to a reduction in the neurogenesis rate. In terms of the delayed onset of antidepressant treatment response, it is very likely that alterations in

gene and protein expression could be the reason for the therapeutic effect. For instance, multiple studies have demonstrated that hippocampal neurogenesis-related genes, namely brain-derived neurotrophic factor (BDNF), play an important role in depression and antidepressant treatment (Duman and Voleti, 2012). It was shown that stress reduces BDNF synthesis, whereas antidepressants increase BDNF synthesis and signaling in the prefrontal cortex and HC (reviewed in (Zhao et al., 2008)).

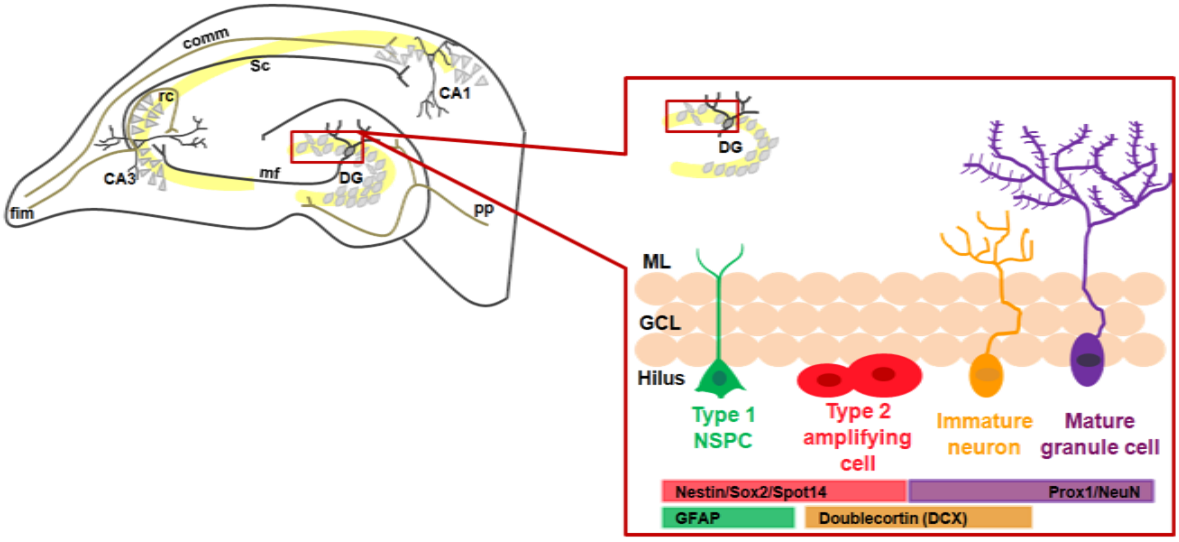

Figure 2: Signaling pathway and neurogenesis in the adult hippocampus in the mouse. The DG receives input from the ec and then pass on the signal to the CA3 neurons via the mossy fibers (mf). The pyramidal cells of the CA3 target mainly the CA1. The principle hippocampal output is formed by the CA1 pathway. Adult neurogenesis occurs in the SGZ of the HC, where NSPCs reside. Type 1 cells, extent a radial process through the granular cell layer into the molecular layer and can then be activated to generate proliferating type 2 non-radial NSPCs. The type 2 cells give rise to immature neurons, which begin to branch out. Immature neurons migrate into the granular cell layer and newborn granule cell neurons form large dendritic arbor, the so called mature granule cells.

1.4 Gene expression profiling in depression

Gene expression profiling is a very propitious technique, and has successfully identified promising genes, such as SLC6A15 (Kohli et al., 2011). Within the past years, unbiased approaches, including microarray analysis or next-generation sequencing, have become attractive techniques to detect novel candidates and pathways, which underlie antidepressant treatment outcome (Ising et al., 2009; Tansey et al., 2013).

Genetic factors strongly contribute to the development of many mental disorders. More and more studies have already shown that variations in specific alleles in combination with environmental factors affect individual susceptibility to develop mental disorders. For instance, Bradley and colleagues found a significant gene x environment interaction in

various SNPs in the CRHR1, a gene involved in the HPA axis. They demonstrated that specific CRHR1 polymorphisms were able to moderate the effect of childhood abuse on the risk of adult depressive symptoms (Bradley et al., 2008). Within the last years, genome-wide association studies (GWAS) gained more and more importance as their methodical properties as well as their statistical power to detect gene variations became more sensitive (Bush and Moore, 2012; Stranger et al., 2011; van der Sijde et al., 2014). Such studies aim to detect genetic factors that contribute to complex diseases, which often results from a combination of multiple genetic as well as environmental risk factors (Freimer and Sabatti, 2007). GWAS studies are carried out in two stages: first the discovery phase and in a second step, the replication phase. The discovery phase is used to screen the whole genome. In the replication phase, a subset of SNPs are tested in an independent cohort (Flint and Kendler, 2014). In comparison to candidate-gene studies that use either resequencing or association studies of specific genes, one advantage of GWAS studies is that the approach is unbiased, aiming to identify novel targets that may contribute to the examined disorder (Hirschhorn and Daly, 2005). Recently, GWAS have been performed for many common disorders, and in some cases, genomic regions with a strong linkage to the disease were identified, such as in type 1 diabetes (Nisticò et al., 1996). However, for many diseases, these association studies showed limited success. When it comes to depressive disorders, and especially antidepressant treatment outcome, a meta-analysis combining three genome-wide pharmacogenetic studies, the Genome-Based Therapeutic Drugs for Depression (GENDEP) project, the Munich Antidepressant Response Signature (MARS) project, and the STAR*D study, was performed aiming to identify biomarkers predicting antidepressant response. As depressed patients show a large heterogeneity in regard to treatment outcome, it was suggested that genetic variations might contribute to this variability (GENDEP Investigators et al., 2013). However, they were not able to detect reliable predictors of antidepressant treatment outcome (GENDEP Investigators et al., 2013). The authors suggest that sub-cohorts should be analyzed in the future, as they were able to detect a variant associated within the SSRI treated patients with early SSRI response (after 2 weeks of treatment). However, they state that this finding would not survive further statistical correction in their analysis (GENDEP Investigators et al., 2013). This study once again demonstrates that the outcome of antidepressant treatment is a very complex and heterogenic phenomenon. Therefore, it might be worthwhile to assess individual treatment outcomes in future studies.

1.5 SRY-box containing gene 11 (Sox11) - a novel antidepressant-inducible gene

One of the genes that was extensively studied in this thesis is SRY-box containing gene 11 (Sox11). The male sex determination gene Sry (sex-determining region Y), was the first of the Sox gene family that was discovered in the 1990s (Kiefer, 2007). All Sox genes, including Sox11, are transcription factors, and have been identified throughout the animal kingdom (Guth and Wegner, 2008).

Structure and function of SoxC genes

Ten Sox gene families have been described so far, SoxA – SoxH, grouped according to their amino acid identity (within one group > 70%) (Guth and Wegner, 2008). All of them contain a DNA-binding high-mobility group (HMG) domain that encodes the DNA-binding domain of a protein (Guth and Wegner, 2008). During the past decades, the role of Sox genes was receiving more attention in developmental processes, such as embryogenesis, gastrulation and stem cells (Guth and Wegner, 2008). Sox4, Sox11 and Sox12 are members of the SoxC family. SoxC genes are expressed in committed, postmitotic neuroblasts, which suggests that they are involved in the latter steps of neuronal development (Bergsland et al., 2006). Studies have shown that the SoxC group is mainly expressed in developing neurons, oligodendrocytes and astrocytes in the human brain (Bergsland et al., 2006; Jay et al., 1995). Furthermore, previous studies have shown that overexpression of SoxC activates panneuronal markers, namely tubulin, beta 3 class III (Tubb3) and microtubule-associated protein 2 (Map2) (Bergsland et al., 2006). Sox11 is expressed in the developing mouse nervous system (Bergsland et al., 2006), however is absent in many adult tissues (Xu and Li, 2010). Haslinger and colleagues revealed that within the adult mouse brain, Sox11 is mainly expressed in the DG of the HC and in the subventricular zone of the olfactory bulb. Furthermore, they showed that Sox11 is stage-specifically expressed in cells of adult neurogenic lineage, whereas the transcriptional targets of Sox11 adult neurogenesis are still unknown (Haslinger et al., 2009).

Sox11 and its involvement in diseases

Sox11 is expressed in virtually all aggressive mantel cell lymphomas and was recently recognized as a diagnostic and prognostic antigen (Zeng et al., 2012). Apart from its role as a diagnostic marker in cancer research, very little is known about the physiological roles of Sox11 in adult organisms. It has been shown that Sox11-deficient mice present

various craniofacial and skeletal malformations, asplenia and hypoplasia of the lung and stomach. Importantly, these Sox11 malformations are in line with the human malformation syndrome (Sock et al., 2004). To-date there is a paucity information describing the behavioral characteristics of Sox11 in adult mice. The association between neurogenesis and psychiatric disorders suggests that insufficient neuronal proliferation, differentiation and connectivity during brain development and/or insufficient adult neurogenesis may contribute to the risk of illness (Sha et al., 2012) and therefore Sox11 would be an interesting candidate to investigate.

1.6 Animal model of depression

Modeling a neuropsychiatric disorder, for example depression, in rodents is a challenge on account of the complexity and vastness variety of symptoms in depressed patients. Furthermore, the psychological aspect cannot be modeled in animals as psychological parameters cannot be interpreted in rodents. Willner and colleagues developed a number of criteria that should be fulfilled in a potential valid animal model of disease (Willner, 1984). The first criterion is the aspect of face validity within an animal model. High face validity means that there is a high degree of uniformity between the disease symptoms in humans and rodents. For depression this would include e.g. anhedonia, increased anxiety, alteration in HPA axis activity or sleep disturbances (Müller and Holsboer, 2006). Another very important aspect of any potential animal model is its predictive validity. This is achieved when treatment approaches, which are successful in the clinical situation, exert the same effects in the animal model. Finally, the third criterion is construct validity. High construct validity implies that the etiological processes underlying the disease state is the same in the animal model as in humans (Chadman et al., 2009). An example of high construct validity includes modeling a persisting genetic variant is present in the human disease state, either by overexpression or knockdown of a known disease-causing genetic mutation (Nestler and Hyman, 2010).

Modeling antidepressant treatment

Animal models aiming to investigate the influence of antidepressant treatment are commonly used within preclinical psychiatric research. However, such model systems present some limitations in terms of predictive validity (Figure 3).

Is the dosage used in the animal model comparable to the clinical situation?

Most animal studies are conducted with very high dosages of antidepressants (for instance paroxetine: 18mg/kg BW; fluoxetine: 18mg/kg BW (Holick et al., 2007)). In comparison to the human situation (paroxetine and fluoxetine are administered with a dosage of 20 - 40mg per day for an average person of 70kg (≙ 0.29mg/kg - 0.57mg/kg BW)), it can be concluded that most of the studies are potentially overdosing the animals.

How is the antidepressant drug applied?

Many animal studies administer the antidepressant drugs via the drinking water (Wagner et al., 2012; Scharf et al., 2013), gavaging (Ganea et al., 2012; Sillaber et al., 2008; Webhofer et al., 2011) or via i.p. injections (Steru et al., 1985; de Montigny and Aghajanian, 1978). However, in the clinical situation we can see that most of the patients are treated with tablets.

How long should a drug be administered to provoke a robust effect?

In the human situation we can see that the majority of patients start responding to the antidepressant treatment after at least 4 - 6 weeks of treatment. However, in preclinical studies, the longest treatment period is 28d, with most studies employing even shorter treatment periods (Ganea et al., 2012; Fava et al., 2000; Sillaber et al., 2008; Vaugeois et al., 1997). Furthermore, several studies draw conclusions following an acute antidepressant exposure, whereas this acute antidepressant effect is not effective in the clinical practice. Collectively, it is evident that a large gap still exists between preclinical research and the actual clinical setting, and therefore the translational value of animal models for depression could be improved.

Therefore, it would be desirable to mimic the clinical situation as closely as possible to get a better translational approach.

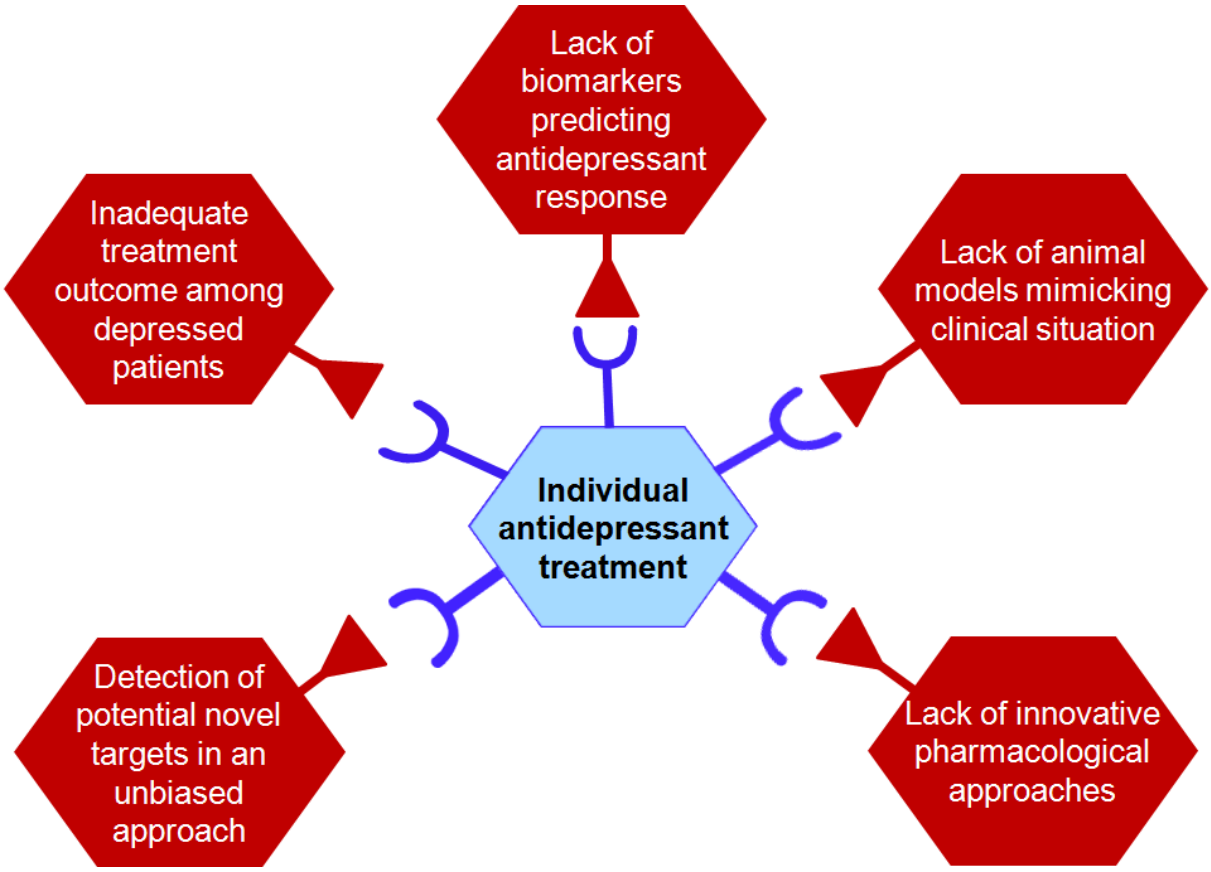

Figure 3: Illustration of the current clinical and preclinical situation of antidepressant response. There are many limitations at the moment when it comes to find the best treatment strategy for each patient. One reason for that is the lack of innovative pharmacological approaches, as most of the antidepressants used at the moment are based on the findings from the 1950s. These antidepressants are in general effective, although many patients do not present an adequate response to the treatment. Additionally, there is a lack of biomarkers that predict antidepressant response in humans. There is also a deficit of appropriate animal models that are mimicking the clinical situation as closely as possible. A first step towards better treatment strategies and biomarkers for antidepressant response might be the detection of novel targets by using an unbiased approach in a novel animal experimental approach.

1.7 Aim of the thesis

The overarching aim of this thesis is to gain a insight into the neurobiology underlying individual treatment response in MDD. We directed our research towards addressing two major problems that currently impede advances in antidepressant drug development employing a translational strategy, namely, we sought to address:

1. Identification of early biomarkers would promote evidence-based selection of antidepressant treatment options, rather than the trial and error approach currently used. As some patients already present a positive treatment effect after 14d of antidepressant treatment, we further aimed to identify novel candidate genes, biomarkers and pathways determining an early antidepressant response.

2. The lack of conceptually novel antidepressant compounds. To further proceed in this field we aimed to establish a novel experimental approach that models antidepressant responsiveness in mice, and to subsequently implement this approach in order to identify novel targets mediating individual antidepressant response. To gain a better understanding of individual antidepressant response and the basis for the heterogeneity in antidepressant treatment outcome, we aimed to mimic the clinical situation as closely as possible.

2 Materials and Methods

2.1 Animals

The experiments were carried out with male DBA/2J mice obtained from Charles River (Charles River Laboratories, France). Animals were single housed in polycarbonate cages (21 x 15 x 14cm) with standard bedding and nesting material, with a 12L:12D cycle (lights on at 7am) as well as constant temperature (23 ± 2°C) and humidity (55 ± 5%). Standard mouse chow (Altromin 1324, Altromin GmbH, Germany) and tap water were provided ad libitum. All experiments were carried out in the animal facility of the Max Planck Institute of Psychiatry in Munich, Germany, in accordance with the European Communities Council Directive 2010/63/EU. All efforts were made to minimize animal suffering during the experiments. The protocols were approved by the committee for the Care and Use of Laboratory animals of the Government of Upper Bavaria, Germany.

2.2 Experimental design

2.2.1 Validation of a novel approach to investigate antidepressant response in mice

2.2.1.1 Paroxetine - Dosage

Dosage: 1mg/kg BW

The aim of this study was to identify the minimum effective paroxetine dosage for the DBA/2J strain. Therefore, 41 male DBA/2J mice were randomly assigned to either the vehicle (n=11) or paroxetine (n=30) experimental group. Upon arrival, animals were at the age of 7 - 9 weeks and housed singly. Pharmacological treatment started at the age of 9 - 11 weeks. The animals were treated with 1mg/kg body weight (BW) paroxetine or vehicle for 28 days twice a day (for details see 262.3). After the treatment interval the animals were subjected to a Forced Swim Test (FST) and sacrificed directly afterwards (Figure 4A). Trunk blood and whole brains of the animals were collected and stored until further processing (for details see 2.4).

Dosage: 5mg/kg BW

To identify the minimum effective dosage, a second experiment was performed using a paroxetine concentration of 5mg/kg BW. Animals were at the age of 7 - 12 weeks at the arrival and housed singly from the beginning on. Paroxetine treatment started at the age of 9 - 14 weeks. The animals were treated with 5mg/kg BW paroxetine (n=100) or vehicle (n=58) for 28d twice a day (for details see 2.3). On treatment day 29, the animals were subjected to a FST and sacrificed directly after the FST (Figure 4B). Trunk blood and brains of the animals were collected and stored until further use (for details see 2.4).

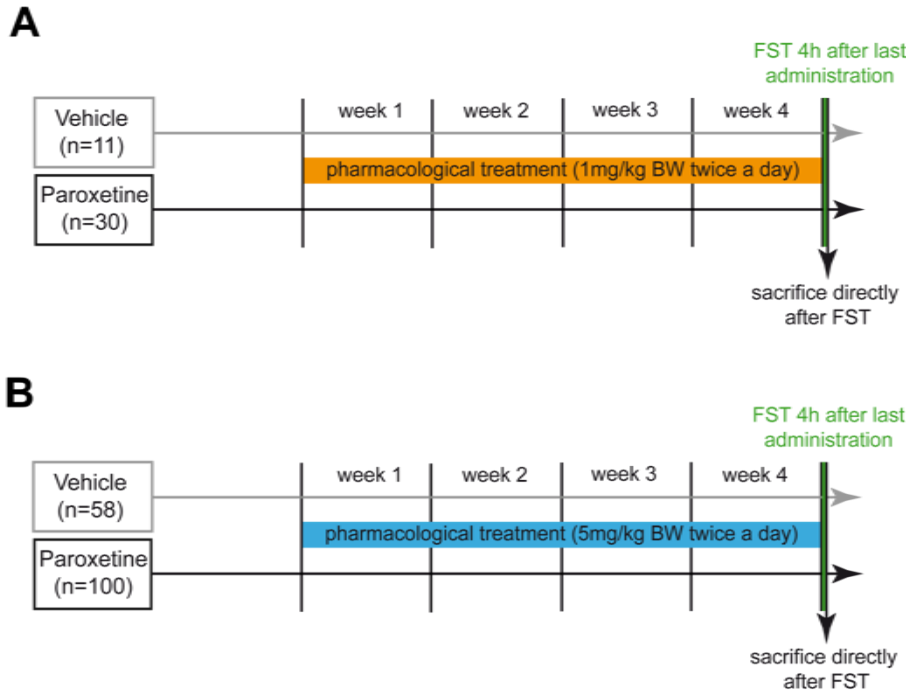

Figure 4: Experimental time course. (A) Animals were randomly divided in vehicle and paroxetine treatment groups. Animals were treated with either 1mg/kg BW paroxetine or vehicle for 28d twice a day. Last drug administration was given to the animals on day 29 in the morning (6am). 4h later the animals were subjected to a FST and killed directly after the FST. (B) Animals were randomly divided in vehicle and paroxetine treatment groups. They were treated with either 5mg/kg BW paroxetine or vehicle for 28d twice a day. Last drug administration was given to the animals on day 29 in the morning (6am). 4h later the animals were subjected to a FST and sacrificed directly after the FST

2.2.1.2 Paroxetine - Acute treatment effects

In a next step, we investigated the effects of an acute paroxetine treatment and therefore male DBA/2J mice were either treated with 5mg/kg BW paroxetine (n=30) or vehicle

(n=50). Animals were between 12 - 14 weeks old and treated on the day of the behavioral testing, with one acute dosage of 5mg/kg BW paroxetine, 4h before the behavioral test and then sacrificed directly after the FST (Figure 5). Trunk blood and brains of the animals were collected and stored until further processing (for details see 2.4).

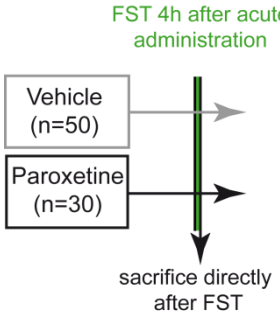

Figure 5: Overview of experimental time course. Animals were treated on the day of the behavioral testing with one acute administration paroxetine (5mg/kg BW). 4h later the animals were subjected to a FST and directly sacrificed after the test.

2.2.1.3 Route of administration: Acute administration of mouse pellets versus intraperitoneal injection (i.p.)

I.p. injection is a common used technique to administer pharmacological agents to mice. We investigated in this study whether the pharmacokinetic effects of the customized palatable mouse pellets is comparable to i.p. injections. Therefore, 10 male DBA/2J mice were i.p. injected once with 5mg/kg BW dosage of paroxetine. The mouse pellet control group (n=30) originated from the acute treatment experiment (see chapter 2.2.1.2). Trunk blood and whole brains were collected at sacrifice to measure paroxetine levels (for details see chapter 2.7.2).

2.2.1.4 Pharmacokinetics of paroxetine

In order to get a better understanding of the pharmacokinetic profile of paroxetine, especially with regard to the pharmacological half-life in the mouse, 20 male DBA/2J mice were treated with 5mg/kg BW paroxetine twice a day for 28d (animals were 9 - 10 weeks old at the beginning of the treatment) (for details see 2.3). After the treatment period animals were killed at different time points (1d (n=5), 3d (n=5), 7d (n=5) or 14d (n=5))

(Figure 6). Trunk blood and whole brains were collected at sacrifice and stored until further use (for details see 2.4).

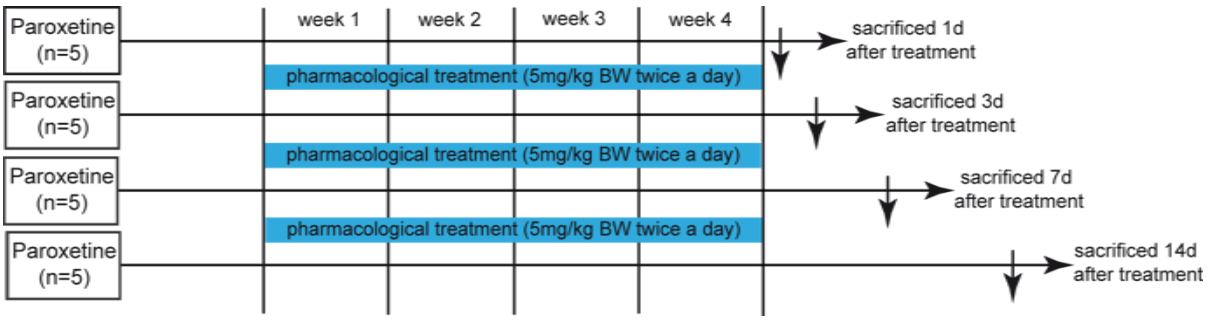

Figure 6: Overview of the experimental time course. Animals were treated with 5mg/kg BW paroxetine twice a day for 28d. After the treatment period animals were killed at different time points after discontinue with the paroxetine treatment. Animals were sacrificed 1d (n=5), 3d (n=5), 7d (n=5) or 14d (n=5) after discontinue the paroxetine treatment.

2.2.1.5 The Forced Swim Test as a readout parameter for antidepressant response

This study was designed to assess whether the FST is a suitable behavioral test to investigate the variability of antidepressant treatment response in mice. Animals were tested before and after the antidepressant treatment in the FST. This repeated testing was used to investigate whether differences in treatment response of the animals could be due to preexisting inherent characteristics. Therefore, 60 male DBA/2J mice were subjected to the first FST at the age of 8 - 9 weeks. After one week of recovery, the animals were treated twice a day for 28d with either 5mg/kg BW paroxetine (n=40) or vehicle (n=20) (for details see 2.3). On the last day of treatment the animals were tested in the FST for the second time (Figure 7). Animals were killed directly after the FST, trunk blood and whole brains were collected at sacrifice and stored until further processes (for details see 2.4).

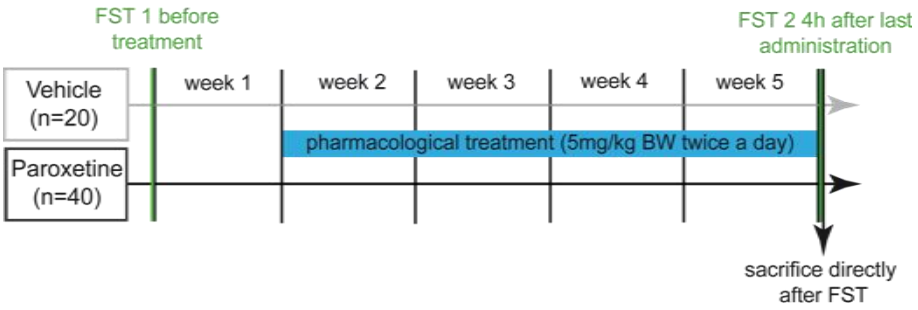

Figure 7: Overview of the experimental time course. Male DBA/2J mice were tested at the age of 8 - 9 weeks in the FST for the first time. After one week of recovery, the animals were treated twice a day for 28d with either 5mg/kg BW paroxetine. On the last day of treatment the animals were tested in the FST. Animals were sacrificed directly after the FST.

2.2.2 Detection of potential novel candidate genes after chronic paroxetine treatment

In a next step, we were aiming to detect novel molecular targets mediating an individual antidepressant response after chronic paroxetine treatment within our novel experimental approach. Therefore, 158 male DBA/2J, aged 9 - 14 weeks, were treated with 5mg/kg BW paroxetine (n=100) or vehicle (n=58) for 28d twice a day (for details see 2.3). Subsequently, the mice were sacrificed directly after the FST (Figure 8). To investigate differences in antidepressant treatment response, the animals were divided into good, intermediate and poor treatment responders according to their performance in the FST (for details see chapter 2.5). Trunk blood and brains were collected and stored until further use (for details see 2.4).

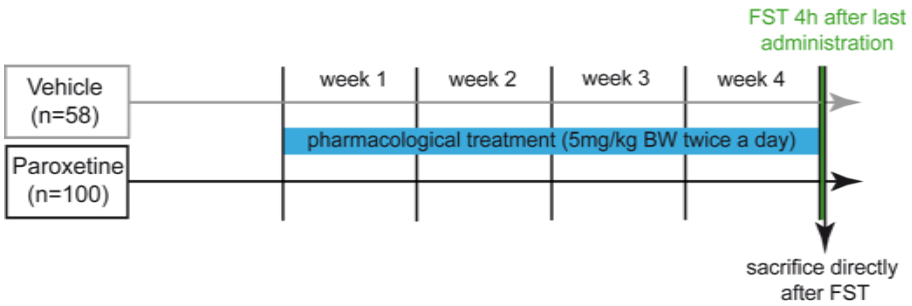

Figure 8: Overview of the experimental time course. Animals were randomly divided in vehicle and paroxetine treatment groups. Animals were treated with either 5mg/kg BW paroxetine or vehicle for 28d twice a day. Last drug administration was given to the animals on day 29 in the morning. Animals were subjected to a FST 4h later and sacrificed directly after the FST.

2.2.3 The role of Sox11 in antidepressant response and depression

2.2.3.1 Characterization of Sox11 under different treatment conditions

Based on the results obtained in 2.2.2 Sox11 was identified as a promising novel candidate gene. In order to investigate the influence of paroxetine treatment on Sox11 expression, brains from the previous experiments (see chapter 2.2.1.3, 2.2.2 and 2.2.4) were processed for *in situ* hybridization (ISH) (2.7.8).

2.2.3.2 The effects of reboxetine on Sox11 expression

The aim of this study was to assess, whether the altered Sox11 messenger RNA (mRNA) expression is a SSRI-dependent effect or a general antidepressant effect. A total of 25 male DBA/2J mice were treated for 28d with either vehicle (n=10) or reboxetine (n=15), a norepinephrine reuptake inhibitor (for details see 2.3). At the end of the treatment period, the animals were subjected to the dark-light box (DaLi) and the FST. Animals were sacrificed directly after the FST (Figure 9). Trunk blood and whole brains were collected and stored until further use (for details see 2.4).

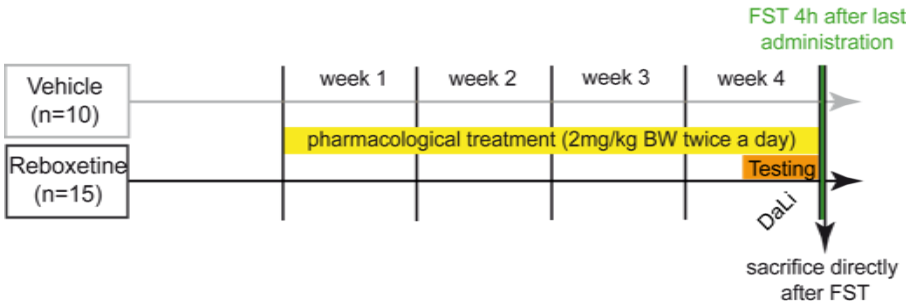

Figure 9: Overview of the experimental time course. DBA/2J mice were treated for 28d with either vehicle (n=10) or reboxetine (n=15). To characterize the behavioral effects of Reboxetine more detailed, the DaLi was used in addition to the FST. Animals were sacrificed directly after the FST.

2.2.3.2 Influence of Sox11 overexpression on antidepressant-like behavior

To provide a better insight into a putative function of Sox11 on emotional behavior, region-specific overexpression (OE) of Sox11 in the DG of the HC formation was achieved by using a recombinant adeno-associated virus (AAV) (Schmidt et al., 2011b) (methodological details can be found in chapter 2.8). AAV-Sox11OE (n=23) and AAV-empty (n=20) mice were generated through stereotaxic injection of the virus and allowed

to recover for 4 weeks from the surgery. This time interval ensured a sufficient transgene expression. As Sox11 was upregulated after 28d of paroxetine treatment the animals were tested another four weeks later (in total eight weeks after the surgery). This time frame was chosen to activate potential downstream pathways in the same way as the chronic antidepressant treatment. The behavioral testing battery included an open field test (OF), a FST, DaLi, novelty induced hypophagia (NIH) and a Y-Maze (Figure 10). Animals were sacrificed under basal conditions and perfused for immunohistochemical confirmation as well as ISH of Sox11 OE. Whole brains were collected and stored until further processing (for details see 2.4).

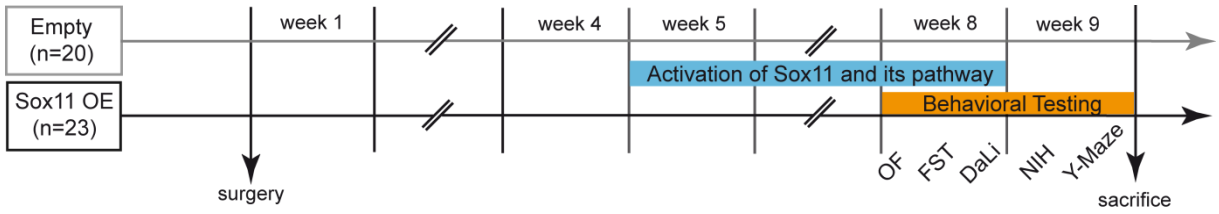

Figure 10: Overview of the experimental time course. Animals were randomly distributed to either AAV9 Sox11 OE or the AAV9 empty groups. After the surgery, the animals were allowed to recover for 4 weeks from the surgery. An upregulation of Sox11 was found after 28d of paroxetine treatment. To ensure that potential pathways will be activated due to the viral OE the animals were tested another 4 weeks later. The behavioral testing battery included an OF, FST, DaLi, NIH and a Y-Maze. Animals were sacrificed under basal conditions.

2.2.3.3 Sox11 OE and its influence on neurogenesis

We next asked whether an overexpression of Sox11 would also affect neurogenesis, thereby mimicking this known cellular antidepressant effect (Warner-Schmidt and Duman, 2006; Sahay and Hen, 2007). 23 male DBA/2J mice were injected with either an AAV9-Sox11 OE or AAV9-empty. Viral injection was performed in 12 - 13 weeks old DBA/2J male mice. 1µl of either AAV9-Sox11OE (n=12) or AAV9-emtpy (n=11) was injected bilaterally in the dorsal hippocampal DG region (for details see 2.8). After that, the animals were allowed to recover for four weeks from the surgery, which ensured a sufficient stable transgene expression. 5-bromo-2-deoxyuridine (BrdU) (Sigma Aldrich, Germany) was solved in 0.9% sodium chloride. Animals were then injected on three consecutive days with a 100mg/kg pulse. 16 animals (Sox11OE n=8; Empty control n=8) were perfused 2h after the last BrdU injection. This time point was used to investigate the proliferation rate of new DG cells as a readout of the viral overexpression of the Sox11. To investigate the maturation status of the new-born neurons (8 weeks after the surgery) 7 animals (Sox11OE n=4; Empty control n=3) were perfused 28d after the last BrdU injection.

Animals were perfused under basal conditions and whole brains were collected until further processing (for details see 2.4).

2.2.3.4 Sox11 knockdown in combination with paroxetine treatment and its influence on antidepressant-like behavior

To examine the effects of a Sox11 knockdown (KD) in combination with a chronic paroxetine treatment, viral injection was performed on 12 - 13 weeks old DBA/2J mice as previously reported (Schmidt et al., 2011b). AAV1/2-Sox11KD (n=35) and AAV1/2 scrambled (SCR) (n=34) mice were generated (for details see 2.8) and allowed to recover for 4 weeks from the surgery to ensure a sufficient transgene expression. Subsequently, the animals were randomly assigned to either a vehicle control or a paroxetine treated groups and treated for 28d with paroxetine or vehicle. The behavioral testing battery included an OF, DaLi, NIH and a FST (Figure 11). Animals were sacrificed under basal conditions and perfused for immunohistochemical confirmation as well as ISH to verify the Sox11 KD (for details see 2.7.8 and 2.7.9).

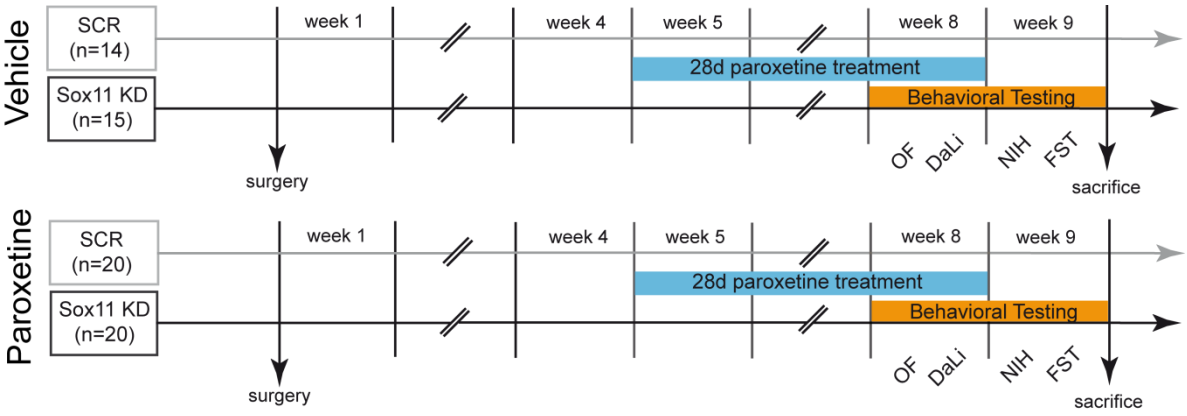

Figure 11: Overview of the experimental time course. Animals were randomly distributed to either AAV1/2 Sox11 KD or the AAV1/2 SCR groups. After the surgery, the animals were allowed to recover from the surgery for 4 weeks. Subsequently, the animals were either treated for 28d with paroxetine or vehicle. The behavioral testing battery included an OF, DaLi, NIH and a FST. Animals were sacrificed under basal conditions.

2.2.4 Detection of potential novel candidates after subchronic paroxetine treatment in the brain and periphery

In order to detect potential novel biomarkers mediating antidepressant response and to identify candidates modulating an early antidepressant response in particular, a shorter treatment period was used for this study. Therefore, 140 male DBA/2J mice were treated

with either 5mg/kg BW paroxetine (n=90) or vehicle (n=50) for 14d twice a day (for details see 2.3). At the beginning of the paroxetine treatment animals were at the age of 9 - 12 weeks. Subsequently, the animals were subjected to a FST and sacrificed directly after that. The animals were divided into good, intermediate and poor treatment responder according to their performance in the FST (for details see chapter 2.5) (Figure 12). Trunk blood and brains were taken at sacrifice and stored until further use (for details see 2.4).

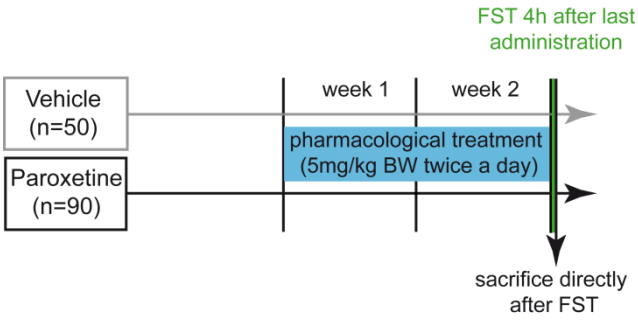

Figure 12: Overview of the experimental time course. Animals were randomly divided in vehicle and paroxetine treatment groups. Animals were treated with either 5mg/kg BW paroxetine or vehicle for 14d twice a day. Last drug administration was given to the animals on day 15 in the morning (6am). 4h later the animals were subjected to the FST and directly killed after the testing.

2.3 Antidepressant treatment

Paroxetine, a commonly used SSRI was chosen for the antidepressant treatment, with the exception of the reboxetine experiment (chapter 2.2.3.2). It could be demonstrated previously that DBA/2J mice are responsive to oral antidepressant treatment under basal and stress-free conditions (Sillaber et al., 2008; Sugimoto et al., 2011; Ohl et al., 2003; Yilmazer-Hanke et al., 2003). If not stated differently, paroxetine (Paroxetine hydrochloride; Sigma-Aldrich, Germany) or vehicle was (voluntarily self-) administered via customized palatable mouse pellets (40mg PQPellets, Phenoquest AG, Martinsried, Germany) with different concentrations of paroxetine. The animals were treated with 5mg/kg BW paroxetine or vehicle for 1, 14 or 28 days twice a day (8am and 6pm) with the exception of the dose finding experiment where the animals were treated with a concentration of 1mg/kg BW (see 2.2.1.1). Body weight was assessed twice a week and according to the animal's body weight, each mouse was assigned to different treatment categories to ensure the right dosage for each animal (Table 1). On the last day of treatment, the last dosage was administered at 6am, 4h prior the behavioral testing in order to avoid acute treatment effects. For chapter 2.2.3.2 Reboxetine was used for the antidepressant treatment. Animals were treated twice a day (8am and 6pm) with 2mg/kg

BW reboxetine or vehicle for 28 days. Administration procedure was performed in the same way as stated for the paroxetine treatments.

Table 1: Paroxetine and reboxetine treatment categories according to the animal's body weight. Body weight was assessed twice a week. Animals were assigned to the respective treatment categories according to their body weight.

Treatment category	Body weight
Category I	19 - 22g
Category II	23 - 25g
Category III	26 - 28g
Category IV	29 - 31g
Category V	31 - 35g

The consumption of the palatable mouse pellets was monitored after every administration. Animals that did not consume the pellets were excluded from the analysis (on average 10% of the animals).

2.4 Sampling procedure

Before sacrificing the animals, they were anesthetized with isoflurane (Abbott GmbH & Co. KG, Germany) and decapitated. Trunk blood was collected in 1.5ml EDTA-coated microcentrifuge tubes (Kabe Labortechnik, Germany) or PCR-clean 1.5ml tubes filled with 966µl PAXgene™ solution (ribonucleic acid (RNA) stabilizer reagent) (for detailed information see chapters 2.2.4 and 2.7.3.1). All blood samples were immediately placed on ice and centrifuged at 8000rpm for 15min at 4°C. Plasma was transferred to clean 1.5ml microcentrifuge tubes and stored at -20°C until further processing. If not stated differently, the animals were sacrificed directly after the FST in order to avoid potential alterations in gene expression levels.

Whole brains were removed and if the left hippocampal formation was extracted (chapter 2.2.2 and 2.2.4) it was done on ice. The rest of this hemisphere was used for the measurement of paroxetine brain tissue concentration. The other hemisphere was collected for ISH. Whole brains or dissected brain tissues were immediately snap-frozen in pre-cooled 2-methylbutane (Carl Roth GmbH, Germany) and stored at -80°C. For immunohistochemistry, animals were deeply anesthetized with isoflurane and slowly perfused intracardially with 0.9% saline followed by 4% paraformaldehyde. Brains were post-fixed overnight in 4% paraformaldehyde followed by 3 nights incubation in 20% sucrose solution at 4°C and then stored at –80°C.

2.5 Modeling antidepressant response in mice with the FST

A large heterogeneity in antidepressant treatment outcome is known from the clinical situation. To-date, there are no common approaches to investigate individual antidepressant response in mice. Therefore, we raised the question whether the heterogeneity in antidepressant treatment outcome can in general be modeled in mice in general. We hypothesized that we can modulate this large heterogeneity within a large experimental group (Figure 13), and thus mimicking the clinical situation. According to the animals' performance in the FST, the animals were divided into good, intermediate and poor treatment responders. Animals with a high time floating (top 20%) were classified as poor treatment responders, whereas animals that showed a very low time floating (bottom 20%) were characterized as good treatment responders. Animals that performed like the average of the paroxetine treated animals were defined as intermediate treatment responders. The animals that performed around the mean of the vehicle treated group were used as the non-treated control group. According to the literature, the treatment duration seems to play an important role in the clinical situation. Many patients show a delayed onset of antidepressant response and most of them do not start responding earlier than 3 - 4 weeks after the beginning of the treatment (Taylor et al., 2006). However, a minority of patients already show an antidepressant response after 2 weeks of antidepressant treatment (so-called "early responder") (Papakostas et al., 2006). These clinically relevant time points were considered in this mouse model approach, i.e. a chronic antidepressant treatment (28d) and a subchronic antidepressant treatment (14d), the latter representing an early antidepressant response. To further mimic the clinical situation, the animals were dosed with paroxetine via customized mouse pellets.

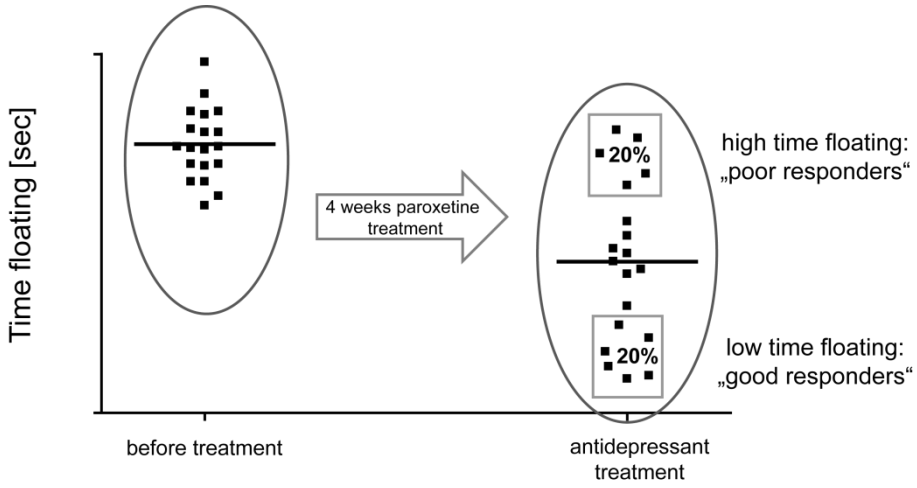

Figure 13: Illustration of the heterogeneity in the FST of mice. Illustration of the heterogeneity in the FST of mice after 4 weeks of antidepressant treatment. This figure illustrates our hypothesis stating that if a large number of animals is treated with an antidepressant, in this case paroxetine, the animals will respond differently in the FST. Although all of them were treated the same this would postulate that not all of the animals will respond equally to the treatment.

2.6 Behavioral testing

In this study, various behavioral tests were performed. Tests were accomplished in a separate room in which the mice were housed during the testing period. Animals were allowed to habituate to the testing room for at least 7 days prior the testing. Housing conditions were the same as described for standard housing (see 2.1). All tests were performed during the light phase, between 7am and 12am to avoid potential behavioral alterations due to circadian variation of corticosterone levels (Barriga et al., 2001). All tests were recorded and analyzed (either automatically or manually) with the automated video tracking system ANY-maze (ANY-maze 4.5; Stoelting Co., Wood Dale, USA).

2.6.1 Open field test

The OF is used to investigate general and basic locomotion of the experimental animal (Crawley, 1985). Furthermore, the OF can also be used to screen anxiety related behavior in mice. The OF consists of square, enclosed arena (50 x 50 x 50cm) made of gray polyvinyl chloride (PVC). For the analysis, the area was virtually divided into a center zone (20 x 20cm), which was illuminated with 20lux and an outer zone illuminated with approximately 16lux. Animals were placed in the lower left corner of the apparatus at the beginning of the testing. The total test duration was 15min. The OF arena was cleaned thoroughly with tap water and dried after each animal. The main readout parameters in

this test were the preference of the inner zone (analyzed via entries, time, distance) as well as total distance traveled.

2.6.2 Dark-light box

As the DaLi is based on the conflict of spontaneous explorative behavior in a novel environment and the natural aversion of mice to avoid highly illuminated areas, it is a common test to investigate anxiety-related behavior in mice (Hascoet et al., 2001). The apparatus consists of a small, secure and dark compartment (15 x 20 x 25cm, with dimmed light condition < 10lux) and a larger, aversive and brightly illuminated compartment (30 x 20 x 25cm, brightly lit with 600lux), which are connected by a 4cm long tunnel. Animals were placed in the lower left corner of the dark chamber at the beginning of a 10min testing period. The DaLi was cleaned thoroughly with tap water and dried after each animal. The main readout parameter in this test was the preference of the light compartment (analyzed via latency to enter, total entries, total time, total distance in the lit compartment).

2.6.3 Novelty induced hypophagia

As the NIH is based on the conflict of the desire of a highly palatable food and the natural aversion of mice to avoid highly illuminated areas, it is a common test to investigate anxiety-related behavior in mice (Dulawa and Hen, 2005). The apparatus consists of a highly illuminated (600 - 1000lux) empty polycarbonate cage (21 x 15 x 14cm) located on a white surface to increase the aversiveness. The test comprises three days of habituation and two testing days. During the habituation period, the 30% sweetened condensed milk was presented to the mice in their home cage for 30min. Consumption was monitored, animals that did not consume any condensed milk during the habituation period were excluded from the analysis (less than 1%). On the first testing day, the sweetened condensed milk was presented to the animals in their home cage for 30min. Latency to consume as well as the amount was recorded. Animals that did not consume any condensed milk or with a latency of at least 300s were excluded from the analysis (less than 1%). On the second day, the mice were placed in the aversive environment for 30min, again with the highly palatable food. Latency to consume and the total consumption of the condensed milk was measured at the end of the testing period.

2.6.4 Y-Maze

The Y-maze test is a common test to investigate hippocampus-dependent spatial memory (Dellu et al., 2000; Dellu et al., 1992). The apparatus consisted of three arms (30 x 10 x 15cm), made of gray PVC, which were arranged in an angle of 120° between two arms. This Y-shaped apparatus consisted of three separate zones all connected by a center zone. The whole apparatus was evenly illuminated with 15lux to avoid preferences based on illumination levels. Each arm was marked differently by easily recognizable symbols (triangle, bar and plus-sign). The testing comprises two different trials. During the first trial, the acquisition phase, one arm was completely blocked by a gray PVC wall. The mouse was placed in the center zone and was allowed to explore the two accessible arms freely for 10 minutes before returning to the home cage. After an intertrial interval of 30min mice were re-introduced to the apparatus facing one of the already known arms. During this retrieval phase (5min), all three arms were accessible. An indicator for spatial memory performance was the percentage of time spent in the novel arm compared to the familiar arms. Significantly higher percentage than chance level (33.3%) was rated as successful spatial memory.

2.6.5 The Forced Swim Test

The FST is a common test to model behavioral despair and antidepressant-like behavior in rodents (Porsolt et al., 1977a; Porsolt et al., 1977b). It is still the most commonly used test paradigm for screening antidepressant action of compounds. A glass beaker (height 24cm, diameter 13cm) was filled with 21 ± 1°C water up to a height of 15cm, that the animal is not able to touch the ground or escape the situation. The animals were gently placed in the glass beaker for 5 minutes testing period. After this period, the animals were removed, dried and placed back into their home cage. Parameters of interest were time swimming, time floating and time struggling.

2.7 Molecular methods

2.7.1 Radioimmunoassay

Radioimmunoassay (RIA) was performed with a commercially available double antibody kit with a sensitivity of 6.25ng/ml (ImmunoChemTM Double AntibodyCorticosterone 125I RIA Kit, MP Biomedicals, USA) according to manufacturers' manual in order to analyze corticosterone concentrations in the plasma of the animals.

2.7.2 Paroxetine concentrations in the brain and plasma

Paroxetine was extracted out of mouse blood or brain according to Uhr et al. (Uhr et al., 2003). In short, to analyze paroxetine concentrations in the homogenized samples, the high-performance liquid chromatography (HPLC) analysis was used. A mobile phase gradient was used for the chromatographic analysis of paroxetine and its metabolites. The substances and its metabolites were determined by UV absorption or fluorescence at the described wavelength. The coefficient of variance was less than 15% for the different methods used. To avoid differences due to day-to-day variability, experimental procedure, extraction procedure and HPLC were carried out in alternating order (Uhr et al., 2003). Plasma and brain samples were calibrated by using spiked samples at different concentrations. The concentrations were in the measurement range to the respective substances. Quantification was performed by calculating the analyte: internal-standard peak-area ratio, and a regression model was fitted to the peak-area ratio of each compound to internal standard versus concentration (Uhr et al., 2003).

2.7.3 RNA isolation

2.7.3.1 Whole blood

RNA isolation out of blood was performed with blood samples originating from the experiments described in chapter 2.2.4. Trunk blood was collected individually in 1.5ml tubes. The blood was further processed according to the PAXgene™ blood miRNA Kit. 350µl of this freshly collected trunk blood was immediately transferred into 1.5ml tubes filled with 966µl PAXgene™ solution (RNA stabilizer reagent), gently inverted 10 times and then incubated at RT for 2 – 24 hours and stored at -20°C before RNA isolation (Krawiec et al., 2009). Volume ratio of RNA stabilizer reagent to blood samples was kept at 2.76 according to the manufacturer's protocol. RNA was isolated according to Krawiec and colleagues (Krawiec et al., 2009). Shortly, frozen samples were brought to room temperature for 45min, then inverted several times and then centrifuged at 5000 x g for 10min at 22°C. The supernatant were aspirated and the pellet was resuspended in 0.5ml of RNase-free water by vortexing until the pellets were visibly dissolved. All following steps were conducted according to the manufacturers' manual with the exception that proteinase K digestion at 55°C was performed for 60min at 700rpm/min on an Eppendorf shaker. The remaining trunk blood of each animal was collected in labeled 1.5ml EDTA-coated microcentrifuge tubes (Kabe Labortechnik, Germany).

2.7.3.2 Whole blood RNA globin reduction

Blood consists of a heterogeneous cell population of erythrocytes, granulocytes, and other peripheral mononuclear cells (PBMC) (Rainen et al., 2002). Due to this heterogeneity it is difficult to detect differences in gene expression levels. Blood itself contains a high amount of globin mRNA transcripts, which might mask differences in other mRNA transcripts. Therefore, we used the Ambion® GLOBINclear™-Mouse/Rat Kit after the RNA isolation. Globin reduction was performed according to the manufactures manual. Input RNA was quantified before the Globin reduction with a Nanodrop. This globin reduced RNA was then further processed, amplified and then used for microarray experiments.

Globin-depleted total RNA was quantified with a Nanophotometer (Nanodrop 2000, Fisher Scientific) and quantified and quality-controlled by capillary gel electrophoresis (2100 Bionanalyzer, Agilent; RNA 6000 nano Assay). The obtained RNA integrity numbers (RIN) were greater than 7.5 in all total RNA samples derived from blood before globin depletion and dropped slightly after globin depletion (RIN > 6.3 for all samples that were further analyzed).

2.7.3.3 Hippocampus

RNA isolation out of the left HC was performed with samples originated from the experiments described in chapter 2.2.2 and 2.2.4. Hippocampal RNA was isolated using the TRIZOL reagent (Invitrogen) as described previously (Schmidt et al., 2010), except that the tissue was homogenized with syringes. For RNA quality and integrity analysis Agilent 2100 Bioanalyzer (Agilent Technologies, Inc., Waldbronn, Germany) as well as RNA Nano LabChips (Agilent Technologies, Inc., Waldbronn, Germany) were used. The measurements were performed according to manufacturers' protocol. Among other parameters, the 28S:18S ratio of the RNA bands, was analyzed and should lie about 2.0. The Agilent software is able to calculate the RIN of the sample by using the 28S:18S ratio and other features. Samples with a RIN < 7.0 were excluded from the analysis (less than 5%).

2.7.4 RNA amplification

Globin-depleted RNA as well as hippocampal RNA were labeled and linearly amplified to complementary RNA (cRNA) in a commercial form of the classical procedure by Eberwine

(Van Gelder et al., 1990). 250ng of RNA was used as input for the Illumina® TotalPrep™-96 RNA Amplification Kit (Life technologies) and sample processing was performed according to the manufacturers' protocol. RNA was again quantified and quality checked as performed with total RNA. All samples underwent photometric analysis (Epoch Spectrophotometer with Take3 Trio Micro-Volume Plate, BioTek Instruments GmbH) and a selected cross section of the samples has been additionally checked on the Bioanalyzer.

2.7.5 cDNA transcription

The VILOSuperScript Kit (Life Techologies) was used for the transcription of RNA to complementary DNA (cDNA) for the quantitative reverse transcription polymerase chain reaction (qRT-PCR). The transcription was performed according to the manufacturers' protocol. Thereafter, samples were loaded into a thermal cycler, using the protocol indicated in the manufacturers' manual. Transcribed cDNA was then stored at -80°C until further use.

2.7.6 Microarray analysis

For transcriptome analysis the MouseWG-6 v2.0 BeadChips (Illumina Inc.) were used, allowing the identification of about 45.281 gene-sequences (50mer oligonucleotides). The preparation of the samples for the microarray chips was done according the Illumina protocols. Chips were analyzed using the BEADARRAY package (www.bioconductor.org) with additional required packages. The animals for the microarray study were part of the cohort described in chapter 2.2.2 (poor responders n=13; intermediate responders n=8; good responders n=12; vehicle n=9) and 2.2.4 (poor responders n=12; intermediate responders n=8; good responders n=12; vehicle n=12) and selected according their behavioral performance in the FST and RNA quality.

The animals selected for the blood microarray were the same animals as used for the brain microarray (for details see 2.2.4) except of the intermediate responder group, which was not included in this analysis.

2.7.7 Quantitative reverse transcription PCR

In order to investigate differences in gene expression levels, quantitative reverse transcription PCR (qRT-PCR) was used. 1µl of each cDNA was analyzed with the Nanodrop, for quality control. cDNA originated from the same samples as the microarray

samples (for details see chapter 2.2.2 and 2.2.4) and were analyzed by qRT-PCR, using the QuantiFast SYBR Green PCR Kit (Qiagen GmbH, Hilden, Germany) according to the manufacturers' instructions. Experiments were performed in duplicates with the Lightcycler 2.0 instrument (Roche Diagnostics, Mannheim, Germany) under the following PCR conditions: initial denaturation at 95°C for 10min, followed by 40 cycles of denaturation (95°C for 10sec) and a combined annealing and extension phase (60°C for 30sec). At the end of every run, a melting curve (50 – 95°C with 0.1°C s^{-1}) was generated to ensure the quality of the PCR product. Experimental analyses were performed on the crossing points, which were calculated by the LightCycler Software 4.0 (Roche Diagnostics GmbH) using the absolute quantification fit point method. Noise band and threshold were set to the same level in all compared runs. Relative gene expression was determined by the $2^{-\Delta\Delta CT}$ method (Livak and Schmittgen, 2001) using the real PCR efficiency calculated from an external standard curve. Crossing points were normalized to the housekeeping gene Hprt. All measurements were normalized to vehicle (vehicle being 1) or poor treatment responders (poor treatment responders being 1) to provide relative expression levels. Primers were designed with the free-online tool Primer3Plus (Rozen and Skaletsky, 2000). Detailed information for the primer used in this experiment can be found in Table 2 and Table 3.

Table 2: Primers used for quantitative reverse transcriptase PCR in hippocampal brain tissue. The left column indicates the most common used symbols in public databases. The middle and right columns indicate the sequences of the forward and reversed primers used in the validation experiment. They are represented here in 5' to 3' direction.

Symbol	Forward Primer	Reverse Primer
Acvr1c	TCAGACGGTGATGCTGAGAC	GAGCCCTGCTCGTGATACTC
Adra2c	TACTGTGCTGGTTCCCCTTC	GGATCGGCTACTGCAACAGT
Arsj	AGCCTGCTCACCTATGGCTA	GTGCCTGCTTCAGGTCTCTC
Bgn	GACAACCGTATCCGCAAAGT	CCTGGTTCAAAGCCACTGTT
C1ql2	GCAATCACTACGACCCCACT	CCACGCATGAGAATGTGGTA
Cd9	TGTCTCAGTCGGTTGTCGAG	GGCATGGTACAAGCTGGAGT
Cort	AAAACCTTCTCCTCGTGCAA	ATTCAGGTCTCGTTGGCATC
Cxcl12	CCAACGTCAAGCATCTGAAA	TGTGCATTGACCCGAAATTA
Drd1a	GGCATACCTAAGCCACTGGA	GGGTAACGGGTTGGATCTTT
Gfap	ACCAAATCCGTGTCAGAAGG	CTCACATCACCACGTCCTTG
Igfbp6	CAGAGACCGGCAGAAGAATC	AGGGGCCCATCTCACTATCT
Il16	TCACCTTGCAACAACAGCTC	GGGCTCTGTGAGACCTTCTG
Mylk	GCTGTGAGAGGAACCAAAGC	TCTGGGGACTTGGACAGTTC
Ntf3	TGCAACGGACACAGAGCTAC	TGCCCACATAATCCTCCATT
Pnck	TCTTTGGATCTCTGGGGATG	CCTGGCAAAATTCTTCTGGA
Ptpn21	GCCACCACAGGTTTGAAGAT	CTTTGAGGTCTTCGGGACAG
Serpina3n	CAATCGGCCTTTCCTGATAA	GTCTCATTTGGGGTTGGCTA
Serpinf1	AACGTCCTGCTGTCTCCACT	GTAGAGAGCCCGGTGAATGA
Slc14a1	TTCTGGTGGGACTTCTGGTC	AAGAGGGCTGTCAGAGTGGA
Sox11	TCATGTTCGACCTGAGCTTG	TCCAGGTCCTTATCCACCAG
Stat3	CGGAGAAGCATTGTGAGTGA	CTTCCAGTCAGCCAGCTCTT
Trpc6	TCGAGTTGGGGATGCTTTAC	CGCTAACCTTTTGCCTTCAG
Vim	TGAAGGAAGAGATGGCTCGT	TCCAGCAGCTTCCTGTAGGT
Wisp	CCCCTACAAGTCCAAGACCA	AGGTTGCAGAAGCAAGCATT

Table 3: Primers used for quantitative reverse transcriptase PCR in peripheral blood. The left column indicates the common used symbols in public databases. The middle and right columns indicate the sequences of the forward and reversed primers used in the validation experiment. They are represented here in 5' to 3' direction.

Symbol	Forward Primer	Reverse Primer
Axol12	ACCACTCCCTCTGTCCTCCT	CCCTTCACATACCTGGCAGT
Chchd1	GATTGTTCTTCCAGGGCTCA	TGGTCATCTTGTGGGGAGAT
Peli	GTGATGCATCCACGTAATGG	TGAGCTGATCTGGTTTCACG
Add1	AGCCCCATGTAATTGTGAGC	TCCACCTCTCGTCGGTATTC
Tomm7	GCAAAGAAGCCAAACAGAGG	GGATCTGCACCCCTTGTAAA
Smim11	TATATCCTGGCGGCAAAAAC	CTGCTTGCAGTTTTCCTTCC
Pdpk1	CTCACAGAAGGGCCACATTT	GCTTCTGGTCGGAGTTCTTG
Sp4	GGAGGTGGGACAGCTCTTGC	ATTCGAATCTTGGGAAATGG
Napa	GCCAACAAGTGTCTGCTGAA	CCCCACCTGCTCATAGATGT
P2RX1	ACTGGGAGTGTGACCTGGAC	CAGGTTCTTCTCCCCGTACA
Sdcbp1	TGACAGGTAACGATGCTGGA	GCCCAATTTTTCCATCTTGA
Elf1	AACCCTCACAGGCTCCCTAT	TGGCTATGGTTGCTTCCTCT
Mapk3	CGGCTGAAGGAGTTGATCTT	CAGGACCAGATCCAAAAGGA
Ddrx12	AAGGGCCTTCTGAGGATGAT	GGGGCTCCTTTTTCTTCTTG
Fbxl6	TGGCATATCTGATGGCTTGA	ACTGAAGTCCAGCTCCCTCA
Rpl13a	CACTCTGGAGGAGAAACGGAAGG	GCAGGCATGAGGCAAACAGTC
Hprt	ACCTCTCGAAGTGTTGGATACAGG	CTTGCGCTCATCTTAGGCTTTG

2.7.8 *In situ* hybridization

Frozen brains were sectioned at -20°C in a cryostat microtome at 18µm, thaw mounted on Super Frost Plus slides, dried and stored at -80°C. ISH using a ^{35}S UTP labeled ribonucleotide probe for Sox11 (Forward primer: TCATGTTCGACCTGAGCTTG; Reverse primer: CACGATAAAGGACGGGAAGA; transcript size: 480 nucleotides) was performed as described previously (Schmidt et al., 2007). The slides were exposed to Kodak Biomax MR films (Eastman Kodak Co., Rochester, NY) and developed following 6d of exposure. Autoradiographs were digitized, and expression was determined by optical densitometry utilizing the freely available NIH ImageJ software. The mean of two measurements of two

different brain slices were calculated for each animal. The data was analyzed blindly, always subtracting the background signal of a nearby structure not expressing the gene of interest from the measurements.

2.7.9 Immunohistochemistry and immunostaining

Immunohistochemistry was used to quantify AAV-Sox11-induced protein expression. Serial coronal sections were cut at 25µm thickness at -20°C. Double-labeling immunofluorescence (Goat-anti-Sox11, 1:250, Santa Cruz, C-20; donkey-anti-goat 555, 1:500, Alexa) was performed on free-floating sections (Sox11 OE n=8; Empty n=8) as described previously (Wang et al., 2013).

BrdU and NeuN immunostaining was performed by Lie and his colleagues according to a previously published paper (Garrett et al., 2012).

2.8 Stereotactic surgery

To provide a better insight into a putative function of Sox11 in the brain, a region-specific overexpression and knockdown of Sox11 in the dorsal DG was achieved by using a recombinant AAV.

2.8.1 Viral vector construct

Viral overexpression of Sox11 was performed as described previously (Schmidt et al., 2011b). A custom-made AAV9 vector (preparation according to previously published protocols (Foust et al., 2009; Mu et al., 2012a)) was used for this experiment (kindly provided by Chichung D. Lie from the University of Erlangen). For the viral knockdown of Sox11 an AAV1/2 vector was used (GeneDetect, New Zealand) containing the U6--Mouse Sox11 2x shRNA--terminator-CAG-EGFP-WPRE-BGH-polyA. The same vector was used for the control groups (SCR group), expressing only EGFP (U6--GeneDetect SCR 2x shRNA--terminator-CAG-EGFP-WPRE-BGH-polyA).

2.8.2 Stereotactic intra-hippocampal injection

Viral injection was performed according to Monory (Monory et al., 2006). In short, animals were deeply anesthetized with isoflurane (Curamed Pharma GmbH, Germany) and inserted into a stereotactic frame (TSE system GmbH, Germany). The skull was exposed and holes were drilled bilaterally at the injection sites, targeting the dorsal DG of the HC

(1.6mm posterior to bregma, 1.3mm lateral from midline, and 1.7mm below the surface of the skull). 1µl of the corresponding virus (Titers: > 1.2 × 1012 genomic particles/ml) was injected at 0.06µl/min by glass capillaries with tip resistance of 2 - 4MΩ. To avoid reflux, class capillaries were removed five minutes after the injection. The wound was sutured and treated with iodine. The mice were treated after the surgery for 5 days with Metacam® via drinking water.

2.9 Statistics

The data presented are shown as means + standard error of the mean, analyzed by the commercially available software SPSS 16.0. For comparing two independent groups (e.g. vehicle versus paroxetine), data were analyzed with two-tailed, independent samples Student's t-test. For the calculation of the mortality rate, the Fisher's exact test was used. Therefore, the data was uploaded to the free online calculator tool (www.langsrud.com/fisher.htm) and significant level was calculated by generating a 2 x 2 contingency table. For variables with more than two groups, one-way ANOVA was performed followed by Bonferroni post-hoc testing. For more complex datasets (2 x 2 design; e.g. chapter 2.2.3.4), 2-way ANOVA was used. Correlations were analyzed with a two-tailed, bivariate Pearson's correlation analysis. As nominal level of significance $p < 0.05$ was accepted, a trend was recognized at $p \leq 0.1$. Values outside the 95% confidence interval (CI) were defined as statistical outliers and excluded from the analyses.

3 Results

3.1 Antidepressant response in mice - methodological considerations

In order to validate the novel experimental approach, which aimed to investigate antidepressant response in mice, some important questions were raised in the beginning.

3.1.1 Dosing

To identify the minimum effective dosage for the DBA/2J mouse strain, male mice were randomly distributed to either the vehicle or paroxetine experimental group and were treated with different concentrations of paroxetine.

Trial 1: 1mg/kg BW (twice a day)

To investigate, whether a very low dose of paroxetine is sufficient to evoke an adequate behavioral and pharmacological effect, animals were treated with 1mg/kg BW paroxetine (n=30) or vehicle (n=11) for 28 days twice a day (8am and 6pm) and killed on day 29 directly after the FST (Figure 14A).

Clinical studies have reported alterations in body weight gain following antidepressant treatment (Pijl and Meinders, 1996; Vanina et al., 2002), and therefore we also investigated this parameter in our experiment. 28d of paroxetine treatment (1mg/kg BW) led to a significant increase in body weight gain in the paroxetine treated animals compared to the vehicle treated animals ($T_{39} = -2.490$, $p < 0.05$) (Figure 14B). To analyze the effects of a 1mg/kg chronic paroxetine administration on a neuroendocrine level, we examined corticosterone levels and did not detect any significant difference between vehicle and paroxetine treated animals (Figure 14C). This low paroxetine dosage seems to influence physiological parameters, like body weight gain, but was not able to evoke a treatment effect on a neuroendocrine level.

As the FST is the main readout parameter to investigate antidepressant treatment response in this model, we analyzed the animals' performance in the FST after 28d of antidepressant treatment. Paroxetine treated animals showed a tendency in a lower time floating compared to vehicle treated animals ($T_{39} = 1.979$, $p = 0.55$) (Figure 14D), but neither time swimming nor time struggling was significantly different between the groups (Figure 14E).

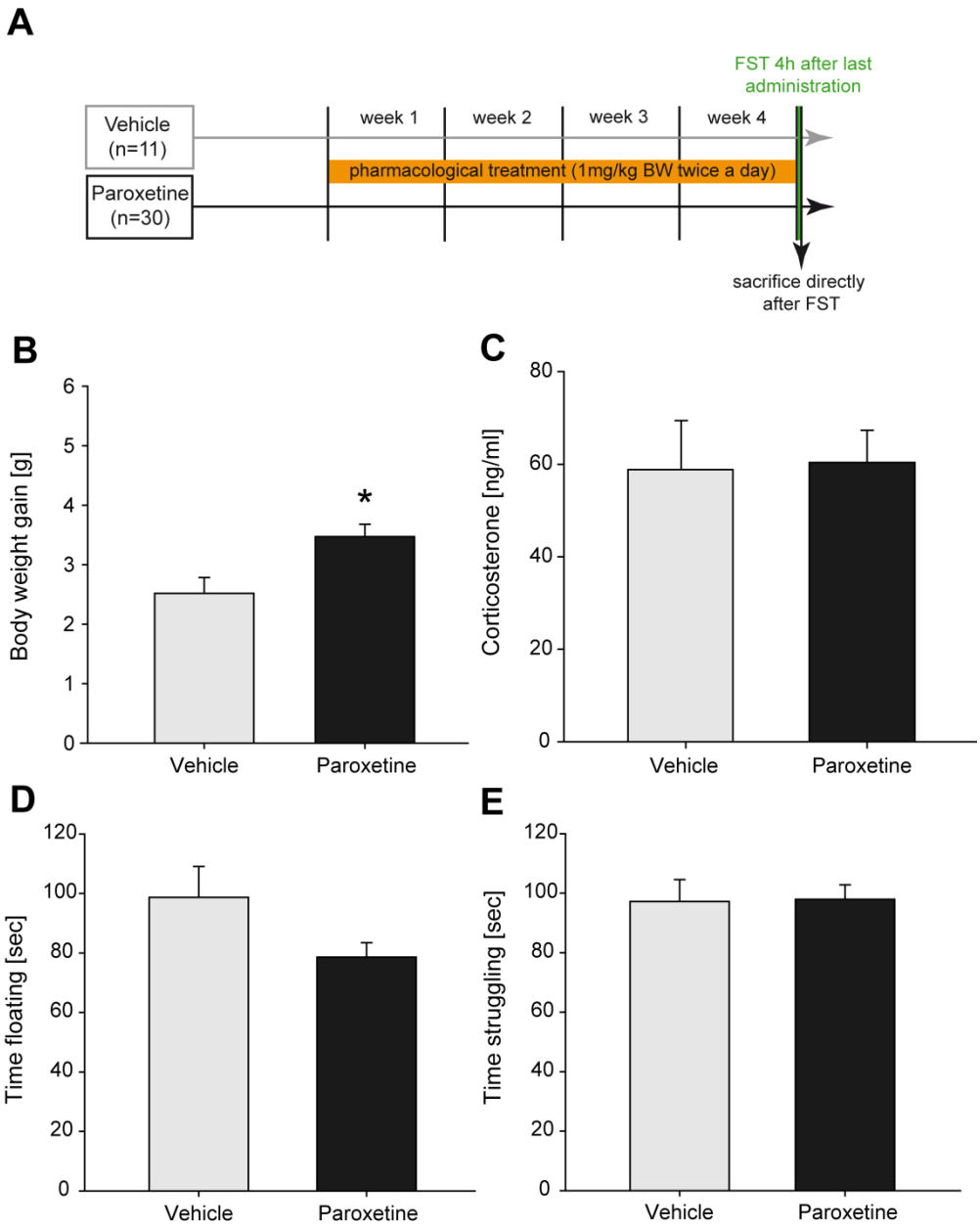

Figure 14: Neuroendocrine, physiological and behavioral parameters from the dosing experiment (1mg/kg BW). (A) Experimental time course of the study. (B) 28d of 1mg/kg BW paroxetine treatment led to an increase in body weight gain in the paroxetine treated animals. (C) Corticosterone levels were not altered due to the treatment. (D) Paroxetine treatment led to a trend in reduced time floating in the treated animals compared to the control group. (E) Chronic treatment did not alter the time struggling in the paroxetine treated group. * significant correlation, $p < 0.05$.

To get a detailed picture of the pharmacological profile of the antidepressant drug in the mouse, paroxetine levels were measured in the brain and the plasma of the treated animals. The animals were split up by the median in two groups according to their performance in the FST. No significant difference was found in paroxetine plasma concentrations within the compared groups (Figure 15A). When investigating the brain

paroxetine levels, no significant difference was detected among the two different behavioral groups (Figure 15B). However, paroxetine brain and plasma concentrations were highly correlated ($r = 0.869$, $p < 0.000$) (Figure 15C).

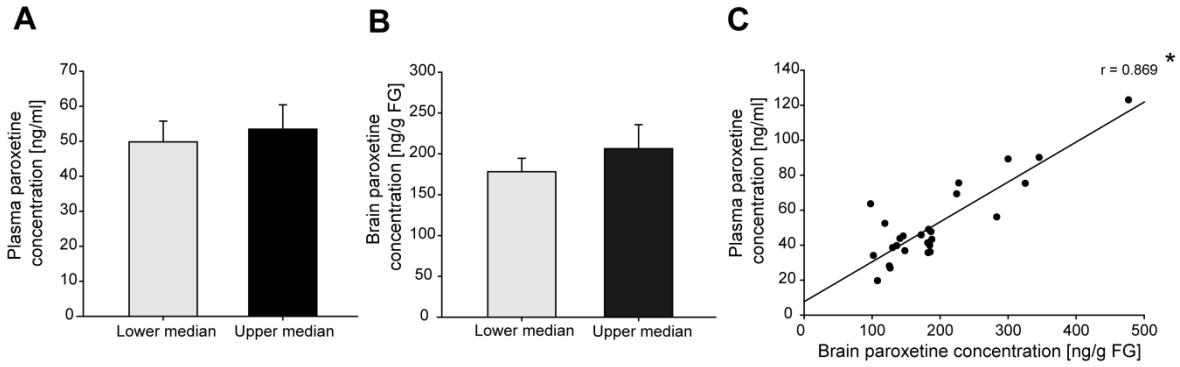

Figure 15: Pharmacological profile of 1mg/kg BW in the mouse brain and periphery. (A) Chronic paroxetine treatment did not change plasma paroxetine concentrations in the upper median group compared to the lower median group. (B) No effect was found in the brain paroxetine concentration among the groups. (C) Higher brain concentrations of paroxetine were accompanied by higher plasma paroxetine concentrations. * significant correlation, $p < 0.05$.

To summarize, we can conclude that 1mg/kg BW was an insufficient dosage to evoke robust behavioral treatment effects in our experimental model.

Trial 2: 5mg/kg BW (twice a day)

As the lower paroxetine concentration did not evoke the intended behavioral phenotype, another paroxetine concentration was tested in male DBA/2J mice. This time, 158 mice were treated with 5mg/kg BW paroxetine (n=100) or vehicle (n=58) for 28d twice a day (8am and 6pm) and were killed on day 29 directly after the FST (Figure 16A). To investigate the effects of the higher paroxetine dosage on physiological parameters, the body weight was assessed in these animals. 28d of paroxetine treatment (5mg/kg BW) led to a significant increase in body weight gain in the paroxetine treated animals compared to the vehicle treated animals ($T_{148.587} = -11.263$, $p < 0.000$) (Figure 16B). The higher paroxetine dosage was also able to evoke a significant reduction in stress-induced circulating corticosterone levels. Paroxetine treated animals showed lower corticosterone levels compared to the vehicle treated control group ($T_{143} = 2.129$, $p < 0.05$) (Figure 16C).

Regarding the behavioral readout of the higher paroxetine dosage, chronic treatment significantly reduced the time floating in the paroxetine treated animals compared to the

vehicle treated group (T_{143} = 9.986, p < 0.000) (Figure 16D). Additionally, paroxetine treated animals showed a significantly higher level of active behavior compared to the vehicle treated animals (Time swimming: T_{143} = -2.633, p < 0.01, vehicle: 105.59sec ± 4.70; paroxetine: 119.71sec ± 3.70; Time struggling: $T_{140.984}$ = -7.820, p < 0.000 (Figure 16E)).

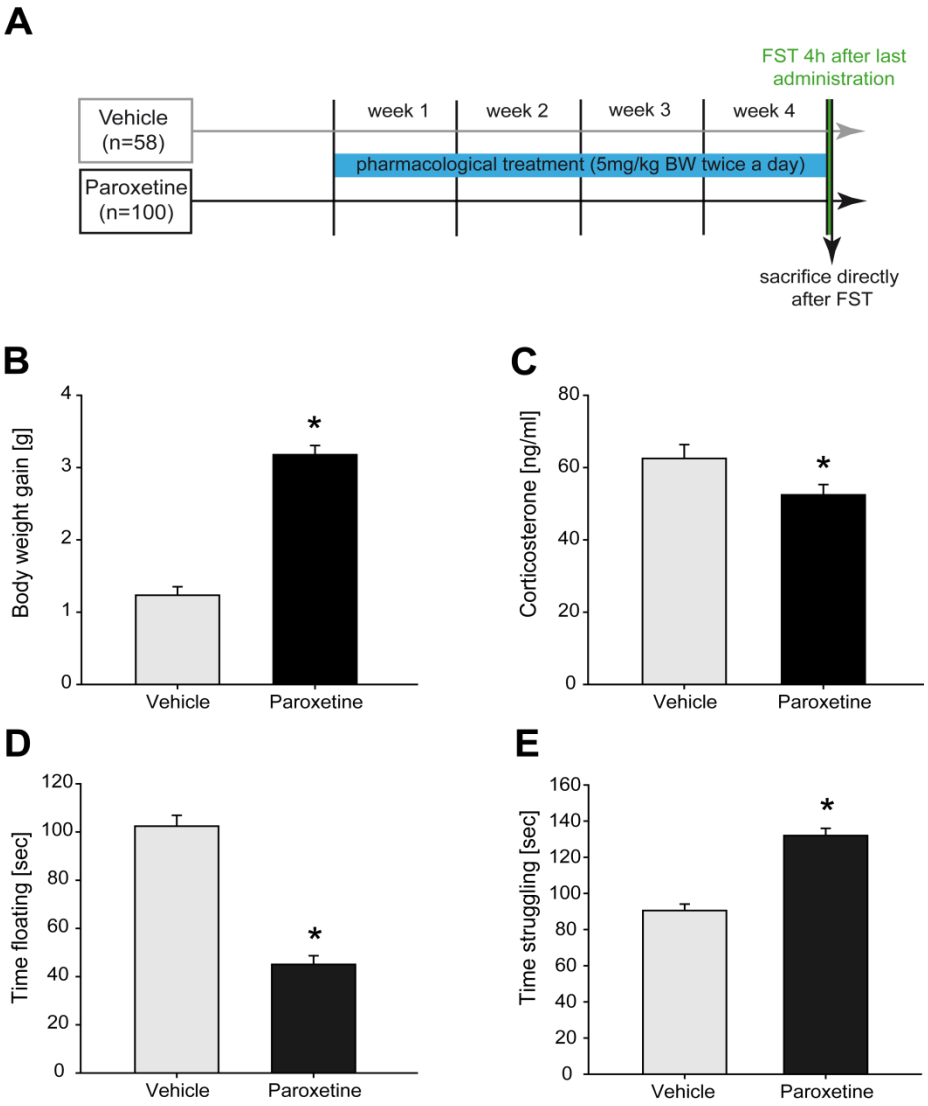

Figure 16: Neuroendocrine, physiological and behavioral parameters from dosing experiment (5mg/kg BW). (A) Experimental time course of the study. (B) 28d of 5mg/kg BW paroxetine treatment led to a significant increase in body weight gain in the paroxetine treated animals. (C) Corticosterone levels were significantly reduced in the paroxetine treated animals. (D) Paroxetine treatment led to a significant decrease in time floating in the treated animals compared to the control group. (E) Chronic treatment significantly increased the time struggling in the paroxetine treated group. * significant correlation, p < 0.05.

After 28d of antidepressant treatment, paroxetine levels were measured in the brain and the plasma of the paroxetine treated animals. No significant difference was found in

paroxetine plasma concentrations (Figure 17A) or paroxetine brain concentrations (Figure 17B) between the different responder groups after 28d of paroxetine treatment. However, we could show again a correlation between paroxetine brain and plasma concentrations ($r = 0.905$, $p < 0.000$) (Figure 17C).

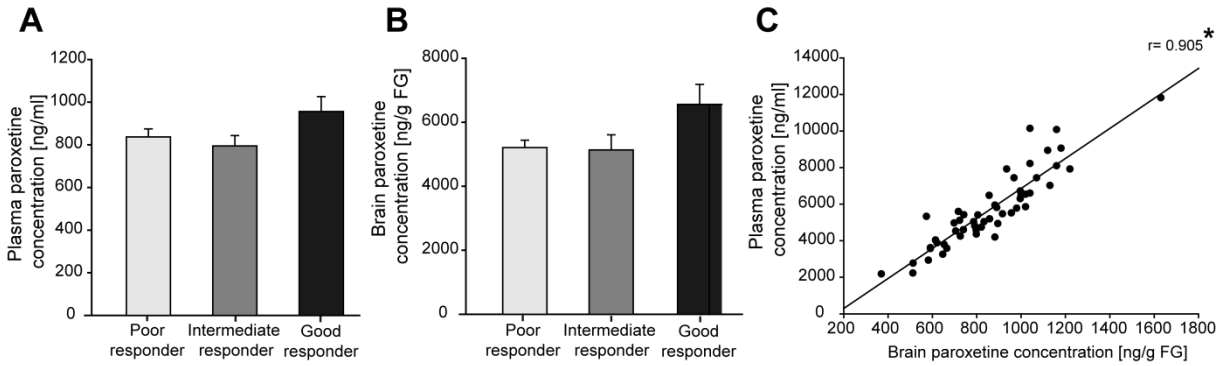

Figure 17: Pharmacological profile of 5mg/kg BW in the mouse brain and periphery. (A) Chronic paroxetine treatment did not change plasma paroxetine concentrations between the behavioral groups. (B) No effect was found in the brain paroxetine concentration among the groups. (C) Higher brain concentrations of paroxetine were accompanied by higher plasma paroxetine concentrations. * significant correlation, $p < 0.05$.

We could conclude from the dosing experiment that 5mg/kg BW is the minimum effective dosage that evoked a robust physiological, neuroendocrine as well as behavioral phenotype in the DBA/2J mouse strain.

3.1.2 Acute antidepressant administration

As acute antidepressant applications are widely used in animal studies, we were interested whether an acute paroxetine administration via the mouse pellets evokes the same behavioral effects as already found in the literature (Cryan et al., 2005; Slattery and Cryan, 2012). Therefore, 80 male DBA/2J mice were treated with 5mg/kg BW paroxetine (n=30) or vehicle (n=50) (Figure 18A).

When investigating physiological parameters, we did not detect a significant difference in body weight gain between the groups. The same counted for neuroendocrine parameters. We did not find any difference in corticosterone concentrations after an acute antidepressant treatment (Figure 18B).

However, an acute paroxetine administration was able to evoke a behavioral response in the FST. Paroxetine treated animals showed a reduction in time floating compared to the vehicle treated control animals (Figure 18C) ($T_{75} = 3.590$, $p< 0.001$) and increased active

behavior (time swimming T_{75} = -2.526, $p < 0.05$, vehicle: 112.05sec ± 4.74; paroxetine: 133.48sec ± 7.61 and time struggling: T_{75} = -2.019, $p < 0.05$) (Time struggling is shown as a representative for active behavior Figure 18D).

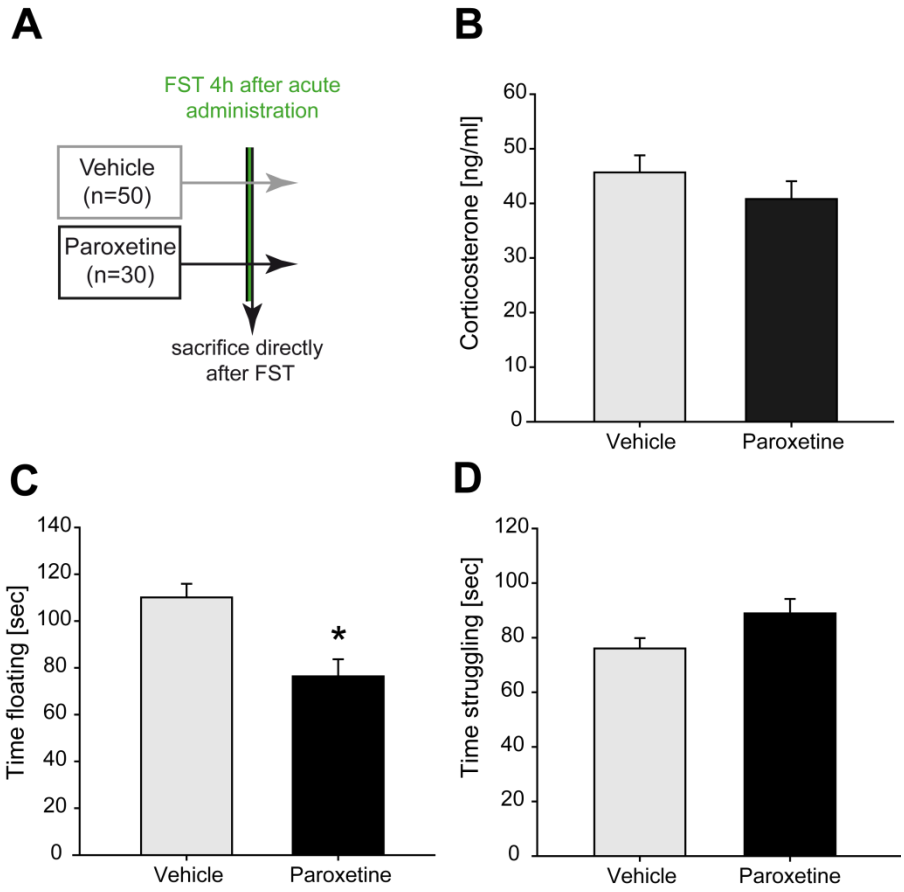

Figure 18: Neuroendocrine, physiological and behavioral parameters after acute paroxetine treatment (5mg/kg BW). (A) Experimental time course of the study. (B) Acute paroxetine treatment (5mg/kg BW) did not alter corticosterone levels. (C) Paroxetine treatment reduced the time floating in the FST in the treated animals compared to the control group. (D) Acute treatment also led to an alteration in time struggling in the paroxetine treated group. * significant difference from vehicle treated control group, $p < 0.05$.

To further investigate the pharmacology of the antidepressant drug in the mouse, paroxetine levels were measured in the brain and the plasma. Treated animals were split up by the median in two groups according to their performance in the FST. For plasma paroxetine levels, no difference was found between the groups, although the upper median group showed a tendency to a higher paroxetine plasma concentrations (T_{23} = 1.965, $p = 0.062$) (Figure 19A). A significant difference in paroxetine concentrations was detected in the brain. Animals subjected to the upper median group showed higher brain paroxetine levels (T_{23} = 2.167, $p > 0.05$) compared to the lower median group (Figure

19B). Nevertheless, we could again demonstrate that paroxetine brain and plasma concentrations were highly correlated (r = 0.861, p < 0.000) (Figure 19C).

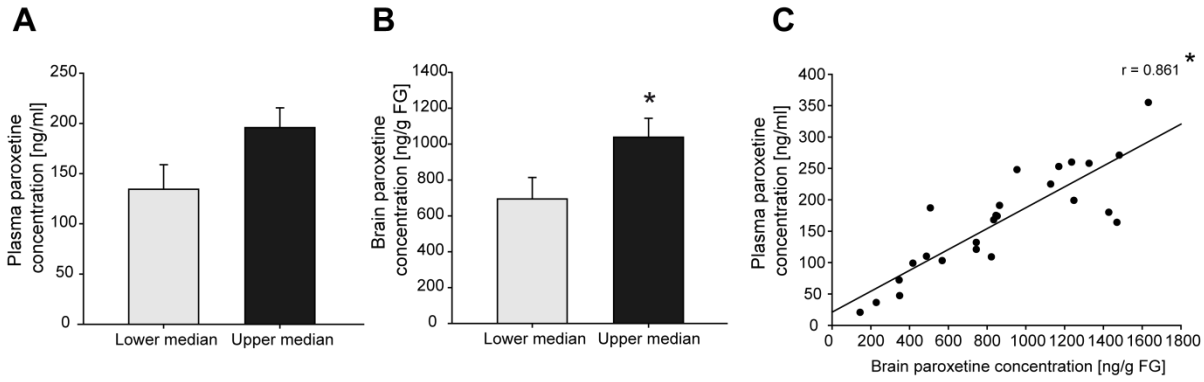

Figure 19: Pharmacological profile of an acute 5mg/kg BW in the mouse brain and periphery. (A) Acute paroxetine treatment did not change plasma paroxetine concentrations between the groups. (B) Animals subjected to the upper median group showed significantly higher brain paroxetine concentration compared to the lower median group. (C) Higher brain concentrations of paroxetine were accompanied by higher plasma paroxetine concentrations. * significant difference between lower and upper median, significant correlation, p < 0.05.

3.1.3 Acute i.p. injection versus acute mouse pellet

I.p. injection is one of the most common tools in preclinical science for pharmacological drug application. To ensure that the mouse pellet is a comparable tool to the commonly used i.p. injection, 10 male mice were injected once with 5mg/kg BW paroxetine. 30 male DBA/2J mice served as a control group (see detailed results in chapter 3.3). I.p. injected animals showed significantly higher plasma paroxetine levels (T_{33} = 2.863, p < 0.01) and brain paroxetine levels (T_{33} = 3.740, p < 0.01) compared to the animals treated with the mouse pellet (Figure 20A-B). We could again show that plasma and brain paroxetine concentrations are correlated (r = 0.883, p < 0.01) after an acute i.p. injection (Figure 20C). These findings are in line with our previous findings from the mouse pellets.

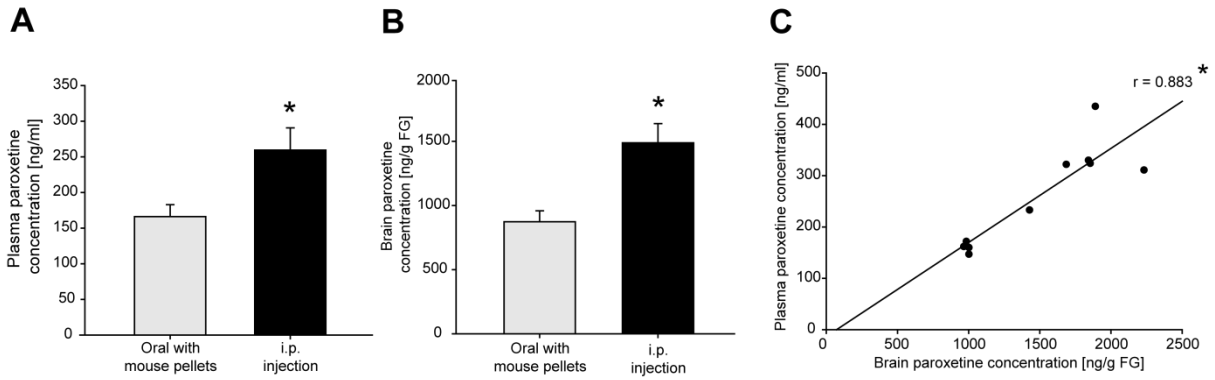

Figure 20: Pharmacological profile of an acute 5mg/kg BW in the mouse brain and periphery. (A) Acute i.p. paroxetine treatment led to higher plasma paroxetine concentrations compared to the mouse pellet treated group. (B) Acute i.p. paroxetine treatment led to higher brain paroxetine concentrations compared to the mouse pellet treated group. (C) After acute i.p. injection of 5mg/kg BW higher brain concentrations of paroxetine were accompanied by higher plasma paroxetine concentrations. *significant difference between i.p. injected group and mouse pellet group, * significant correlation, $p < 0.05$.

3.1.4 Half-life study

After we had identified the minimum effective dosage for the DBA/2J mouse strain (5mg/kg BW), we were aiming to get a better understanding of the pharmacokinetics of paroxetine especially with regard to pharmacological half-life of paroxetine within the mouse organism. 20 male DBA/2J mice were treated chronically with 5mg/kg BW paroxetine twice a day and were killed 1d (n=5), 3d (n=5), 7d (n=5) or 14d (n=5) after discontinuation of the paroxetine treatment (Figure 21A). One day after discontinuation of the antidepressant, the animals showed a 50% reduction of the paroxetine levels compared to the measured values right after the FST. Paroxetine plasma are no longer detectable from day 3 on (Figure 21B). Paroxetine was detectable a little bit longer in the brain, although there was very little left after 3 days of discontinuation of the treatment (Figure 21C).

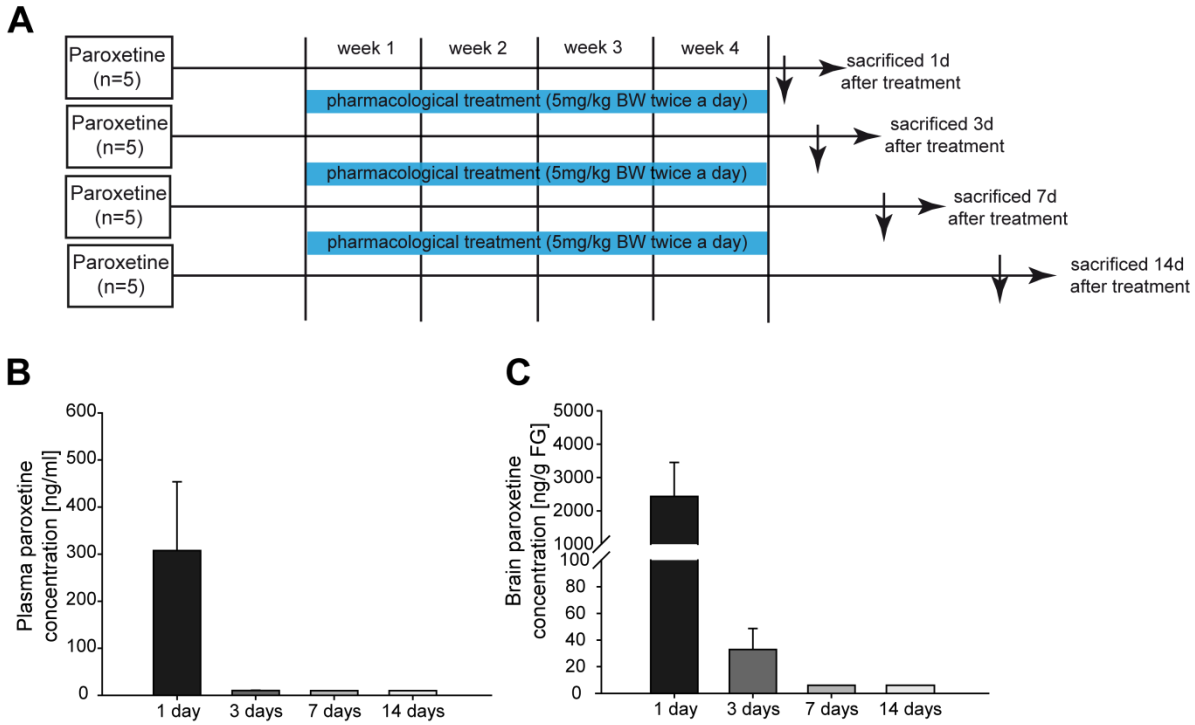

Figure 21: Pharmacological profile after discontinuation of 28d paroxetine treatment (5mg/kg BW) in the mouse brain and periphery. (A) Experimental time course. (B) Paroxetine plasma levels showed a 50% reduction of the paroxetine levels compared to the paroxetine levels data set right after the FST one day after withdrawal of the antidepressant. Already three days after discontinuation of the treatment, no more paroxetine could be detected in these animals. (C) Brain paroxetine levels showed a 50% reduction of the paroxetine levels compared to the paroxetine levels data set right after the FST one day after discontinuation of the antidepressant. Three days after discontinuation of the treatment a small amount of paroxetine could still be detected in these animals.

3.1.5 The FST as a valid readout for antidepressant treatment outcome in mice

In order to analyze whether the differences in individual antidepressant treatment response is due to pre-existing inherent behavioral characteristics, 60 animals were subjected to a FST and following one week of recovery treated for 28d with either paroxetine (n=40) or vehicle (n=20). After the treatment period the animals were screened in a second FST (Figure 22A). After the 28d treatment period, paroxetine treated animals showed a lower time floating ($T_{47} = 4.695$, $p < 0.000$) and higher time struggling compared to the vehicle treated animals ($T_{47} = -2.026$, $p < 0.05$) (Figure 22B-C). Furthermore, time swimming was also increased in the paroxetine treated animals compared to the vehicle treated control group ($T_{47} = -2.328$, $p < 0.05$, vehicle: 117.56 ± 11.54; paroxetine: 152.59 ± 9.48). As the time floating is our main readout parameter in this experimental design, we correlated the time floating of the animals under basal conditions with the time floating after the paroxetine treatment. Our results did not show any significant correlation in the investigated parameters ($r = 1.80$, $p = 0.340$) (Figure 22D).

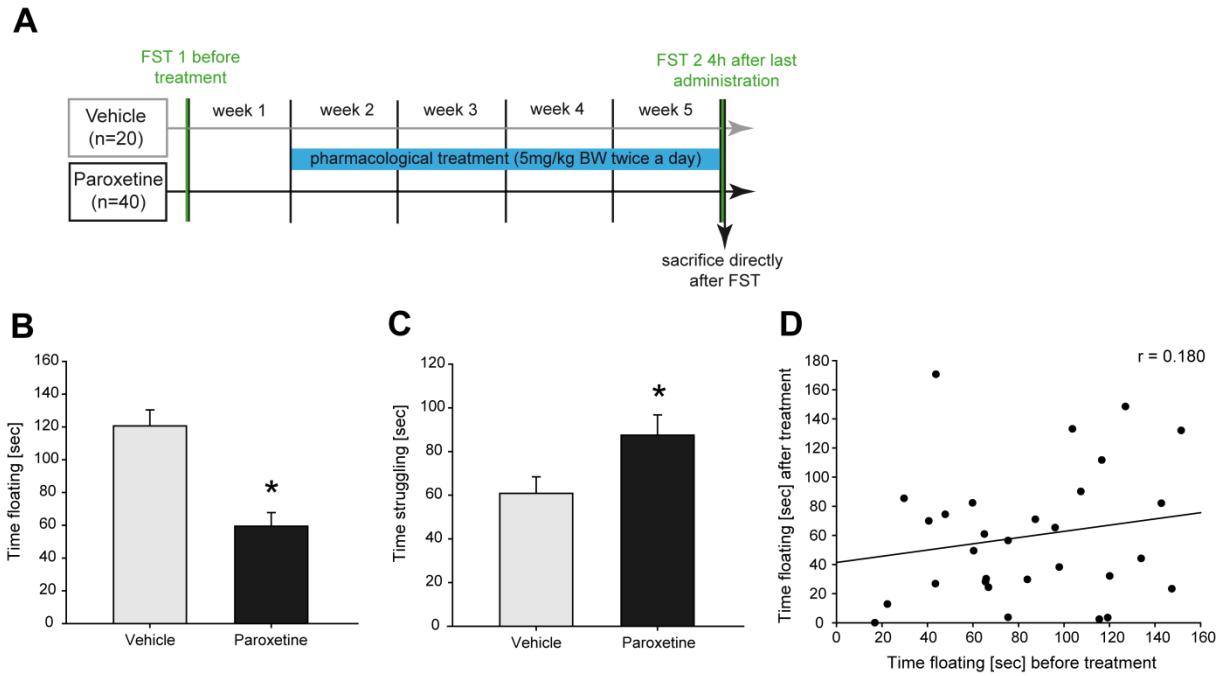

Figure 22: Behavioral profile of a repeated FST after 28d of paroxetine treatment (5mg/kg BW). (A) Experimental time course. (B) Time floating in the second FST following 28d of paroxetine treatment. Paroxetine treated animals showed significant lower time floating compared to the vehicle treated control group. (C) Time struggling in the second FST. Paroxetine treated animals showed significant higher time struggling compared to the vehicle treated control group. (D) When correlating the time floating in the FST before and after the paroxetine treatment, no correlation was found between the performance of the animals. * significant difference between vehicle treated control group and paroxetine treated group, $p < 0.05$.

3.2 Genes and pathways modulated after chronic paroxetine treatment

In a next step, we were interested in genes and pathways that are differently regulated in good and poor responders as well as between vehicle and paroxetine treated animals after a chronic antidepressant treatment.

3.2.1 Microarray analysis

158 mice were treated with 5mg/kg BW paroxetine (n=100) or vehicle (n=58) for 28d twice a day (8am and 6pm) and were killed on day 29 directly after the FST. For detailed information and results see chapter 3.1.1, as the here described animals were part of this cohort. As we were aiming to identify novel genes and pathways, mediating an individual antidepressant response, we investigated the individual behavior of the animals. After identifying good (n=12), poor (n=13) and intermediate (n=8) treatment responders as well as the vehicle treated control group (n=9) (for detailed information see 2.5) a whole

genome gene expression microarray was conducted with hippocampal brain tissue (Figure 23).

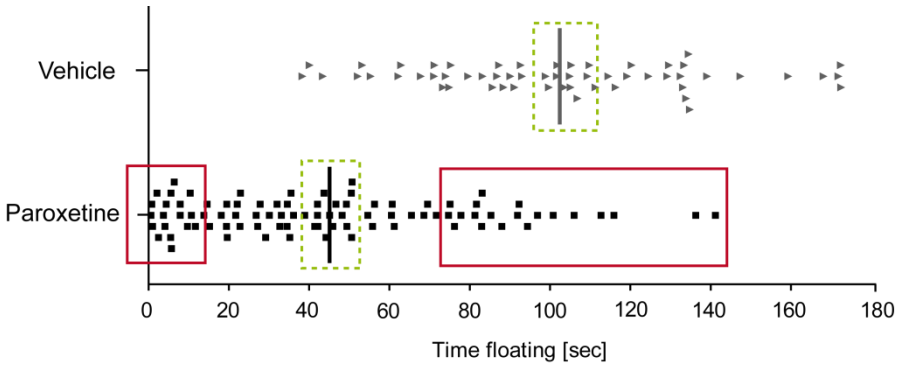

Figure 23: Identification of different responder groups according to their performance in the FST. Animals indicated in the red squares are referred as good and poor treatment responder. Animals that showed a very high time floating represented the poor treatment responder, whereas animals that showed a very low time floating represented the good treatment responder. Animals indicated with the green dotted squares are representing internal control groups. The animals within the paroxetine treated group are representing the intermediate responder group and served as a treated control group. The animals within the vehicle treated group served as a vehicle treated control group.

Analysis of the Illumina microarray chip revealed 36 regulated genes between vehicle treated animals and good responder at a false discovery controlled significant level of 10% ($q < 0.1$). Duplicates were removed in a next step (n=2) as well as genes that were detected by the microarray but were not specific for the respected gene (n=4), resulting in 30 differentially regulated genes. A detailed gene list containing all relevant parameters can be found in Table 4.

Table 4: Significantly regulated genes in the hippocampal DG region 28d after paroxetine treatment. Genes are ordered by their functional classes. Fold Change is normalized to vehicle treated animals.

Functional classification (according to Gene Ontology GO)	PROBE_ID	REFSEQ_ID	SYMBOL	Gene Name	q-Value	Fold change
Calmodulin binding						
	ILMN_1244364	NM_012040.2	Pnck	pregnancy upregulated non-ubiquitously expressed CaM kinase	0.07	0.76
Enzymatic activity						
	ILMN_2642426	NM_001081408.1	Agmat	agmatine ureohydrolase (agmatinase)	0.07	1.32
	ILMN_1237725	NM_173451.2	Arsj	arylsulfatase J	0.02	1.30
Growth factor activity						
	ILMN_2689790	NM_008344.2	Igfbp6	insulin-like growth factor binding protein 6	0.06	1.47
	ILMN_2868220	NM_008380.1	Inhba	inhibin beta-A	0.06	1.63
	ILMN_2859613	NM_008760.2	Ogn	osteoglycin	0.01	0.63
	ILMN_2492264	NM_018865.2	Wisp1	WNT1 inducible signaling pathway protein 1	0.06	1.33
	ILMN_1258734	NM_023653.4	Wnt2	wingless-related MMTV integration site 2	0.07	1.32
Hormone activity						
	ILMN_2955725	NM_007745.2	Cort	cortistatin	0.00	0.67
	ILMN_2777319	NM_009285.3	Stc1	stanniocalcin 1	0.07	0.75
Immune system						
	ILMN_2671473	NM_207233.1	C1ql2	complement component 1, q subcomponent-like 2	0.00	1.62
Protein binding						
	ILMN_1244829	NM_010404.2	Hap1	huntingtin-associated protein 1	0.07	0.75
Receptor activity						
	ILMN_2614086	NM_001033369.2	Acvr1c	Activin	0.00	1.65
	ILMN_1235741	NM_007418.2	Adra2c	adrenergic receptor, alpha 2c	0.06	1.27
	ILMN_2734062	NM_010076.2	Drd1a	dopamine receptor D1A	0.04	1.44
Receptor binding						
	ILMN_2872698	NM_172406.2	Trak2	trafficking protein, kinesin binding 2	0.07	1.33
Structural molecule						
	ILMN_2915232	NM_028071.1	Cotl1	coactosin-like 1 (Dictyostelium)	0.08	1.39
Transcription factor activity						
	ILMN_1235647	NM_009234.5	Sox11	SRY-box containing gene 11	0.00	1.75
Transporter activity						
	ILMN_1237059	NM_010595.3	Kcna1	potassium voltage-gated channel, shaker-related subfamily, member 1	0.07	1.13
	ILMN_2657243	NM_201531.2	Kcnf1	potassium voltage-gated channel, subfamily F, member 1	0.04	0.72
	ILMN_2679229	NM_172861.2	Slc7a14	solute carrier family 7 (cationic amino acid transporter, y+ system), member 14	0.09	1.16
Others						
	ILMN_1253600	NM_001081156.2	2300002D11	MF1-regulated nuclear protein 1	0.07	1.41
	ILMN_2903169	NM_001033356.2	Gm484	netrin 5	0.02	0.63
	ILMN_2719973	NM_016697.2	Gpc3	glypican 3	0.07	0.75
	ILMN_3161834	NM_001030294.1	Olfm4	olfactomedin 4	0.07	1.37
	ILMN_1214118	NM_031257.2	Plekha2	pleckstrin homology domain-containing, family A	0.00	1.45
	ILMN_2643212	NM_023396.4	Rprm	reprimo, TP53 dependent G2 arrest mediator candidate	0.01	1.80
	ILMN_1246800	NM_009252.2	Serpina3n	serine (or cysteine) peptidase inhibitor, clade A, member 3N	0.09	1.35
	ILMN_2639239	NM_011340.3	Serpinf1	serine (or cysteine) peptidase inhibitor, clade F, member 1	0.04	1.49
	ILMN_1219904	NM_146173.2	Tspan33	tetraspanin 33	0.05	0.73

We did not detect any significant difference between good and poor treatment responders after correcting for multiple testing.

3.2.2 Validation of potential candidates with qRT-PCR

12 genes were selected for further investigation. The selection was based on the gene expression pattern (www.brain-map.org) as well as evidences from the literature that these genes are involved in pathophysiological processes, which have been linked to the neurobiology of psychiatric disorders, such as neurogenesis, receptor activity, immune system or intracellular signaling. In a next step, we performed qRT-PCR with the same samples to validate the microarray results in a technical control replicate. Therefore, we

investigated mRNA expression levels with normalization to the housekeeper gene Hprt. We were able to validate 9 out of the 12 selected candidates. Acvr1c was significantly upregulated in the good treatment responders after 28d of paroxetine treatment compared to the vehicle treated control group (T_{19} = -5.5570, $p < 0.000$) (Figure 24A). The same regulation pattern was found for Adra2c ($T_{13.336}$ = -3.125, $p < 0.01$) (Figure 24B), C1ql2 (T_{19} = -3.043, $p < 0.01$) (Figure 24E), Igfbp6 (T_{18} = -3.481, $p < 0.005$) (Figure 24G), Serpina3n ($T_{11.903}$ = -2.891, $p < 0.05$) (Figure 24J), Serpinf1 ($T_{11.658}$ = -3.421, $p < 0.005$) (Figure 24K) and Sox11 ($T_{12.056}$ = -4.775, $p > 0.000$) (Figure 24L). However, we also detected genes that showed a significant downregulation in the good treatment responder after 28d of paroxetine compared to the vehicle treated control group, such as Cort (T_{18} = 3.734, $p < 0.005$) (Figure 24D) and Pnck (T_{19} = 4.853, $p < 0.000$) (Figure 24I). Arsj (Figure 24C), Drd1a (Figure 24F) and Mylk (Figure 24H) did not show any significant gene expression alterations between the two compared groups.

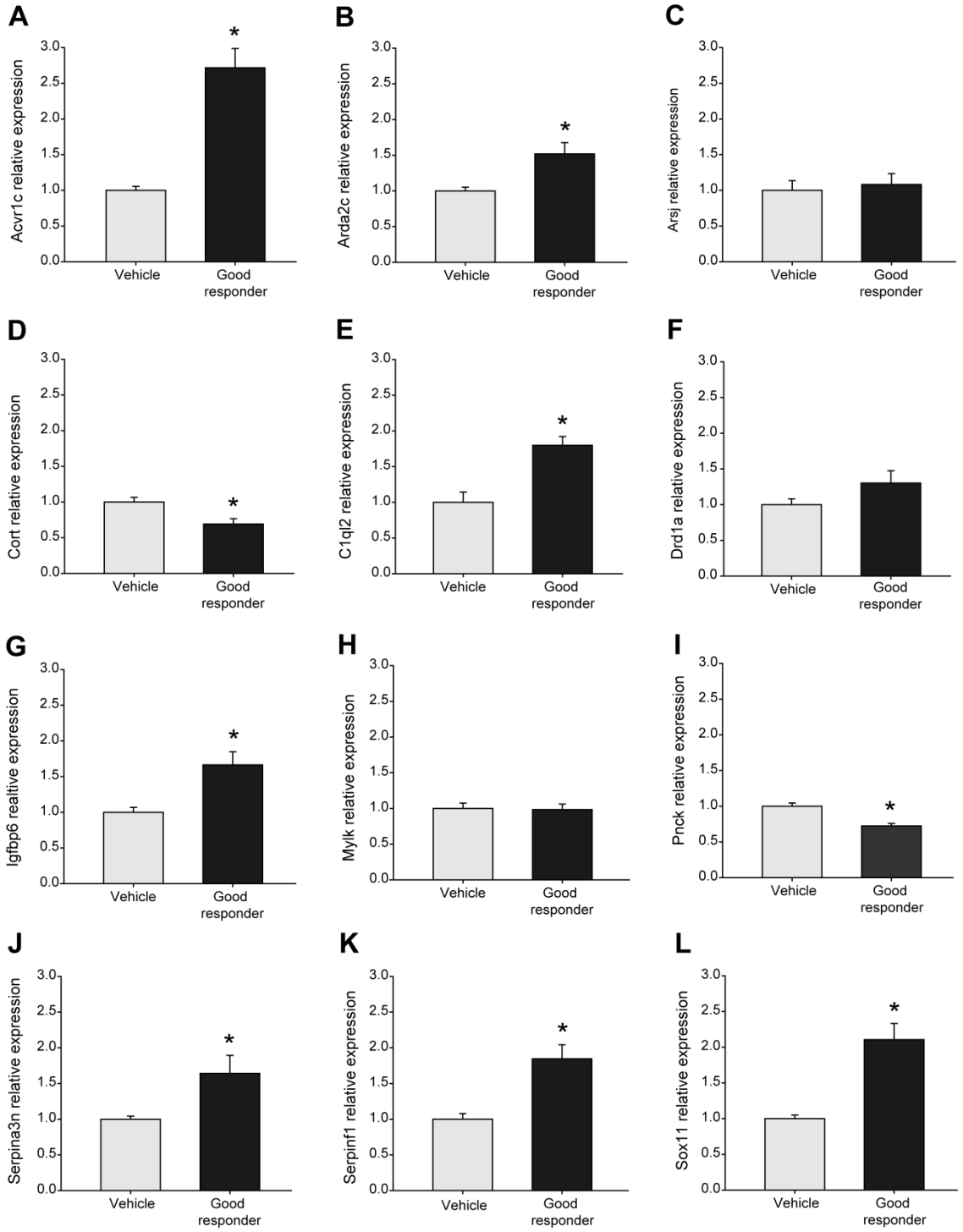

Figure 24: Validation of candidate genes from the microarray. From 12 selected candidates, the mRNA of 9 transcripts were significantly regulated in the hippocampus after 28d of paroxetine treatment (A-L). * significant different to vehicle treated control animals $p < 0.05$.

3.3 Sox11 as a potential novel candidate mediating antidepressant action

Evidences from the literature (Sha et al., 2012; Mu et al., 2012b; Kuhlbrodt et al., 1998; Jankowski et al., 2006; Haslinger et al., 2009) suggests a potential role of Sox11 in adult neurogenesis, thereby we selected Sox11 as a very interesting candidate for further investigations. Consequently, we were interested if different paroxetine treatment durations can also influence Sox11 gene expression.

3.3.1 Chronic paroxetine treatment leads to a robust upregulation of Sox11

To verify the upregulation of Sox11 after 28d of paroxetine treatment, brain samples originating from two independent experiments were used for ISH. The first samples derived from the microarray experiment, but were not selected for the microarray analysis itself. Here, we showed that paroxetine lead to a significant increase in Sox11 mRNA levels in the DG compared to the vehicle treated control group ($T_{17} = -3.932$, $p < 0.005$) (Figure 25A and C). We also investigated other hippocampal areas, but did not find a significant difference between the groups. After further evaluation Sox11 mRNA levels in the different responder groups, we were not able to detect a significant difference between good and poor responders. The second independent sample derived from chapter 3.1.5. Here, we also detected a significant difference in the DG between the treated animals (n=14) and the vehicle treated control group (n=20) ($T_{32} = -6.283$, $p < 0.000$) (Figure 25B and D). Additionally to the DG, we found a significant increase in Sox11 mRNA expression in the paroxetine treated animals in the CA1 region of the HC ($T_{17.593} = -3.671$, $p < 0.01$, vehicle: 11.75 ± 1.01; paroxetine: 21.34 ± 2.41).

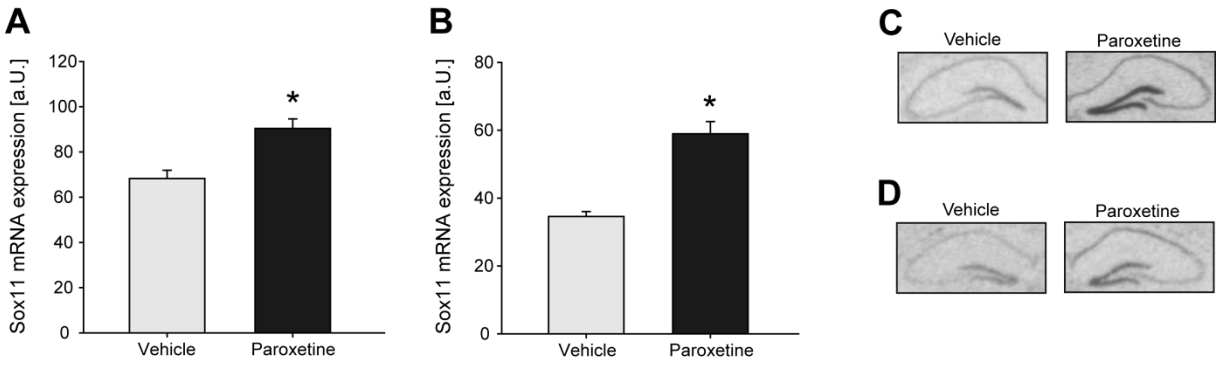

Figure 25: Sox11 mRNA expression after chronic treatment. (A-B) Chronic paroxetine treatment resulted in an increase in Sox11 mRNA expression levels compared to the vehicle treated control group. (C-D) Pictures show representative autoradiographs of Sox11 expression in the hippocampus of vehicle and paroxetine treated animals. * significant difference between vehicle treated control group and paroxetine treated group, $p < 0.05$.

3.3.2 Subchronic paroxetine treatment leads to higher Sox11 mRNA expression

In a next step we were interested in the time course of paroxetine-induced regulation, i.e. the question whether Sox11 is already upregulated after subchronic treatment. Therefore, ISH was performed on brains obtained from chapter 2.2.4. After 14d of drug administration increased Sox11 mRNA expression levels were found in paroxetine treated animals (n=30) compared to the vehicle treated control group (n=12) (T_{40} = -2.958, $p < 0.01$) (Figure 26A-B). A significant increase in Sox11 mRNA expression was also detected in the hippocampal CA1 region of the paroxetine treated animals (T_{40} = -2.875, $p < 0.01$, vehicle: 7.70 ± 0.92; paroxetine: 11.76 ± 0.81).

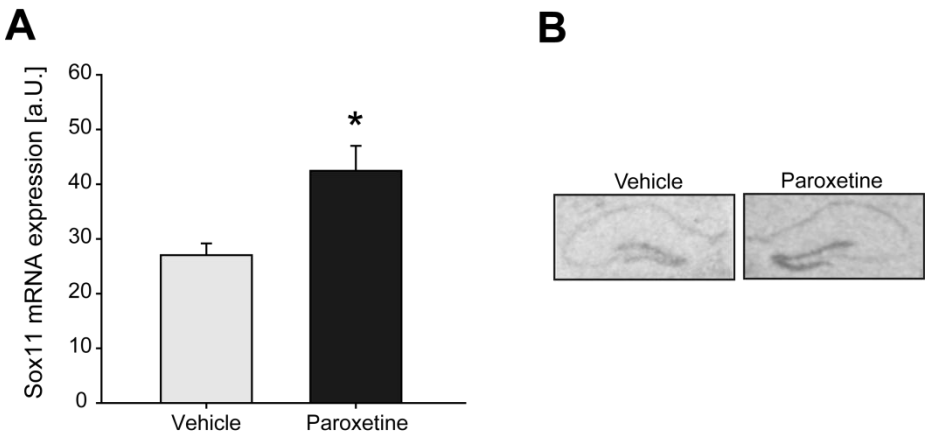

Figure 26: Sox11 mRNA expression after subchronic treatment. (A) Subchronic paroxetine treatment resulted in increased Sox11 mRNA expression levels compared to the vehicle treated control group. (B) Pictures show representative autoradiographs of Sox11 expression in the HC of vehicle and paroxetine treated animals. * significant difference between vehicle treated control group and paroxetine treated group, $p < 0.05$.

3.3.3 Acute paroxetine treatment does not alter Sox11 gene expression

We could show that Sox11 is already upregulated after 14d of paroxetine treatment and this persists at least until 28d of paroxetine treatment. Subsequently, we were interested if this upregulation is already present after one acute dosage of paroxetine. Therefore, ISH was performed on brains obtain from chapter 2.2.1.3. Acute paroxetine administration has no influence on Sox11 mRNA expression in the HC (Figure 27).

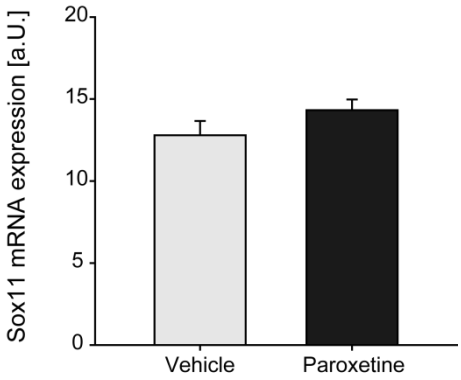

Figure 27: Sox11 mRNA expression in the hippocampal DG after acute treatment. Acute paroxetine administration did not influence Sox11 mRNA expression levels.

3.3.4 Sox11 upregulation is a SSRI specific effect

We demonstrated in the previous chapters that paroxetine is regulating Sox11 mRNA expression in the mouse DG. Subsequently, we were interested whether the gene expression changes are SSRI specific effects or if the change in gene expression are due to antidepressants in general.

Therefore, 25 male DBA/2J mice were treated twice a day for 28d with either vehicle (n=10) or 2 mg/kg BW reboxetine (n=15), a norepinephrine reuptake inhibitor (Figure 28A). Regarding physiological parameters, reboxetine did not alter body weight gain between the vehicle and reboxetine treated animals (Figure 28B). Moreover, we did not detect any difference in corticosterone concentrations after chronic reboxetine treatment.

However, chronic reboxetine administration was able to evoke a behavioral response in the FST. Reboxetine treated animals showed a significant increase in time struggling compared to the vehicle treated control animals (Figure 28C) (T_{22} = -4.301, p< 0.000) but interestingly vehicle treated animals showed a significant increase in time swimming (T_{22} = 3.219, p < 0.005). No significant difference was found between the groups in time floating (Figure 28D). Nevertheless, reboxetine treated animals showed a significant increase in the latency to float in the FST (T_{21} = -2.316, p < 0.05) compared to the vehicle treated animals (Figure 28E). As depression often shows a high comorbidity with anxiety, we were also interested in the effects of reboxetine on anxiety-related behavior and therefore tested these animals in the DaLi. However, we did not detect any differences between the groups in anxiety-like behavior (Figure 28F).

In order to investigate the effects of reboxetine on Sox11 mRNA expression levels, ISH was performed. We did not detect any differences in Sox11 mRNA expression in the HC between vehicle and reboxetine treated animals (Figure 28G).

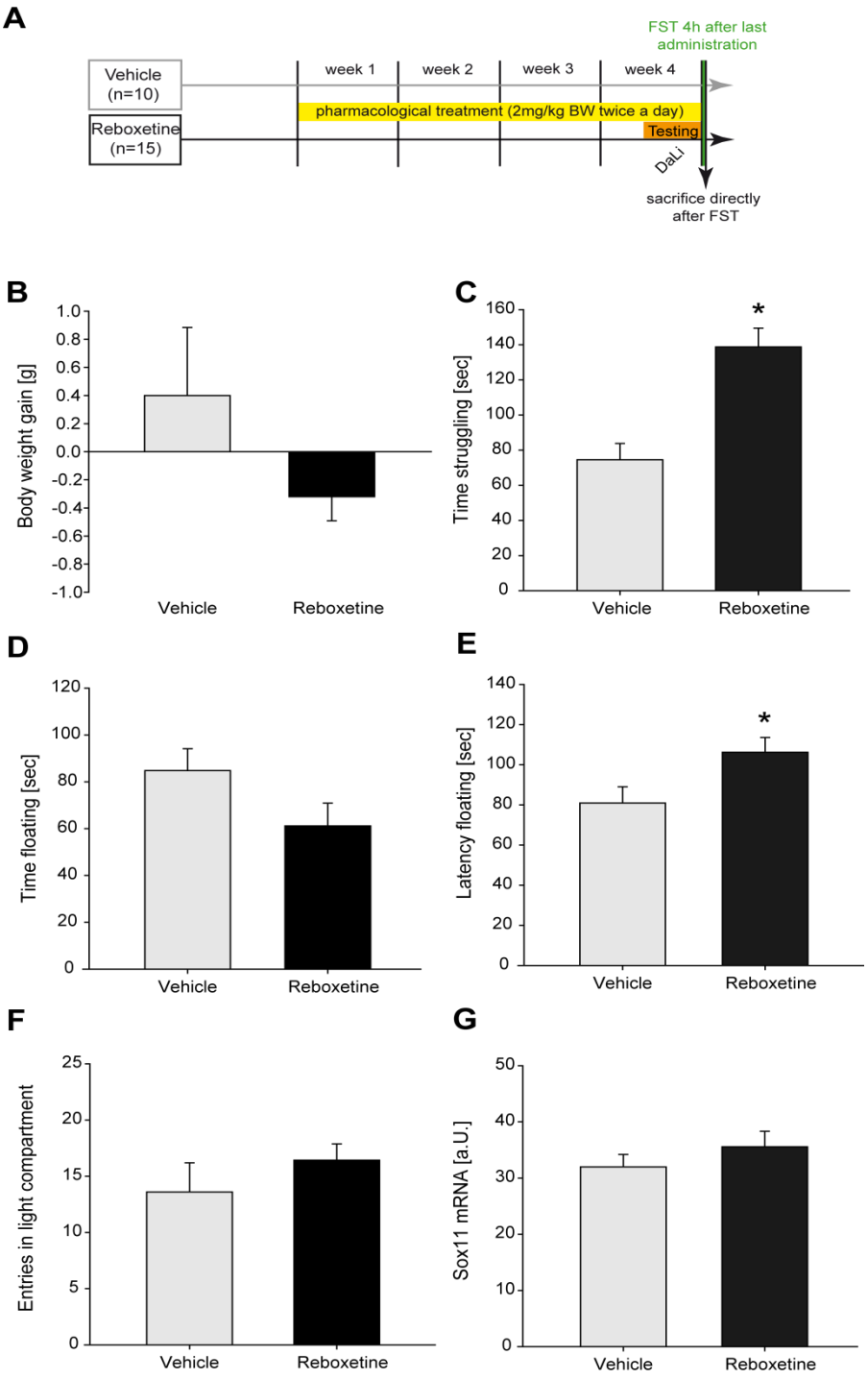

Figure 28: Physiological and behavioral effects of chronic reboxetine treatment. (A) Experimental time course. (B) Reboxetine did not alter body weight gain between the vehicle and reboxetine treated animals. (C) Chronic reboxetine administration was able to evoke a behavioral response in the FST. Paroxetine treated animals showed a significant increase in time struggling compared to the vehicle treated control animals. (D) No significant difference was found between the groups in time floating. (E) Reboxetine treated animals showed a significant increase in latency to float in the FST compared to the vehicle treated animals. (F) When investigating the effects of reboxetine on anxiety-related behavior in the DaLi, we did not detect any differences between the groups. (G) Reboxetine did not alter Sox11 mRNA expression levels. * significant difference between the vehicle treated control and the reboxetine treated group, $p < 0.05$.

3.3.5 Viral overexpression of Sox11 leads to a less anxious phenotype

We could show a paroxetine-induced upregulation of Sox11 as well as the reduction in depressive-like behavior in the FST in the previous chapters. As a consequence, we examined whether a virus-mediated OE of Sox11 mimics the same behavioral phenotype as the paroxetine treatment. Therefore, we performed a region-specific OE of Sox11 in the hippocampal DG, by using AAV-9 Sox11OE (n=23) or empty control (n=20) injections (Figure 29C). ISH confirmed a stable overexpression of Sox11 in the DG region (T_{28} = -8.835, p < 0.000) (Figure 29A-B), with some spreading in the CA3 region of the hippocampal formation ($T_{13.507}$ = -18.105, p < 0.000). Furthermore, we additionally controlled for the viral OE by immunofluorescence (Figure 29D).

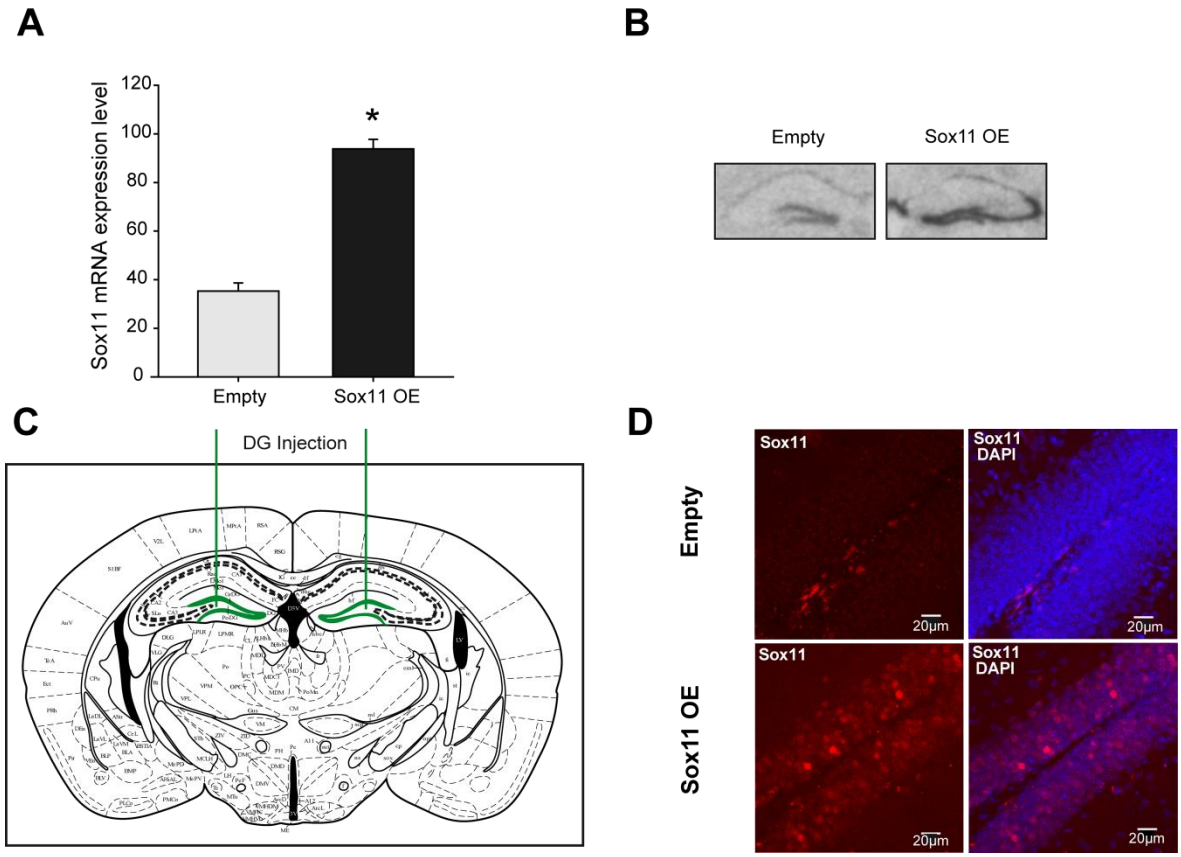

Figure 29: Sox11 OE in the dorsal HC. (A) Sox11 mRNA expression levels in the dorsal HC. (B) Representative autoradiographs of Sox11 mRNA levels in the dorsal HC of control and Sox11 OE animals. (C) Schematic representation of the injection site (green). (D) Visualization of Sox11 expression in the HC 8 weeks after the injection of control (top row) and Sox11 OE (lower row). * significant difference between Empty control group and Sox11 OE group, p < 0.05.

Animals were tested in the OF to investigate general locomotor activity. We could show that the viral overexpression of Sox11 did not change locomotor activity (Figure 30B).

Additionally, we analyzed the parameters of the inner zone in OF apparatus, which are also commonly used parameters to investigate anxiety-like behavior. Sox11 OE animals showed a reduced latency to enter the inner zone ($T_{33} = 2.130$, $p < 0.05$) (Figure 30C) as well as a longer distance travelled in the inner zone ($T_{41} = -2.087$, $p < 0.05$) (Figure 30D). Furthermore, they showed a tendency to spend more time in the inner zone (trend: $T_{40} = -1.944$, $p = 0.059$). To verify this anxiety-like phenotype, we tested the animals additionally in the DaLi. Here, the Sox11 OE animals entered the light compartment more often compared to the empty control animals ($T_{41} = -2.142$, $p < 0.05$) (Figure 30E). Moreover, the Sox11 OE spent more time in the light compartment compared to the control animals ($T_{41} = -2.521$, $p < 0.05$) (Figure 30F). Sox11 OE animals also travelled more in the light compartment compared to their empty control group ($T_{37.824} = -2.457$, $p < 0.05$) (Figure 30G).

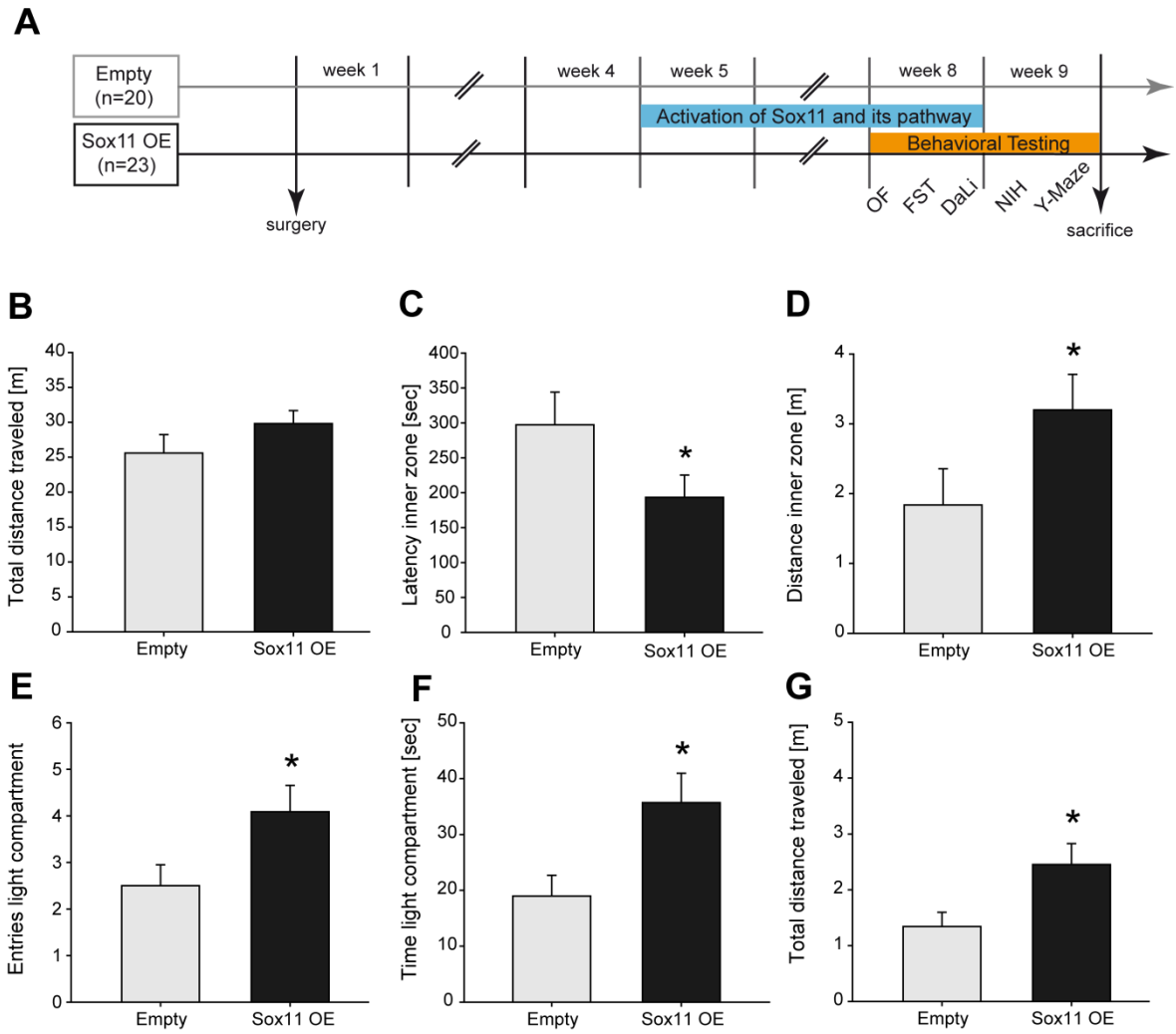

Figure 30: Sox11 OE in the dorsal HC led to a less anxious phenotype. (A) Experimental time course. (B) Sox11 OE had no influence on general locomotion. (C) When analyzing the inner zone of the OF, Sox11 OE animals showed a reduced latency to enter the inner zone (D) as well as a longer distance travelled in the inner zone. (E) Viral OE of Sox11 led to a less anxious phenotype in DaLi compared to the empty control animals. Sox11 OE animals entered the light compartment more often compared to the Empty control animals. (F) Sox11 OE showed a significant increase in time spent in the light compartment compared to the control group. (G) Additionally, Sox11 OE travelled more in the light compartment compared to their Empty control group. * significant difference between Empty control group andSox11 OE group, $p < 0.05$.

To investigate depressive-like behavior in these animals, we subjected them to a FST but no significant difference was found between Sox11 OE and the Empty control group (Figure 31A-B).

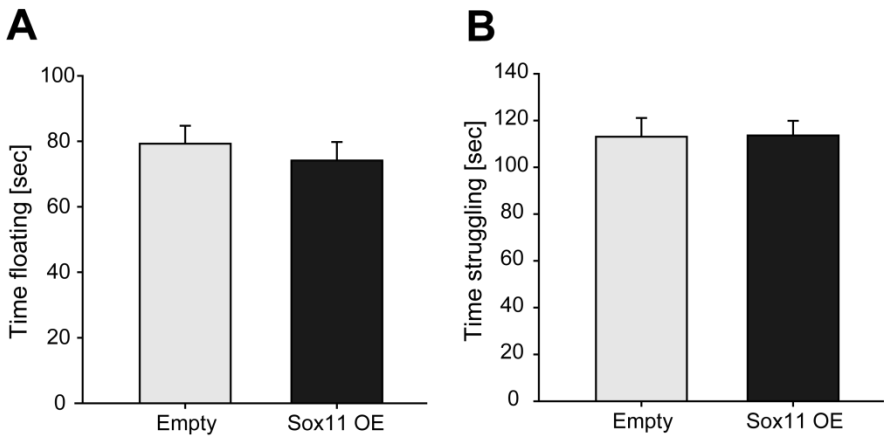

Figure 31: Sox11 OE had no effect on depressive-like behavior. (A) There was no significant difference between Empty and Sox11 OE animals in the time spent floating. (B) No significant difference was found between Empty and Sox11 OE animals in the time spent struggling.

Additionally to the DaLi a NIH test was performed. However, we did not find any significant difference between the two groups in the NIH (Figure 32A-B).

In order to exclude any cognitive deficits in these animals, we subjected them to a Y-Maze. To investigate whether short-term memory performance is still intact in these animals, an inter-trail interval of 30min between the acquisition and the retrieval phase was applied. Both control and Sox11 OE animals performed better than chance level, as they spent significantly more time exploring the novel arm of the Y-Maze. However, we did not detect any difference between the two groups (Figure 32C-D).

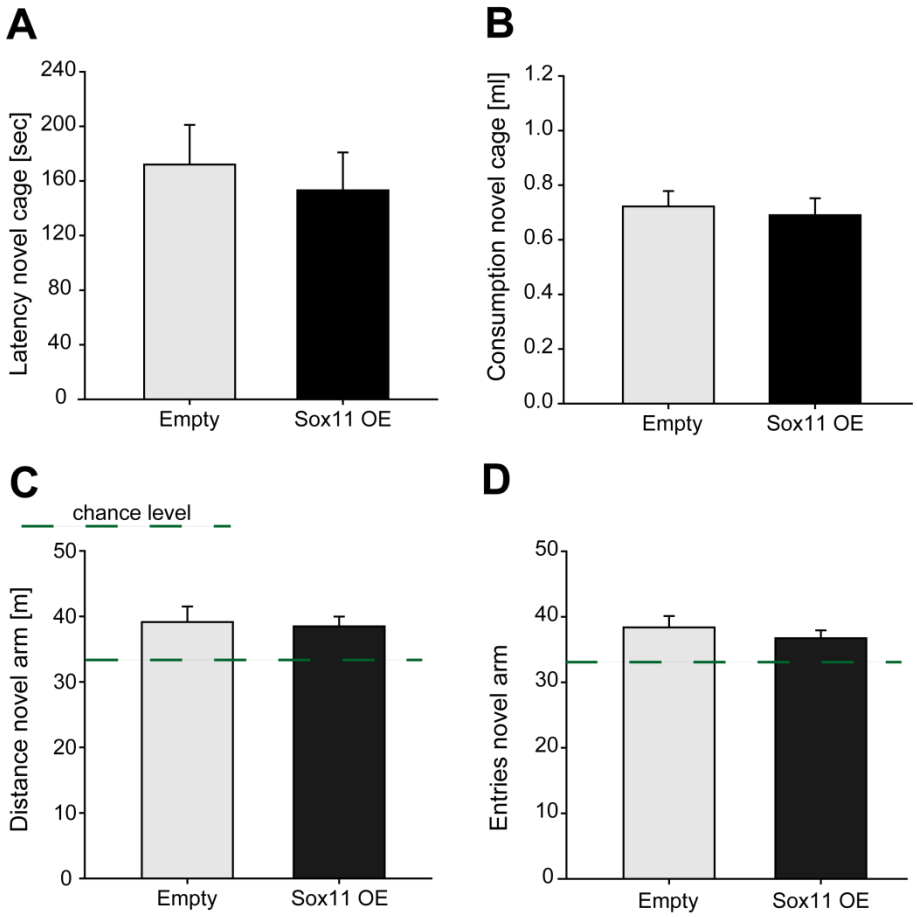

Figure 32: Effects of Sox11 OE in the NIH and the Y-Maze. (A) No significant difference was found between the two groups in the latency to consume the sweetened condensed milk in the NIH. (B) Both groups consumed the same amount of sweetened condensed milk in the NIH. (C) Both testing groups performed better then chance level in the Y-Maze. Sox11 OE and Empty animals travelled more in the novel arm (D) and entered the arm more frequently compared to the already known arms.

3.3.6 Sox11 OE and its influence on neurogenesis

As there are evidences from the literature that Sox11 is involved in neurogenesis (Haslinger et al., 2009), we were interested, whether a region-specific overexpression of Sox11 in the DG also increases the neurogenesis rate. Therefore, 23 male DBA/2J mice were injected with either an AAV9-Sox11OE or AAV9-empty. After 4 weeks of recovery, the animals were then injected on 3 consecutive days with 100mg/kg BrdU pulse (Figure 33A). 16 animals (Sox11OE n=8; Empty control n=8) were perfused on the last day of the BrdU pulse, 2 hours after the last injection (Figure 33A). This time point was chosen to analyze the proliferation rate as a consequence of the viral OE of the Sox11. However, we were not able to detect any differences in BrdU positive cells between the groups. Sox11

OE has no influence on the proliferation rate of NSPCs compared to the Empty control animals (Figure 33B-D).

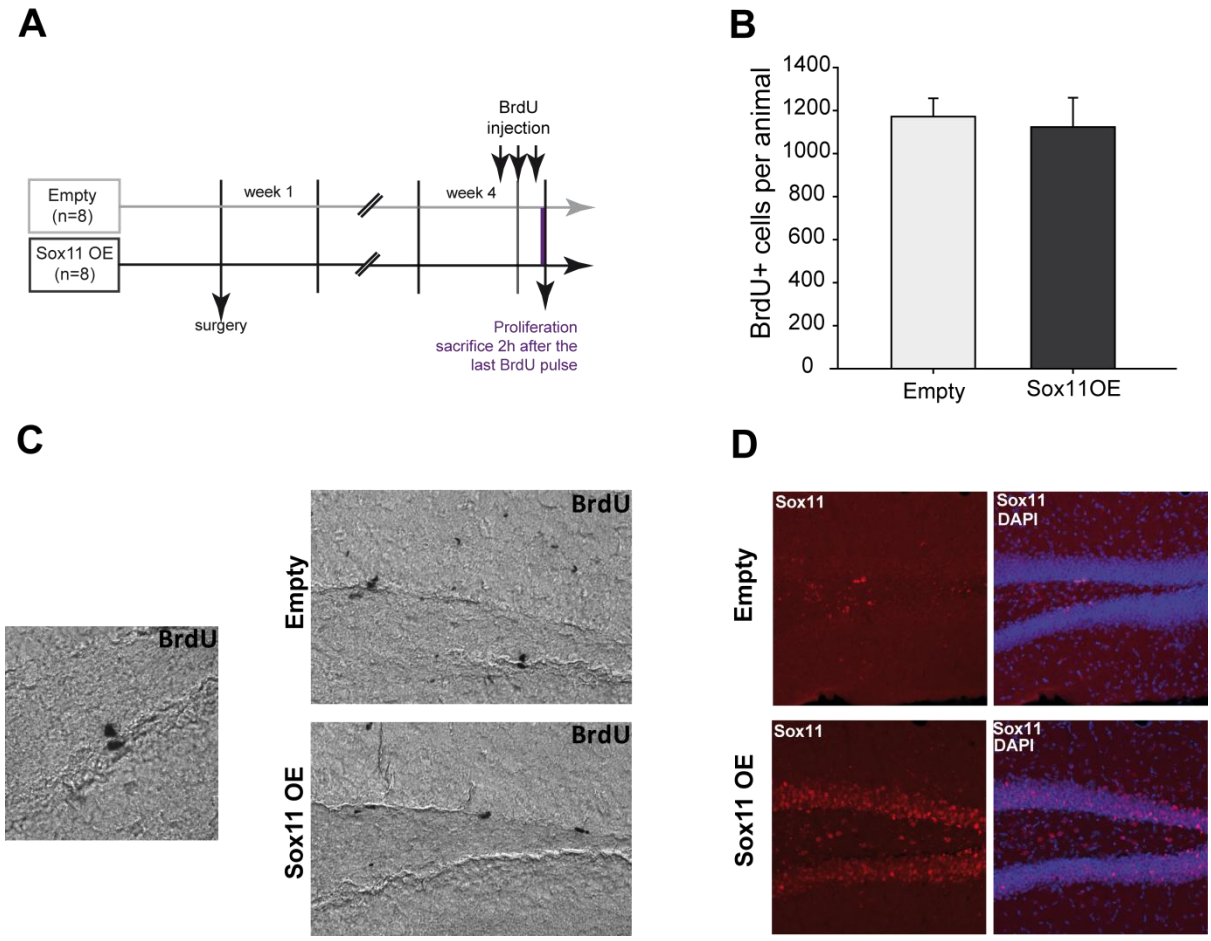

Figure 33: Influence of Sox11 OE on neurogenesis. (A) Experimental time course. (B) Sox11 OE had no influence on proliferation status. (C) BrdU immunoreactivity in the dentate gyrus 2 hours after the last BrdU pulse. (D) Visualization of Sox11 expression in the hippocampus of control (top row) and Sox11 OE (lower row) 4 weeks after the surgery (Scale: 1µm = 4.818pixel).

7 animals (Sox11OE n=4; Empty control n=3) were perfused 28d after the last day of the BrdU pulse (Figure 34A). This time point was chosen to analyze the maturation status as a consequence of the viral OE of the Sox11. However, we did not detect any differences in the percentage of BrdU+ and NeuN+ cells in the BrdU+ labeled cells between the groups. The percentage of novel produced neurons (NeuN+ labeled cells, as NeuN is a marker for neurons) was the same in the compared groups. In order to test, whether an overexpression of Sox11 is leading in general to a higher number of BrdU+ cells and thus more cells, further staining and investigations needs to be performed. However, at this stage we can say, that within the novel produced cells (BrdU+ cells), there is no difference in NeuN+ labeled cells between the groups (Figure 34B).

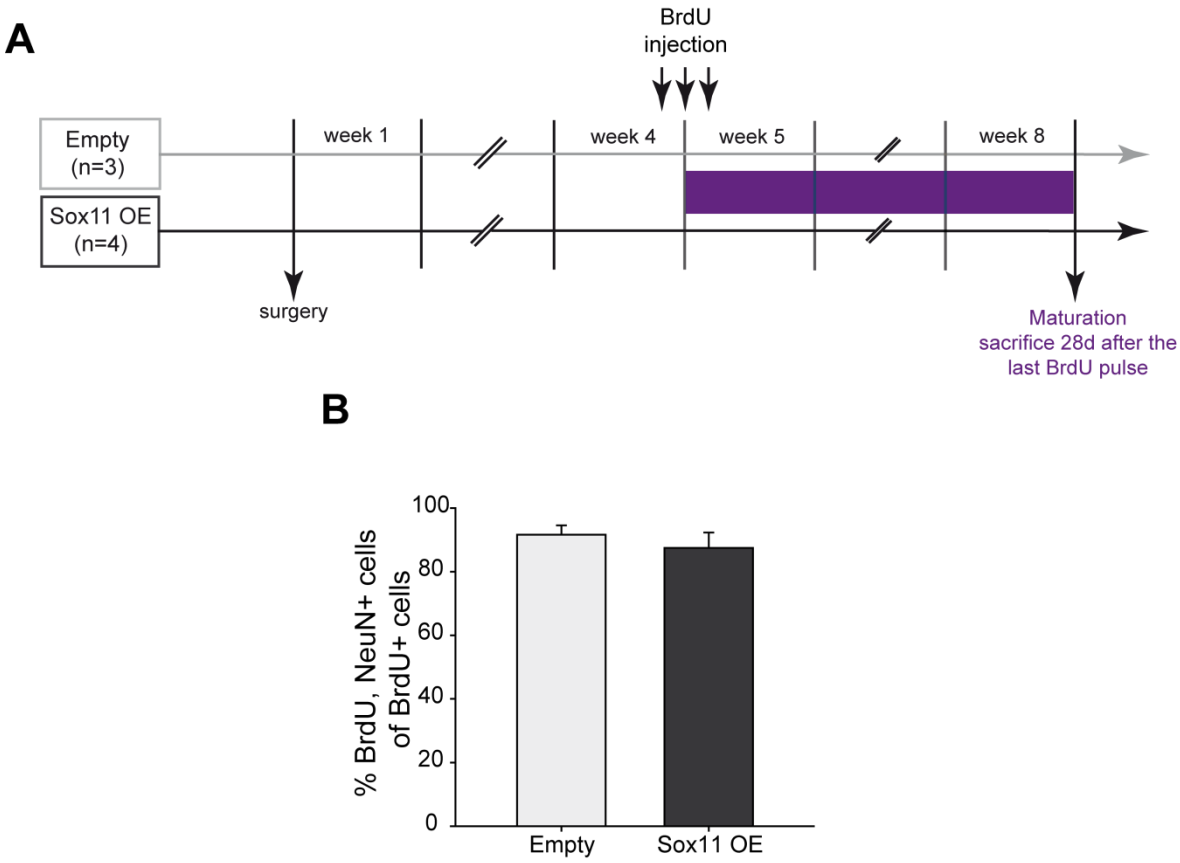

Figure 34: Influence of Sox11 OE on neurogenesis. (A) Experimental time course. (B) Sox11 OE had no influence on proliferation status.

3.3.7 Viral knockdown of Sox11 in combination with paroxetine treatment

Sox11 OE seems to be an important factor in modulating anxiety-related behavior, as we could show in the previous chapter. Consequently, we performed a Sox11 KD to further elucidate its role in anxiety-like behavior and even more, whether paroxetine is able to reverse this hypothesized phenotype. Therefore, we performed a region-specific KD of Sox11 in the dorsal DG, by using an AAV-1/2 (n=35) or an SCR control (n=34) injection (Figure 35C). ANOVA analysis revealed a significant downregulation of Sox11 in the DG region ($F_{1,36} = 12.674$, $p < 0.001$) (Figure 35A, B), with some spreading in the CA3 region of the hippocampal formation. KD efficiency in the DG was 30%.

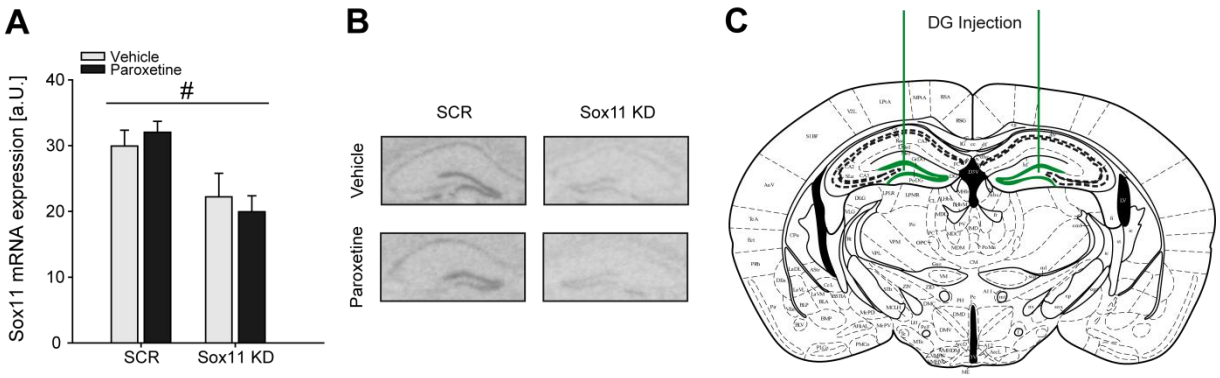

Figure 35: Sox11 KD in the dorsal hippocampus. (A) Sox11 mRNA expression levels in the dorsal HC. (B) Representative autoradiographs of Sox11 mRNA levels in the dorsal HC of vehicle and paroxetine treated animals as well as SCR control and Sox11 KD animals. (C) Schematic representation of the injection site (green). # significant ANOVA condition effect, $p < 0.05$.

We detected an increase in body weight gain after paroxetine treatment in the previous experiments. Therefore, we were also interested in this parameter after 28d of paroxetine treatment under Sox11 KD and control conditions. ANOVA analysis revealed a significant treatment effect in the paroxetine treated animals compared to the vehicle treated control group, independent of the condition ($F_{1,43} = 10.264$, $p < 0.01$) (Figure 36B). To analyze whether the Sox11 KD lead to any locomotor changes, we subjected the animals to the OF. ANOVA analysis revealed a significant treatment effect ($F_{1,43} = 4.887$, $p < 0.05$) but no condition or condition x treatment interaction effect (Figure 36G). Further, paroxetine treated animals were less immobile in the OF compared to vehicle treated animals ($F_{1,43} = 4.585$, $p < 0.05$, Sox11 OE vehicle: 169.22sec ± 21.76; Sox11 OE paroxetine: 148sec ± 10.55; SCR vehicle: 169.22sec ± 27.84; SCR paroxetine: 145.49sec ± 18.38).

As Sox11 OE led to a less anxious phenotype, we hypothesized that Sox11 KD would lead to a more anxious phenotype. Additionally, we were interested whether a chronic paroxetine treatment is able to reverse this effect. Therefore, we tested the animals in the DaLi. ANOVA analysis revealed a condition effect in the parameters distance in the light compartment ($F_{1,46} = 4.180$, $p < 0.05$), entries in the light compartment ($F_{1,46} = 24.290$, $p < 0.05$) (Figure 36E) as well as time in the light compartment ($F_{1,46} = 4.479$, $p < 0.05$) (Figure 36F). Paroxetine treatment did not influence anxiety-related behavior in this test. In order to investigate, depressive-like behavior in these animals we subjected them in a FST. ANOVA revealed that paroxetine treated animals showed significantly more time struggling compared to vehicle treated animals ($F_{1,42} = 23.222$, $p < 0.000$) (Figure 36C). This effect was independent of the genetic manipulation. Furthermore, we found that paroxetine treated animals floated significantly less time compared to vehicle treated

animals ($F_{1,42}$ = 22.967, $p < 0.000$) (Figure 36D) and showed a longer latency to float ($F_{1, 41}$ = 8.305, $p < 0.01$) (Sox11 KD vehicle: 90.32sec ± 8.61; Sox11 KD paroxetine: 110.45sec ± 13.10; SCR vehicle: 81.65sec ± 9.35; SCR paroxetine: 112.12sec ± 7.64).

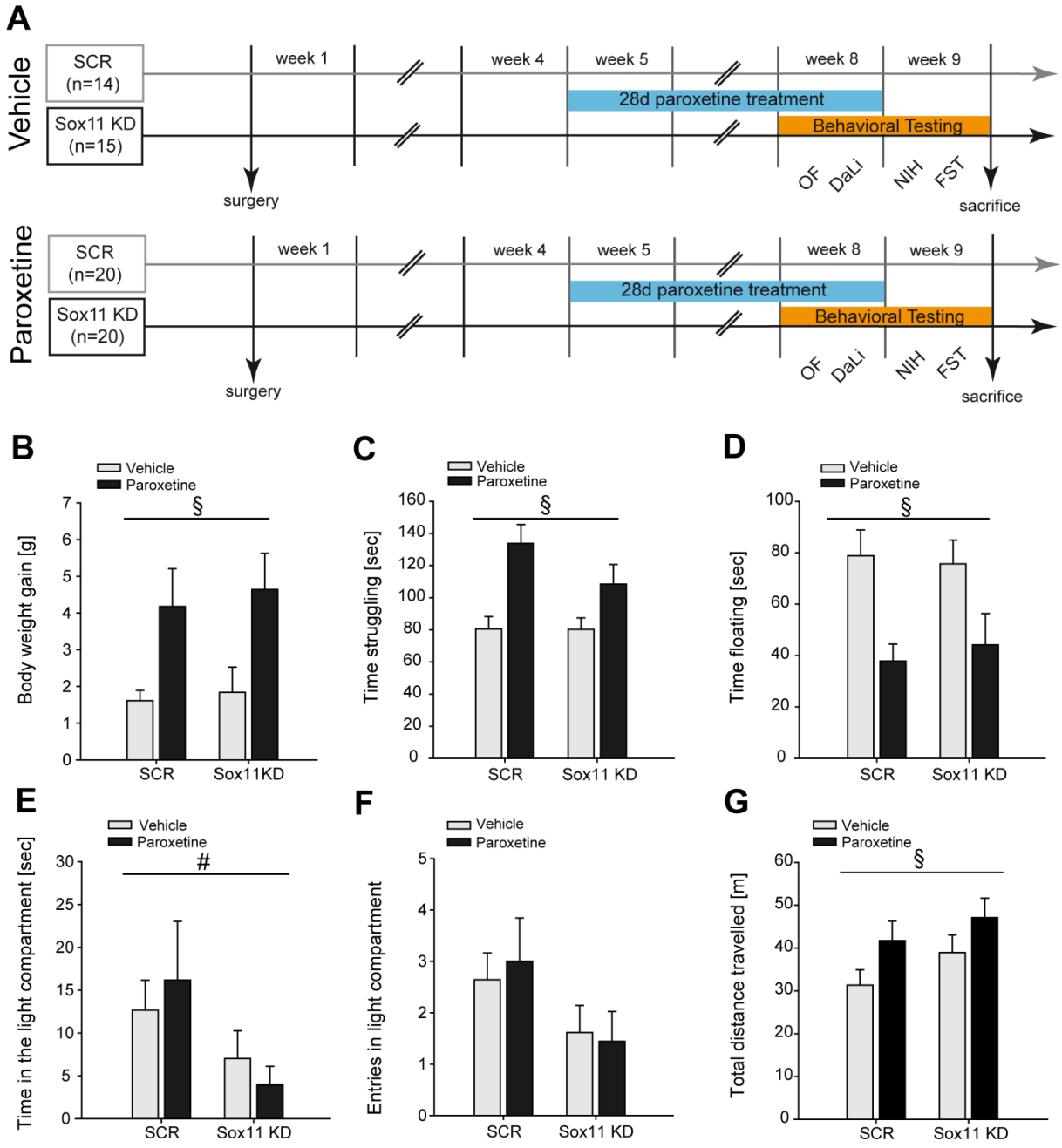

Figure 36: Physiological and behavioral effects of Sox11 KD. (A) Experimental time course. (B) Paroxetine led to an increase in body weight gain compared to vehicle treated animals, independent of the genotype. (C) Paroxetine led to more time struggling in the FST compared to vehicle treated animals, independent of the genotype. (D) Paroxetine led to a decrease in time floating compared to vehicle treated animals, independent of the genotype. (E) Viral KD of Sox11 led to a more anxious phenotype in DaLi compared to the empty control animals, whereas paroxetine was not able to reverse this effect. (F) When comparing entries in the light compartment, no significant difference could be found between the groups. (G) Paroxetine treated animals showed a higher general locomotor activity compared to vehicle treated control animals. This effect is independent of the condition. # overall ANOVA condition effect, $p < 0.05$, § overall ANOVA treatment effect, $p < 0.05$

During this study, we detected a higher mortality rate in the Sox11 KD animals, reflected by 9 (of 35) compared to 0 (of 34) in the SCR control animals (Fisher's exact test: $p < 0.005$).

3.4 Genes and pathways mediating an early onset of antidepressant response

The previous studies demonstrated that a 28d treatment regiment is well-suited to detect novel antidepressant-responsive genes. However, in order to differentiate between good and poor responders and even more to identify potential candidates mediating a more rapid onset of action, a shorter treatment period may be more promising. There is evidence from clinical studies, that some patients start responding to an antidepressant treatment already after 14d of antidepressant administration (Papakostas et al., 2006). According to this finding, we treated 140 male DBA/2J mice subchronically (14d) with 5mg/kg BW paroxetine (n=90) or vehicle (n=50) (Figure 37A).

To analyze the effects of subchronic paroxetine treatment on physiological parameters, body weight gain was assessed in these animals. 14d of paroxetine treatment (5mg/kg BW) led to a significant increase in body weight gain in the paroxetine treated animals compared to the vehicle treated animals ($T_{105} = -8.356$, $p < 0.000$) (Figure 37B). However, a subchronic paroxetine treatment did not significantly reduce corticosterone levels in the paroxetine treated animals compared to the vehicle treated control group. (Figure 37C).

We also investigated paroxetine brain and plasma levels after a subchronic treatment. ANOVA analysis showed a significant increase in plasma paroxetine concentrations in good responders compared to the intermediate responder group and the poor responder group ($F_{2,25} = 3.691$, $p < 0.05$). Further post-hoc analysis revealed a trend between good responders compared to the intermediate responder group and the poor responder group. No significant difference was found between the intermediate and the poor responder groups (Figure 37D). The same pattern was detected for paroxetine brain concentrations. Good responders showed significantly higher brain paroxetine concentrations compared to the intermediate responders and the poor responders ($F_{2,32} = 7.777$, $p < 0.01$). Further post-hoc analysis revealed a significant difference between good responders compared to the intermediate responder group and the poor responder group. No significant difference was found between the intermediate and the poor responders (Figure 37E). However, paroxetine brain and plasma concentrations were highly correlated ($r = 0.554$, $p < 0.000$)

(Figure 37F). For the here presented correlation analysis, we only analyzed poor and good responders.

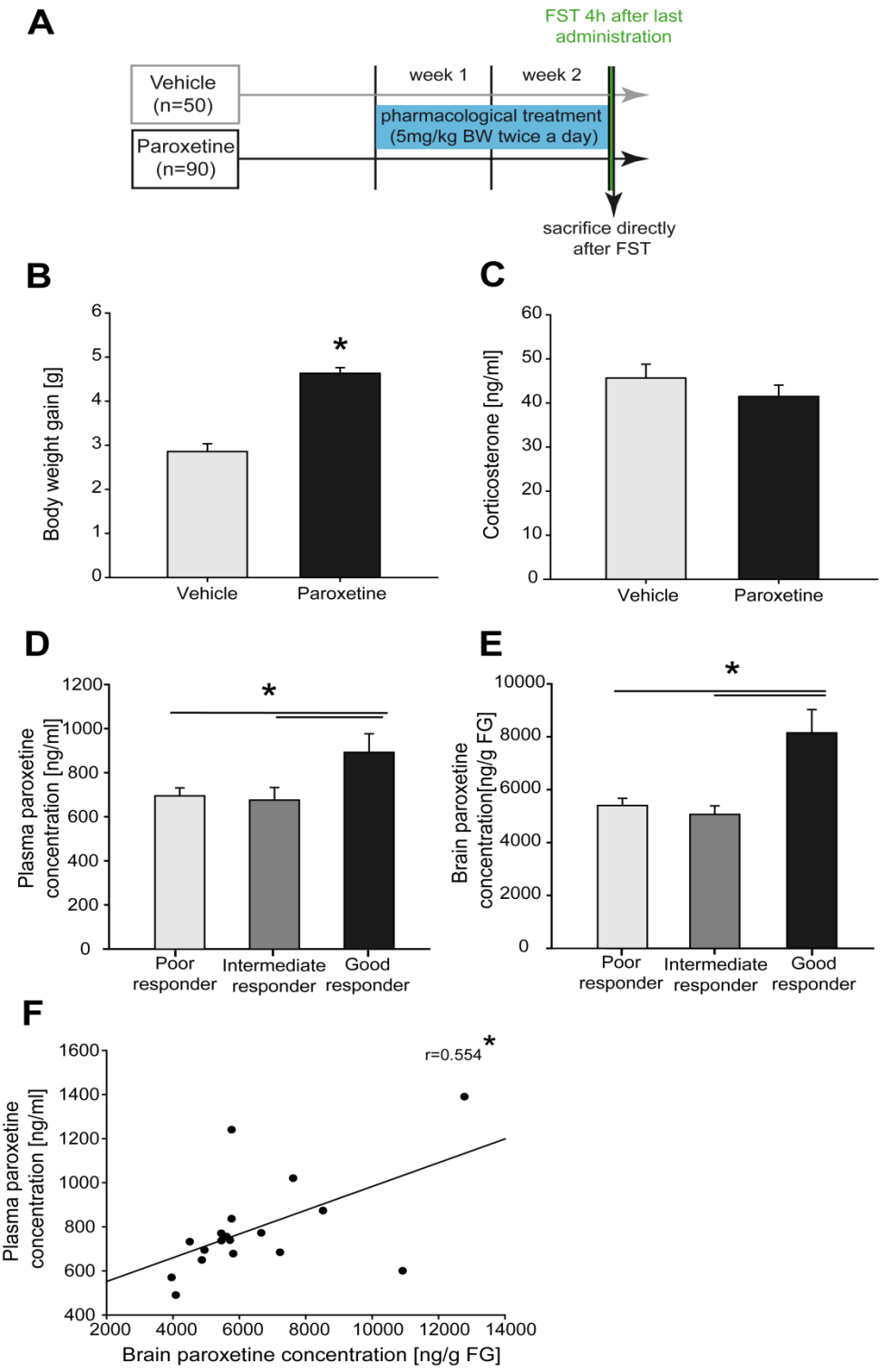

Figure 37: Neuroendocrine, physiological and pharmacological parameters after subchronic paroxetine treatment. (A) Experimental time course. (B) Paroxetine treated animals showed a significant increase in body weight gain compared to vehicle treated animals. (C) No difference was found in corticosterone levels between the groups. (D) Good responders showed significantly higher plasma paroxetine levels compared to poor and intermediate responders. (E) Good responders showed significantly higher brain paroxetine levels compared to poor and intermediate responders. (F) Paroxetine brain and plasma concentrations highly correlated with each other. * significant difference between vehicle treated control group and paroxetine treated group, $p < 0.05$.

To investigate the responder status within the paroxetine treated group, we subjected the animals to a FST. Overall, paroxetine treated animals showed significantly less time floating compared to vehicle treated control animals ($T_{80.701}$ = 9.157, p < 0.000) (Figure 38A and C). Furthermore, paroxetine treated animals also showed more active behavior compared to vehicle treated animals. The time swimming was increased in paroxetine-treated animals (T_{105} = -5.112, p < 0.000, vehicle: 112.05sec ± 4.74; paroxetine: 147.80sec ± 4.99;) as well as the time struggling ($T_{102.624}$ = -4.496, p < 0.000) (Figure 38B).

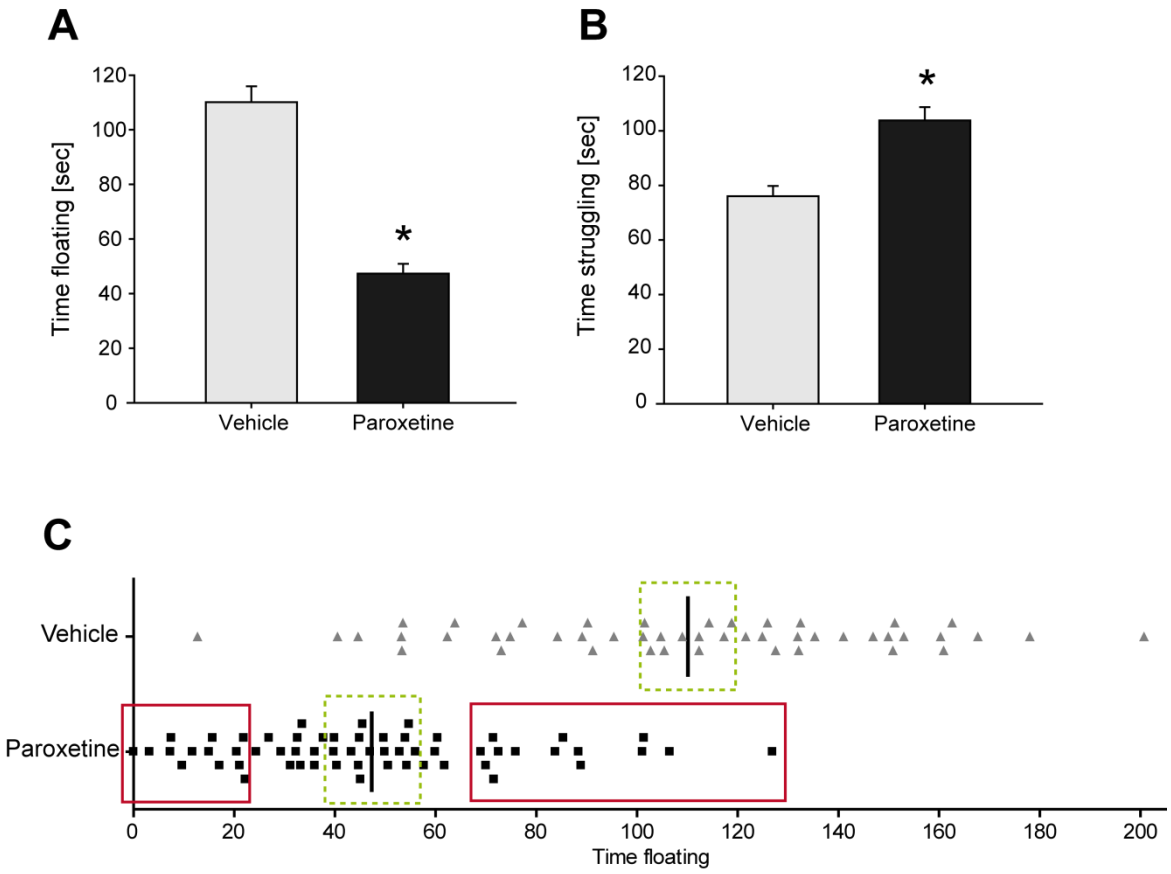

Figure 38: Subchronic paroxetine treatment led to a less depressive-like behavior in the FST. (A) Paroxetine treated animals showed less time floating compared to vehicle treated animals. (B) Paroxetine treated animals showed higher time floating compared to vehicle treated animals. (C) Identification of different responder groups according to their performance in the FST. Animals indicated in the red squares are referred as good and poor treatment responder. Animals that showed a very high time floating represent the poor treatment responder, whereas animals that showed a very low time floating represent the good treatment responder. Animals indicated in the green dotted square are representing internal control groups. The animals within the paroxetine treated group are representing the intermediate responder group and served as a treated control group. The animals within the vehicle treated group served as a vehicle treated control group. * significant difference between vehicle treated control group and paroxetine treated group, p < 0.05.

3.4.1 Brain Microarray analysis

The animals used for the Microarray analysis were part of the in the previous chapter described cohort. As we were aiming to identify novel genes and pathways determining early antidepressant response, we were interested in the individual time floating in the FST of these animals. After identifying good (n=12), poor (n=12) and intermediate (n=8) treatment responders as well as the vehicle treated control group (n=12) (for detailed information see 2.5) a whole-genome expression microarray was conducted with hippocampal brain tissue (Figure 38C). Analysis of the Illumina microarray chip revealed 101 differently regulated genes between vehicle treated animals and good responders at a false discovery controlled significant level of 10% ($q < 0.1$). Duplicates were removed in a next step (n=10) as well as genes that were detected by the microarray but were not specific for the respected gene (n=4). Resulting in 87 differentially regulated genes. A detailed gene list containing all relevant parameters can be found in Table 5. There were no significant differences between good and poor treatment responders.

Table 5: Significantly regulated genes in the hippocampal DG region 14d after paroxetine treatment. Genes are ordered by their functional classes. Fold Changes were normalized to vehicle treated animals.

Functional classification (according to Gene Ontology GO)	PROBE_ID	REFSEQ_ID	SYMBOL	Gene Name	q-Value	Fold change
adenylate cyclase activity						
	ILMN_2607127	NM_009623.2	Adcy8	adenylate cyclase 8	0.10	0.83
ATP binding						
	ILMN_2711562	NM_008846.2	Pip5k1b	phosphatidylinositol-4-phosphate 5-kinase, type 1 beta	0.09	0.84
calcium channel activity						
	ILMN_2915118	NM_013838.1	Trpc6	transient receptor potential cation channel, subfamily C, member 6	0.08	0.78
calcium ion binding						
	ILMN_2867771	NM_007601.1	Capn3	calpain 3	0.03	0.70
	ILMN_2928498	NM_029946.3	Efcab6	EF-hand calcium binding domain 6	0.08	1.31
	ILMN_1260538	XM_132034.1	Pcdh7	protocadherin 7	0.10	1.21
	ILMN_2697410	XM_130497.2	Ryr3	ryanodine receptor 3	0.06	0.80
Calmodulin binding						
	ILMN_1244364	NM_012040.2	Pnck	pregnancy upregulated non-ubiquitously expressed CaM kinase	0.07	0.78
DNA binding						
	ILMN_2730329	NM_175659.1	Hist1h2ah	histone cluster 1, H2ah	0.08	1.22
	ILMN_2725927	NM_009251.1	Serpina3g	serine (or cysteine) peptidase inhibitor, clade A, member 3G	0.09	1.71
	ILMN_1246800	NM_009252.2	Serpina3n	serine (or cysteine) peptidase inhibitor, clade A, member 3N	0.03	1.35
Enzyme activity						
	ILMN_1245509	NM_033149.2	B3galt5	UDP-Gal:betaGlcNAc beta 1,3-galactosyltransferase, polypeptide 5	0.06	0.81
	ILMN_2611295	NM_025869.3	Dusp26	dual specificity phosphatase 26 (putative)	0.07	1.32
	ILMN_2846194	NM_026728.1	Echdc2	enoyl Coenzyme A hydratase domain containing 2	0.03	0.75
	ILMN_1231336		Itih3	inter-alpha trypsin inhibitor, heavy chain 3	0.08	1.27
	ILMN_1225191	NM_172607.3	Naprt1	nicotinate phosphoribosyltransferase domain containing 1	0.08	1.23
	ILMN_2594525	NM_010941.3	Nsdhl	NAD(P) dependent steroid dehydrogenase-like	0.03	1.30
	ILMN_1222733	NM_011877.1	Ptpn21	protein tyrosine phosphatase, non-receptor type 21	0.08	0.81
	ILMN_2600348	NM_009270.3	Sqle	squalene epoxidase	0.08	1.24
	ILMN_2737163	NM_009270.3	Sqle	squalene epoxidase	0.10	1.21
extracellular matrix binding						
	ILMN_2964042	NM_007542.3	Bgn	biglycan	0.03	1.50
Growth factor activity						
	ILMN_2689790	NM_008344.2	Igfbp6	insulin-like growth factor binding protein 6	0.08	1.49
	ILMN_2760161	NM_008742.1	Ntf3	neurotrophin 3	0.08	0.70
	ILMN_2657828	NM_010117.1	Rhbdf1	rhomboid family 1 (Drosophila)	0.10	1.23
	ILMN_2492264	NM_018865.2	Wisp1	WNT1 inducible signaling pathway protein 1	0.10	1.35
GTP binding						
	ILMN_2719702	NM_145216.3	Rasl10a	RAS-like, family 10, member A	0.03	1.43
	ILMN_2653567	NM_023275.2	Rhoj	ras homolog gene family, member J	0.06	1.25
Hormone activity						
	ILMN_2955725	NM_007745.2	Cort	cortistatin	0.05	0.83
Immune system						
	ILMN_2671473	NM_207233.1	C1ql2	complement component 1, q subcomponent-like 2	0.03	1.49
	ILMN_3049559	NM_009780.1	C4b	complement component 4B (Chido blood group)	0.03	1.46
	ILMN_1223697	NM_001039150.1	Cd44	CD44 antigen	0.07	0.62
	ILMN_2725414	NM_007657.2	Cd9	CD9 antigen	0.09	0.82
	ILMN_1226829	NM_010740.3	Cd93	CD93 antigen	0.08	0.82
	ILMN_2671738	NM_010551.3	Il16	interleukin 16	0.09	0.83

Functional classification (according to Gene Ontology GO)	PROBE_ID	REFSEQ_ID	SYMBOL	Gene Name	q-Value	Fold change
Ion channel binding						
	ILMN_2645526	NM_011510.3	Abcc8	ATP-binding cassette, sub-family C	0.01	0.73
Ion channel binding	ILMN_1247335	NM_027782.1	Kctd6	potassium channel tetramerisation domain containing 6	0.07	0.81
metal ion binding						
	ILMN_1237725	NM_173451.2	Arsj	arylsulfatase J	0.09	1.27
	ILMN_2693403	NM_033612.1	Ela1	chymotrypsin-like elastase family, member 1	0.08	1.20
opioid peptide activity						
	ILMN_2719921	NM_001002927.2	Penk1	preproenkephalin	0.04	1.45
phospholipid binding						
	ILMN_2771559		Osbpl5	oxysterol binding protein-like 5	0.09	1.24
Protein binding						
	ILMN_2619107	NM_008495.1	Lgals1	lectin, galactose binding, soluble 1	0.05	1.38
Receptor activity						
	ILMN_2614086	NM_001033369.2	Acvr1c	Activin receptor 1c	0.08	1.53
	ILMN_3152476	NM_007418.2	Adra2c	adrenergic receptor, alpha 2c	0.06	1.36
	ILMN_2734062	NM_010076.2	Drd1a	dopamine receptor D1A	0.08	1.38
	ILMN_2865082	NM_008072.1	Gabrd	gamma-aminobutyric acid (GABA) A receptor, subunit delta	0.08	1.38
	ILMN_2698299	NM_008072.1	Gabrd	gamma-aminobutyric acid (GABA) A receptor, subunit delta	0.08	1.35
	ILMN_3073644	NM_019511.1	Ramp3	receptor (calcitonin) activity modifying protein 3	0.06	0.80
	ILMN_1215120	NM_013658.2	Sema4a	sema domain, immunoglobulin domain (Ig), transmembrane domain (TM) and short cytoplasmic domain, (semaphorin) 4A	0.06	1.29
	ILMN_1229577	NM_009217.1	Sstr2	somatostatin receptor 2	0.06	1.45
Receptor binding						
	ILMN_2872698	NM_172406.2	Trak2	trafficking protein, kinesin binding 2	0.03	1.28
	ILMN_2658908	NM_013655.2	Cxcl12	chemokine (C-X-C motif) ligand 12	0.10	0.84
Signal transduction						
	ILMN_2589790	NM_213659.2	Stat3	signal transducer and activator of transcription 3	0.08	1.27
Structural molecule						
	ILMN_1214715	NM_010277.2	Gfap	glial fibrillary acidic protein	0.08	1.66
	ILMN_2805339	NM_001012401.1	Hspb6	heat shock protein, alpha-crystallin-related, B6	0.09	1.64
	ILMN_1218347	NM_139300.3	Mylk	myosin, light polypeptide kinase	0.03	1.32
	ILMN_1219471	NM_139300.3	Mylk	myosin, light polypeptide kinase	0.08	1.23
	ILMN_1221835	NM_023716.2	Tubb2b	tubulin, beta 2B class IIB	0.06	1.38
	ILMN_2598715	NM_023716.1	Tubb2b	tubulin, beta 2B class IIB	0.08	1.36
	ILMN_1377919	NM_023716.2	Tubb2b	tubulin, beta 2B class IIB	0.08	1.24
	ILMN_2825574	NM_023716.1	Tubb2b	tubulin, beta 2B class IIB	0.09	1.30
	ILMN_2451022	NM_011701.3	Vim	vimentin	0.07	1.36
syntaxin-1 binding						
	ILMN_1227805	NM_001081344.1	Stxbp5	syntaxin binding protein 5 (tomosyn)	0.08	1.20
Transcription factor activity						
	ILMN_1235647	NM_009234.5	Sox11	SRY-box containing gene 11	0.10	1.46
transporter activity						
	ILMN_2622915		Slc14a1	solute carrier family 14 (urea transporter), member 1	0.06	1.26
	ILMN_1235006	NM_028122.3	Slc14a1	solute carrier family 14 (urea transporter), member 1	0.09	1.24
	ILMN_1218441	NM_194333.3	Slc23a3	solute carrier family 23 (nucleobase transporters), member 3	0.08	1.38
	ILMN_2593621	NM_009208.2	Slc4a3	solute carrier family 4 (anion exchanger), member 3	0.08	0.83
	ILMN_1248672	NM_201353.1	Slc6a7	solute carrier family 6 (neurotransmitter transporter, L-proline), member 7	0.06	1.24
zinc ion binding						
	ILMN_1256970		Adamts18	a disintegrin-like and metallopeptidase (reprolysin type) with thrombospondin type 1 motif, 18	0.08	1.35
	ILMN_2655795	NM_007607.1	Car4	carbonic anhydrase 4	0.10	0.82
	ILMN_2606162	NM_019417.2	Pdlim4	PDZ and LIM domain 4	0.08	1.42
Others						
	ILMN_3119914	NM_001081156.1	2300002D11R	TMF1-regulated nuclear protein 1	0.08	1.30
	ILMN_2777175		2310004N11R	serine/threonine kinase 40	0.10	1.38
	ILMN_2700344	XM_001478683.1	2310046A06R	RIKEN cDNA 2310046A06 gene	0.09	0.77
	ILMN_2761585	XM_358687.1	2400009B08R	RIKEN cDNA 2400009B08 gene	0.08	1.23
	ILMN_2641486	XM_126991.8	3830431G21R	RIKEN cDNA 3830431G21 gene	0.09	0.82
	ILMN_1250860	NM_177717.3	4732456N10R	RIKEN cDNA 4732456N10 gene	0.06	1.31
	ILMN_2433166		4933439C10R	RIKEN cDNA 4933439C10 gene	0.03	0.81
	ILMN_2599214		6430548M08I	RIKEN cDNA 6430548M08 gene	0.08	1.26
	ILMN_1221652		B930090K24R	Ensembl kein Ergebnis	0.08	1.33
	ILMN_2463583		C030009J22Ri	Ensembl kein Ergebnis	0.10	1.20
	ILMN_2814927	NM_007693.1	Chga	chromogranin A	0.08	1.42
	ILMN_1213374		D330040L23R	Ensembl kein Ergebnis	0.06	0.78
	ILMN_2963091	NM_175332.3	E130012A19R	RIKEN cDNA E130012A19 gene	0.07	0.65
	ILMN_1244448		E230013M07I	Ensembl kein Ergebnis	0.07	1.25
	ILMN_2984744	NM_010129.1	Emp3	epithelial membrane protein 3	0.06	1.29
	ILMN_2537782	XM_358960.1	LOC385825	Ensembl kein Ergebnis	0.09	0.81
	ILMN_2540103	XR_031145.1	LOC666559	Ensembl kein Ergebnis	0.09	1.24
	ILMN_2991389	NM_027366.1	Ly6g6e	lymphocyte antigen 6 complex, locus G6E	0.06	1.99
	ILMN_3161834	NM_001030294.1	Olfm4	olfactomedin 4	0.09	1.37
	ILMN_1214474	XM_132396.8	Rimbp2	RIMS binding protein 2	0.08	1.24
	ILMN_1251651	NM_001081388.1	Rimbp2	RIMS binding protein 3	0.08	1.23
	ILMN_2643212	NM_023396.4	Rprm	reprimo, TP53 dependent G2 arrest mediator candidate	0.03	1.81
	ILMN_2889832	NM_001034870.2	Serpina3h	serine (or cysteine) peptidase inhibitor, clade A, member 3H	0.05	2.56
	ILMN_2639239	NM_011340.3	Serpinf1	serine (or cysteine) peptidase inhibitor, clade F, member 1	0.03	1.42
	ILMN_2471166	NM_145439.1	Tmc6	transmembrane channel-like gene family 6	0.09	1.24
	ILMN_2513778	NM_145439.1	Tmc6	transmembrane channel-like gene family 6	0.09	1.23
	ILMN_1231705	NM_028355.3	Tmem48	transmembrane protein 48	0.10	1.19
	ILMN_2454692	NM_145500.3	Ubtd1	ubiquitin domain containing 1	0.04	1.29
	ILMN_2789692	NM_009528.2	Wnt7b	wingless-related MMTV integration site 7B	0.07	1.35

3.4.2 Identification of potential networks via pathway analysis in the hippocampus

In order to identify novel genes and pathways that might play a role in mediating an early antidepressant response in DBA/2J mice, we performed a pathway analysis with the 87 genes detected by the microarray. We identified a pathway formed out of 15 genes (Figure 39) that originated from the microarray result, after applying these genes to the Pathway Studio software v7.1 (Ariadne Genomics, Rockville, MD, USA), which contains literature-based relations between proteins, small molecules and cellular processes (Webhofer et al., 2011).

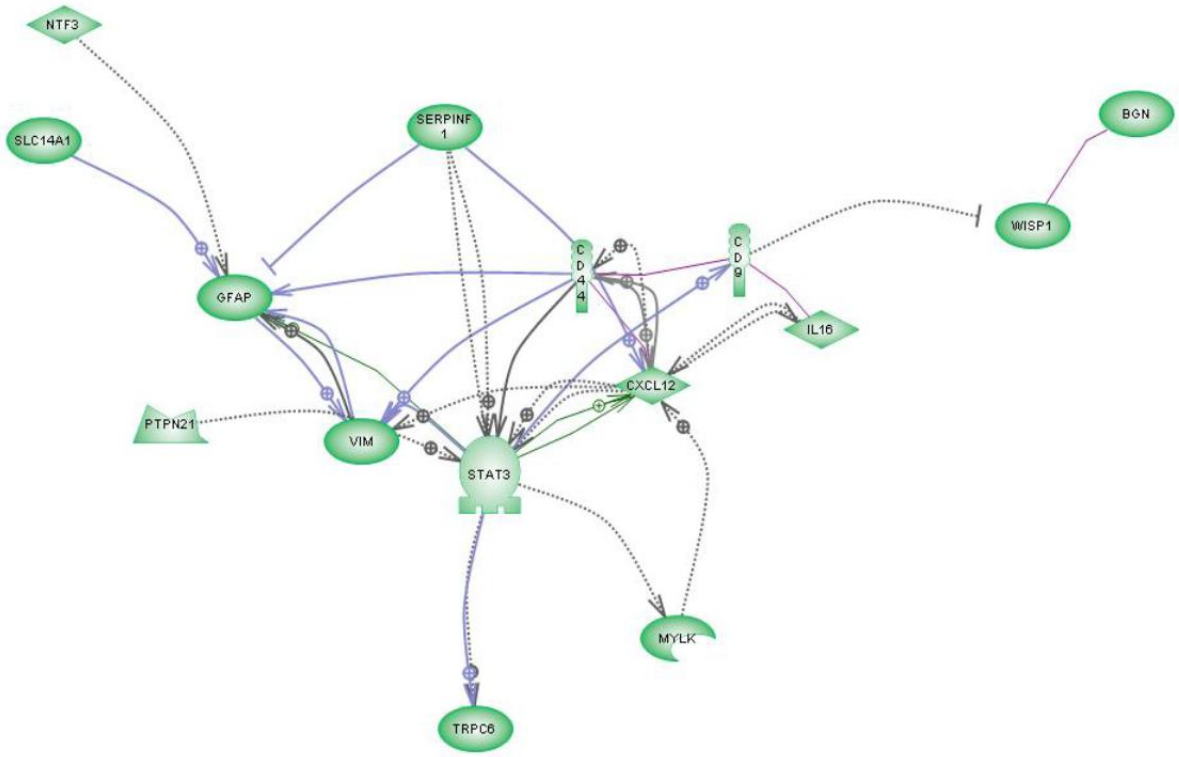

Figure 39: Pathway analysis of altered genes after 14d of paroxetine treatment. 15 out of 87 genes were clustered in a common pathway via the Pathway analysis software.

3.4.3 Validation of potential candidates with qRT-PCR

After performing the pathway analysis, 14 genes were selected for further investigation. The samples derived from the microarray analysis were used for qRT PCR as technical control replicates. We investigated mRNA expression levels with normalization to Hprt. 10 out of the 14 selected candidates could be validated. Bgn was significantly upregulated in the good responders after 14d of paroxetine treatment compared to the vehicle treated

control group (T_{22} = -2.141, $p < 0.05$) (Figure 40A). The same regulation pattern was found for Gfap ($T_{11.360}$ = -2.553, $p < 0.05$) (Figure 40D), Serpinf1 ($T_{17.725}$ = -2.730, $p < 0.05$) (Figure 40I), Slc14A1 ($T_{13.506}$ = -2.289, $p < 0.05$) (Figure 40J), Vim (T_{21} = -2.835, $p < 0.01$) (Figure 40M), Wisp1 (T_{20}= -2.789, $p < 0.05$) (Figure 40N). Good responders showed a trend in Cd9 upregulation compared to vehicle treated animals (T_{22} = -1.997, $p = 0.058$) (Figure 40B). However, we also detected genes that show a significant downregulation in the good treatment responders after 14d of paroxetine treatment compared to the vehicle treated control group, such as Cxcl12 (T_{22} = 2.2.39, $p < 0.05$) (Figure 40C),Il16 (T_{22} = 3.319, $p < 0.005$) (Figure 40E), Ntf3 (T_{22} = 4.537, $p < 0.000$) (Figure 40G) and Trpc6 (T_{22}= 2.995, $p <0.01$) (Figure 40L). Mylk (Figure 40F), Ptpn21 (Figure 40H) and Stat3 (Figure 40K) did not show any significant gene expression alterations between the two treatment groups.

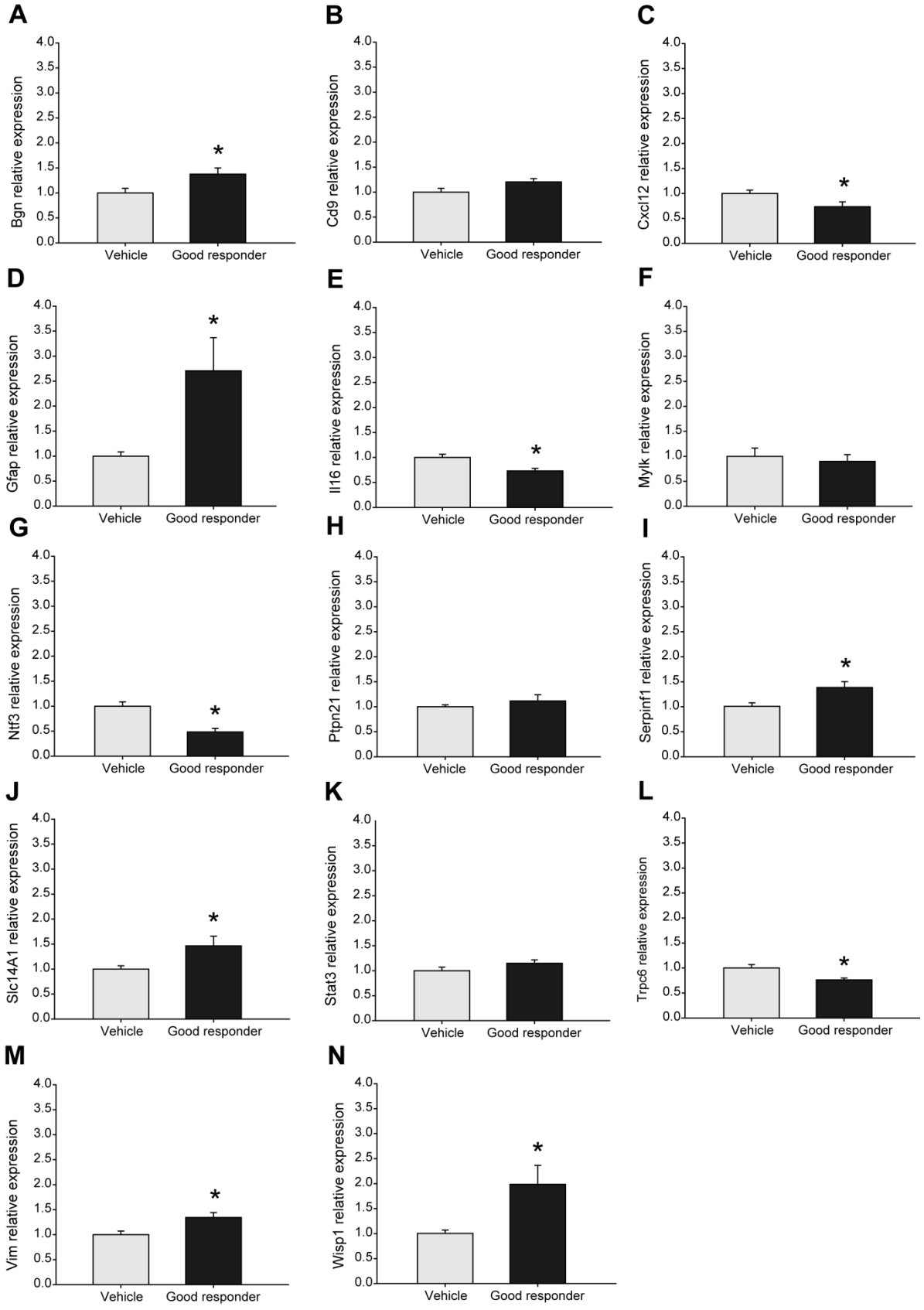

Figure 40: Validation of candidate genes from the microarray. Out of 14 selected candidates, the mRNA of 10 transcripts were significantly differently regulated in the hippocampus after 14d of paroxetine treatment (A-N). * significant different to vehicle treated control animals $p < 0.05$.

3.4.4 Time course of gene expression regulation during antidepressant treatment in the mouse hippocampus

Interestingly, more genes were regulated following subchronic paroxetine treatment compared to chronic treatment. When comparing the gene expression profiles of the two treatment time points, we identified an overlap of 15 genes differently regulated following both treatment intervals (Table 6). The 15 detected genes in the overlap were equivalent to 17.2% of the total number of genes found after 14d of treatment and 50% of the genes detected after 28d of treatment.

Table 6: Differently regulated genes after 14d and 28d of paroxetine treatment. When comparing the genes differently regulated after 14d and 28d, we detected an overlap of 15 genes, which were regulated after both treatment time points.

Gene symbol	Gene name	Fold Change 14d	Fold Change 28d
Acvr1c	activin A receptor, type 1c	1.53	1.65
Adra2c	adrenergic receptor, alpha 2c	1.36	1.27
Arsj	arylsulfatase J	1.27	1.30
C1ql2	complement component 1, q subcomponent-like 2	1.49	1.62
Cort	cortistatin	0.83	0.63
Drd1a	dopamine receptor D1A	1.38	1.44
Igfbp6	insulin-like growth factor binding protein 6	1.49	1.47
Olfm4	olfactomedin 4	1.37	1.37
Pnck	pregnancy up-regulated nonubiquitously expressed CaM kinase	0.78	0.76
Serpina3n	serine (or cysteine) peptidase inhibitor, clade A, member 3N	1.35	1.35
Serpinf1	pigment epithelium-derived factor	1.42	1.49
Sox11	SRY-box containing gene 11	1.46	1.52
Sstr2	somatostatin receptor 2	1.45	1.46
Trak2	trafficking protein, kinesin binding 2	1.28	1.33
Wisp1	WNT1 inducible-signaling pathway protein 1	1.35	1.33

3.4.5 Transcriptome signatures predicting antidepressant response in the periphery

We aimed at the detection of novel genes and pathways in the periphery of DBA/2J mice mediating an early antidepressant response not only in the brain but also in the periphery. This could potentially provide novel information on individual antidepressant treatment outcome after subchronic treatment. Therefore, we conducted a whole-genome expression microarray analysis by using peripheral blood. For this purpose gene expression data sets of vehicle treated animals (n=12), good responders (n=12) and poor responders (n=12) were created and analyzed. In pairwise group comparisons both treatment effect and response status of mice were evaluated in respect to antidepressant treatment. Technical batch effects in the data set and measured drug concentrations in

blood were used as covariates in an ANOVA based statistical model. Although no robust gene regulation was apparent when comparing treatment groups (independent of response) with the control group. However, there was a pronounced effect within the treatment group. Interestingly, we were able to detect a set of 259 transcripts that show a significant change in expression due to antidepressant response status at a false discovery controlled significance level of 10% ($q < 0.1$) (Table 7).

Table 7: Significantly regulated genes in the peripheral blood between good and poor responders after 14d of paroxetine treatment. Genes are ordered according their functional classes. Fold changes are normalized to poor responders.

Functional classification (according to Gene Ontology GO)	PROBE_ID	REFSEQ_ID	SYMBOL	Gene Name	q-Value	Fold change
1-phosphatidylinositol-3-kinase activity						
	ILMN_3128616	NM_008840.2	Pik3cd	Phosphatidylinositol-4,5-Bisphosphate 3-Kinase, Catalytic SubunitDelta	0.09	0.92
actin binding						
	ILMN_3007072	NM_024427.2	Tpm1	Tropomyosin 1 (Alpha)	0.04	1.18
	ILMN_1219471	NM_139300.3	Mylk	Myosin Light Chain Kinase	0.09	1.35
	ILMN_3033533	NM_001024458.1	Add1	Adducin 1 (Alpha)	0.06	1.12
	ILMN_2955973	NM_013870.1	Smtn	smoothelin	0.09	1.15
	ILMN_2604521	XM_150115.1	Cotl1	Coactosin-Like 1 (Dictyostelium)	0.04	1.21
	ILMN_2977404	NM_021883.1	Tmod1	Tropomodulin 1	0.03	1.32
antioxidant activity						
	ILMN_1252204	NM_009156.2	Sepw1	Selenoprotein W, 1	0.03	1.18
apoptotic process						
	ILMN_2674095	NM_134141.4	Ciapin1	Cytokine Induced Apoptosis Inhibitor 1	0.05	0.87
ATP-dependent DNA helicase activity; mRNA binding						
	ILMN_2774825	NM_013716.2	G3bp1	GTPase Activating Protein (SH3 Domain) Binding Protein 1	0.03	0.88
ATP-dependent helicase activity						
	ILMN_3025192	NM_001081107.1	Hel308	Helicase, POLQ-Like	0.10	0.91
calcium ion binding						
	ILMN_2628757	NM_010119.5	Ehd1	EH-Domain Containing 1	0.10	1.13
	ILMN_2718589	NM_007995.3	Fcna	Ficolin (Collagen/Fibrinogen Domain Containing) A	0.09	1.08
	ILMN_1216871	NM_008879.3	Lcp1	Lymphocyte Cytosolic Protein 1 (L-Plastin)	0.09	1.10
cation channel activity						
	ILMN_2932453	NM_008771.2	P2rx1	Purinergic Receptor P2X, Ligand-Gated Ion Channel, 1	0.09	1.20
cell surface						
	ILMN_2700292	NM_010376.3	H13	histocompatibility 13	0.05	0.88
choline transmembrane transporter activity						
	ILMN_1254938	NM_133891.2	Slc44a1	Solute Carrier Family 44 (Choline Transporter), Member 1	0.03	1.12
chromatin binding						
	ILMN_3154409	NM_010238.3	Brd2	Bromodomain Containing 2	0.03	0.86
	ILMN_2652187	NM_198602.2	Cux1	Cut-Like Homeobox 1	0.03	1.26
cysteine-type peptidase activity						
	ILMN_2706451	NM_001003971.1	Senp7	SUMO1/Sentrin Specific Peptidase 7	0.06	0.86
cytochrome-c oxidase activity						
	ILMN_2764551	NM_183405.1	Cox6b2	Cytochrome C Oxidase Subunit VIb Polypeptide 2 (Testis)	0.09	1.16
cytokine receptor activity; transmembrane signaling receptor activity						
	ILMN_1226499	NM_010823.1	Mpl	Myeloproliferative Leukemia Virus Oncogene	0.06	1.15
cytoplasm						
	ILMN_2684300	NM_026549.3	Pdcd2l	Programmed Cell Death 2-Like	0.08	0.89
	ILMN_1246770	AK029441	Ybx3	Y Box Binding Protein 3	0.09	0.89
cytoplasmic microtubule; microtubule associated complex						
	ILMN_2495703	NM_001039162.1	Clip2	CAP-GLY Domain Containing Linker Protein 2	0.03	1.14
DNA binding						
	ILMN_1252136	NM_175661.1	Hist1h2af	Histone cluster 1, H2af	0.04	1.20
	ILMN_2680066	NM_009087.1	Polr1d	Polymerase (RNA) I Polypeptide D, 16kDa	0.02	0.86
DNA-directed RNA polymerase activity; protein kinase activity						
	ILMN_2874443	NM_145632.1	Polr2h	Polymerase (RNA) II (DNA Directed) Polypeptide H	0.04	0.86
double-stranded RNA binding; ATP-dependent RNA helicase activity						
	ILMN_2546724	NM_019553.2	Ddx21	DEAD (Asp-Glu-Ala-Asp) Box Helicase 21	0.02	0.83
electron carrier activity						
	ILMN_1250947	NM_145367.3	Txndc5	Thioredoxin Domain Containing 5 (Endoplasmic Reticulum)	0.07	0.88
enzyme activator activity						
	ILMN_2780167	NM_145131.1	Pitrm1	Pitrilysin Metallopeptidase 1	0.09	1.15
eutral amino acid transmembrane transporter activity						
	ILMN_1229667	NM_001083809.1	Slc43a1	Solute Carrier Family 43 (Amino Acid System L Transporter), Member 1	0.07	1.19
exocyst						
	ILMN_2841290	NM_009396.1	Tnfaip2	Tumor Necrosis Factor, Alpha-Induced Protein 2	0.07	1.21
extracellular matrix structural constituent						
	ILMN_2609813	NM_007695.2	Chi3l1	Chitinase 3-Like 1 (Cartilage Glycoprotein-39)	0.08	1.24
galactosyltransferase activity						
	ILMN_2754594	NM_146045.1	B4galt7	Xylosylprotein Beta 1,4-Galactosyltransferase, Polypeptide 7	0.06	0.90
GTP binding						
	ILMN_1240466	NM_178041.1	Eif5	Eukaryotic Translation Initiation Factor 5	0.08	1.22
	ILMN_1236553	NM_174960.2	Gimap9	GTPase, IMAP Family Member 7	0.07	0.86
	ILMN_3161289	NM_010311.3	Gnaz	Guanine Nucleotide Binding Protein (G Protein), Alpha Z Polypeptide	0.09	1.21
	ILMN_2623184	NM_028024.2	Nkiras2	NFKB Inhibitor Interacting Ras-Like 2	0.09	1.14
	ILMN_2887208	NM_029576.1	Rab1b	RAB1B, Member RAS Oncogene Family	0.08	1.11
GTPase activator activity						
	ILMN_2954575	NM_001005508.1	Arhgap30	Rho GTPase Activating Protein 30	0.09	0.88
	ILMN_1238871	NM_025709.2	Gapvd1	GTPase Activating Protein And VPS9 Domains 1	0.08	1.12
	ILMN_2862760	NM_010273.1	Gdi1	GDP Dissociation Inhibitor 1	0.09	1.11

Functional classification (according to Gene Ontology GO)	PROBE_ID	REFSEQ_ID	SYMBOL	Gene Name	q-Value	Fold change
histone acetyl-lysine binding						
	ILMN_3154409	NM_010238.3	Brd2	Bromodomain Containing 2	0.03	0.86
histone deacetylase binding; protein serine/threonine kinase activity						
	ILMN_2768805	NM_178654.3	Pkn2	Protein Kinase N2	0.06	1.26
hydrolase activity						
	ILMN_1257102	NM_144815.2	Cecr5	Cat Eye Syndrome Chromosome Region, Candidate 5	0.04	0.89
	ILMN_2759598	NM_026871.1	Hint2	Histidine Triad Nucleotide Binding Protein 2	0.09	0.91
	ILMN_1234759	NM_026623.3	Nudt21	Nudix (Nucleoside Diphosphate Linked Moiety X)-Type Motif 21	0.04	0.84
identical protein binding						
	ILMN_1217102	NM_145853.2	Tpcn1	Two Pore Segment Channel 1	0.10	1.09
integral to membrane						
	ILMN_2795854	NM_138743.2	1190017O12Rik	RIKEN cDNA 1190017O12 gene	0.01	0.86
	ILMN_2698221	XM_913080.3	Bean	Brain Expressed, Associated With NEDD4, 1	0.10	1.15
	ILMN_2992541	NM_025516.2	Ergic3	ERGIC And Golgi 3	0.09	1.08
	ILMN_2906430	NM_017480.1	Icos	Inducible T-Cell Co-Stimulator	0.08	0.87
	ILMN_1221624	NM_134060.2	Slc35b3	Solute Carrier Family 35 (Adenosine 3'-Phospho 5'-Phosphosulfate Transporter), Member B3	0.09	0.91
	ILMN_2696272	NM_146103.1	Tmem185b	Transmembrane Protein 185B	0.09	0.92
	ILMN_2473122	NM_207301.1	Wrb	Tryptophan Rich Basic Protein	0.07	0.89
	ILMN_1226325	NM_033569.2	Cnnm2	Cyclin M2	0.06	1.17
	ILMN_1219904	NM_146173.2	Tspan33	Tetraspanin 33	0.03	1.30
integrin binding						
	ILMN_1215847	NM_010277	Gfap	Glial Fibrillary Acidic Protein	0.05	1.15
ion channel binding						
	ILMN_2713285	NM_001077361.1	Fhl1	Four And A Half LIM Domains 1	0.09	1.15
iron ion binding						
	ILMN_2827535	NM_007440.2	Alox12	Arachidonate 12-Lipoxygenase	0.09	1.15
kinase binding						
	ILMN_1215847	NM_010277	Gfap	Glial Fibrillary Acidic Protein	0.05	1.15
	ILMN_2690460	NM_178394.3	Jakmip1	Janus Kinase And Microtubule Interacting Protein 1	0.05	0.86
lavin adenine dinucleotide binding; N,N-dimethylaniline monooxygenase activity						
	ILMN_1230890	NM_010232.3	Fmo5	Flavin Containing Monooxygenase 5	0.03	1.14
lysosomal membrane						
	ILMN_1237208	NM_010684.2	Lamp1	Lysosomal-Associated Membrane Protein 1	0.04	1.15
magnesium ion binding						
	ILMN_1232884	NM_011451.2	Sphk1	Sphingosine Kinase 1	0.07	1.16
MAP kinase activity						
	ILMN_2715744	NM_011952.1	Mapk3	Mitogen-Activated Protein Kinase 3	0.06	1.14
metal ion binding						
	ILMN_2596534	NM_172124.2	B3gat2	Beta-1,3-Glucuronyltransferase 2 (Glucuronosyltransferase S)	0.06	1.20
	ILMN_2668996	NM_032540.2	Kel	Kell Blood Group, Metallo-Endopeptidase	0.08	1.28
	ILMN_1214899	NM_153104.2	Phospho1	Phosphatase, Orphan 1	0.03	1.25
	ILMN_3046846	NM_001033865.1	Rps27a	Ribosomal Protein S27a	0.09	0.90
molecular function						
	ILMN_2664726	XM_203393.1	3110013H01Rik	Centromere Protein V	0.06	1.16
	ILMN_2605694	NM_025327.2	Krtcap2	Keratinocyte Associated Protein 2	0.09	0.92
	ILMN_2630018	NM_018810.2	Mkrn1	Makorin Ring Finger Protein 1	0.09	1.19
	ILMN_1223346	NM_011354.2	Serf2	Small EDRK-Rich Factor 2	0.08	1.12
	ILMN_2804559	NM_178638.2	Tmem108	Transmembrane Protein 108	0.03	0.86
NAD+ ADP-ribosyltransferase activity enzyme binding						
	ILMN_1221470	XM_917270.3	Tnks2	Tankyrase, TRF1-Interacting Ankyrin-Related ADP-Ribose Polymerase 2	0.01	0.83
NADH dehydrogenase (ubiquinone) activity						
	ILMN_1216007	NM_026614.2	Ndufa5	NADH Dehydrogenase (Ubiquinone) 1 Alpha Subcomplex, 5	0.08	0.89
	ILMN_2976591	NM_024220.1	Ndufc2	NADH Dehydrogenase (Ubiquinone) 1, Subcomplex Unknown, 2, 14.5kDa	0.03	0.86
no information on genecards						
	ILMN_1259814	AK003858	1110020G09Rik	no information on genecards	0.05	1.23
	ILMN_1259764	XM_203453	1500005K14Rik	no information on genecards	0.07	0.86
	ILMN_1235281	NM_174987.3	1810063B05Rik	no information on genecards	0.04	0.87
	ILMN_2490820	N/A	2310005L22Rik	no information on genecards	0.06	0.88
	ILMN_1227110	AK009331	2310014B11Rik	no information on genecards	0.04	1.23
	ILMN_2673380	NM_025605.2	2400001E08Rik	no information on genecards	0.06	0.90
	ILMN_2452717	N/A	2610019E17Rik	no information on genecards	0.06	0.90
	ILMN_1256701	XM_001474596.1	2900016B01Rik	no information on genecards	0.05	0.87
	ILMN_1221714	NM_197959.1	3000004C01Rik	no information on genecards	0.09	1.09
	ILMN_2807335	NM_025626.3	3110001A13Rik	no information on genecards	0.06	0.89
	ILMN_1235047	NM_028439.1	3110009E18Rik	no information on genecards	0.10	0.90
	ILMN_2943685	NM_133797.1	4833439L19Rik	no information on genecards	0.07	1.13
	ILMN_2869623	NM_029528.2	6330503C03Rik	no information on genecards	0.06	1.10
	ILMN_3109491	NM_145836.1	6430527G18Rik	no information on genecards	0.05	0.86
	ILMN_1244531	AK034086	9330155C01Rik	no information on genecards	0.09	1.12
	ILMN_1245887	N/A	9626100_224	no information on genecards	0.08	1.12
	ILMN_1243621	AK037550	A130026C10Rik	no information on genecards	0.09	0.87
	ILMN_2552983	AK037815	A130052C08Rik	no information on genecards	0.04	0.88
	ILMN_2568488	AK041191	A530089A20Rik	no information on genecards	0.07	1.16
	ILMN_2595814	XM_145254	A630082K20Rik	no information on genecards	0.07	1.23
	ILMN_2603662	NM_172691.2	B230312A22Rik	no information on genecards	0.03	1.35
	ILMN_2598927	XM_356186.1	B930007L02Rik	no information on genecards	0.05	0.88
	ILMN_2746830	NM_177564.4	BC022224	no information on genecards	0.09	1.21
	ILMN_2656422	NM_153513.1	BC028528	Chromosome 1 Open Reading Frame 54	0.08	0.90
	ILMN_2484932	N/A	C030002B11Rik	no information on genecards	0.07	0.90
	ILMN_1244149	NM_177994.4	C030046I01Rik	no information on genecards	0.09	1.17
	ILMN_1223511	NM_207265.2	C230071H18Rik	no information on genecards	0.09	0.89

Functional classification (according to Gene Ontology GO)	PROBE_ID	REFSEQ_ID	SYMBOL	Gene Name	q-Value	Fold change
no information on genecards	ILMN_1222071	N/A	C920004C08Rik	no information on genecards	0.08	1.17
	ILMN_2755492	NM_138587.3	D6Wsu176e	no information on genecards	0.08	0.89
	ILMN_1227976	AK088915	E430031D18Rik	no information on genecards	0.06	0.89
	ILMN_2681030	XM_894495.2	EG629595	no information on genecards	0.08	0.89
	ILMN_2742647	XM_984926.2	EG666609	no information on genecards	0.03	0.84
	ILMN_1256844	XR_002259.2	EG668850	no information on genecards	0.10	0.86
	ILMN_3161168	NM_001033488.1	Gm1964	no information on genecards	0.10	1.24
	ILMN_3161500	NM_001033780.2	I830077J02Rik	no information on genecards	0.07	1.17
	ILMN_1236868	AK013239	Idb2	no information on genecards	0.04	0.87
	ILMN_2499056	N/A	IGKV2-137_AJ2312	no information on genecards	0.06	0.88
	ILMN_1239776	XM_001474366.1	LOC100040243	no information on genecards	0.05	0.87
	ILMN_1260447	XM_001479822.1	LOC100043192	no information on genecards	0.09	0.83
	ILMN_2628271	XR_032154.1	LOC100045967	no information on genecards	0.08	1.11
	ILMN_1222674	XM_001476743.1	LOC100046746	no information on genecards	0.10	1.20
	ILMN_2725464	XM_001477084.1	LOC100046930	no information on genecards	0.04	0.86
	ILMN_1255556	XM_001477665.1	LOC100047214	no information on genecards	0.08	1.19
	ILMN_2739156	XM_001477752.1	LOC100047260	no information on genecards	0.07	1.14
	ILMN_2437513	XM_001479238.1	LOC100047963	no information on genecards	0.09	1.12
	ILMN_2531208	XM_124826.2	LOC232606	no information on genecards	0.03	0.80
	ILMN_1240350	XM_354604.1	LOC380692	no information on genecards	0.09	0.88
	ILMN_2536116	XM_356731.1	LOC382885	no information on genecards	0.07	0.86
	ILMN_2736999	XR_031998.1	LOC621824	no information on genecards	0.08	1.20
	ILMN_1259869	XR_032410.1	LOC622655	no information on genecards	0.04	0.83
	ILMN_1229210	XM_925296.2	LOC640739	no information on genecards	0.08	1.11
	ILMN_1217489	XM_001473434.1	LOC671878	no information on genecards	0.04	0.88
	ILMN_1221126	XM_001479274.1	LOC675440	no information on genecards	0.04	0.91
	ILMN_2674666	XM_987671.1	LOC676136	no information on genecards	0.09	0.84
	ILMN_1251853	XM_992449.1	LOC676724	no information on genecards	0.03	0.85
	ILMN_1237466	XM_001003781.1	LOC677008	no information on genecards	0.04	0.89
	ILMN_2549544	AK008185	Mapbpip-pending	no information on genecards	0.06	0.89
	ILMN_2722938	NM_008654.1	Myd116	no information on genecards	0.07	1.19
	ILMN_2965417	NR_002702.1	Npm3-ps1	no information on genecards	0.07	0.89
	ILMN_3059476	NM_001013370.1	Sesn1	Sestrin 1	0.03	0.85
nucleic acid binding						
	ILMN_2971481	NM_023162.3	Znrd1	Zinc Ribbon Domain Containing 1	0.07	0.84
nucleotide binding						
	ILMN_2603834	NM_016865.2	Htatip2	HIV-1 Tat Interactive Protein 2, 30kDa	0.08	1.12
	ILMN_1240979	NM_019547.2	Rbm38	RNA Binding Motif Protein 38	0.04	1.18
nucleus						
	ILMN_1216690	NM_173736.2	Samd11	Sterile Alpha Motif Domain Containing 11	0.08	1.19
ornithine decarboxylase inhibitor activity						
	ILMN_2683794	NM_010952.2	Oaz2	Ornithine Decarboxylase Antizyme 2	0.03	1.19
others						
	ILMN_2908981	NM_028768.1	Armc8	Armadillo Repeat Containing 8	0.03	0.89
	ILMN_1239632	NM_023893.3	Ng23	Suppressor APC Domain Containing 1	0.08	0.89
	ILMN_2862093	NM_019817.1	Copz1	Coatomer Protein Complex, Subunit Zeta 1	0.03	1.15
phosphatase binding						
	ILMN_1237964	NM_013709.4	Sh3yl1	SH3 Domain Containing, Ysc84-Like 1 (S. Cerevisiae)	0.06	1.26
	ILMN_2715744	NM_011952.1	Mapk3	Mitogen-Activated Protein Kinase 3	0.06	1.14
phosphatidate phosphatase activity						
	ILMN_2759079	NM_008247.2	Ppap2a	Phosphatidic Acid Phosphatase Type 2A	0.09	1.16
phosphatidylinositol binding						
	ILMN_2674752	NM_028965.3	Snx11	Sorting Nexin 11	0.04	0.87
phosphatidylinositol phospholipase C activity						
	ILMN_1236465	NM_010170.4	F2rl2	Coagulation Factor II (Thrombin) Receptor-Like 2	0.09	1.18
phosphatidylinositol-4,5-bisphosphate 4-phosphatase activity; phosphatidylinositol-3,4-bisphosphate 4-phosphatase activity						
	ILMN_1226239	XM_134427.3	Inpp4b	Inositol Polyphosphate-4-Phosphatase, Type II, 105kDa	0.03	0.84
phospholipid binding						
	ILMN_2755666	NM_019456	Apbb1ip	Amyloid Beta (A4) Precursor Protein-Binding, Family B, Member 1 Interacting Protein	0.05	1.11
	ILMN_2749448	NM_153119.2	Plekho2	Pleckstrin Homology Domain Containing, Family O Member 2	0.04	1.16
photoreceptor cell development						
	ILMN_1244303	NR_002321.1	Tug1	Taurine Upregulated 1 (Non-Protein Coding)	0.05	0.89
plasma membrane						
	ILMN_2803920	NM_010742.1	Ly6d	Lymphocyte Antigen 6 Complex, Locus D	0.06	0.86
	ILMN_2431046	NM_133835.1	Ubac1	UBA Domain Containing 1	0.08	1.23
prenylated protein tyrosine phosphatase activity						
	ILMN_2655260	NM_008975.2	Ptp4a3	Protein Tyrosine Phosphatase Type IVA, Member 3	0.07	1.19
protein binding						
	ILMN_1228231	NM_025366.2	Chchd1	Coiled-Coil-Helix-Coiled-Coil-Helix Domain Containing 1	0.02	0.88
	ILMN_1255335	NM_133865.2	Dclre1b	DNA Cross-Link Repair 1B	0.09	1.16
	ILMN_2638404	NM_133865.2	Dclre1b	DNA Cross-Link Repair 1B	0.10	1.19
	ILMN_1229042	NM_018796.2	Eef1b2	Eukaryotic Translation Elongation Factor 1 Beta 2	0.05	0.88
	ILMN_2987107	NM_027342.1	Fam162a	Family With Sequence Similarity 162, Member A	0.04	0.86
	ILMN_1240677	NM_183358.3	Gadd45gip1	Growth Arrest And DNA-Damage-Inducible, Gamma Interacting Protein 1	0.07	0.89
	ILMN_1231420	NM_133852.2	Golga2	Golgin A2	0.02	0.83
	ILMN_3113787	NM_010815.2	Grap2	GRB2-Related Adaptor Protein 2	0.06	1.19
	ILMN_2740646	NM_025888.5	Kctd20	Potassium Channel Tetramerization Domain Containing 20	0.07	1.15
	ILMN_2725429	NM_138721.1	Lsm10	LSM10, U7 Small Nuclear RNA Associated	0.08	0.85
	ILMN_2883907	NM_133939.1	Lsm8	N(Alpha)-Acetyltransferase 38, NatC Auxiliary Subunit	0.03	0.88

Functional classification (according to Gene Ontology GO)	PROBE_ID	REFSEQ_ID	SYMBOL	Gene Name	q-Value	Fold change
protein binding	ILMN_2732961	NM_029409.2	Mff	Mitochondrial Fission Factor	0.09	1.21
	ILMN_1215647	NM_023431.5	Mum1	Melanoma Associated Antigen (Mutated) 1	0.06	0.85
	ILMN_2887065	NM_080638.1	Mvp	Major Vault Protein	0.08	1.09
	ILMN_2430813	NM_026131	Pdlim7	PDZ And LIM Domain 7 (Enigma)	0.09	1.18
	ILMN_2973925	NM_026398.2	Pop5	Processing Of Precursor 5, Ribonuclease P/MRP Subunit	0.09	0.90
	ILMN_2612635	NM_026943.1	Snrpd2	Small Nuclear Ribonucleoprotein D2 Polypeptide 16.5kDa	0.09	0.89
	ILMN_2949605	NM_026861.2	Ubac2	UBA Domain Containing 2	0.05	0.88
	ILMN_2972063	NM_027086.1	Ubl7	Ubiquitin-Like 7 (Bone Marrow Stromal Cell-Derived	0.08	1.15
	ILMN_2951120	NM_016757.1	Wbp1	WW Domain Binding Protein 1	0.05	1.18
	ILMN_1249698	NM_016852.2	Wbp2	WW Domain Binding Protein 2	0.07	1.16
	ILMN_2862214	NM_025392.1	Bccip	BRCA2 And CDKN1A Interacting Protein	0.04	0.87
	ILMN_2859659	NM_027151.1	Dctn2	Dynactin 2 (P50)	0.02	1.10
	ILMN_2971946	NM_025520.2	Lsm5	LSM5 Homolog, U6 Small Nuclear RNA Associated (S. Cerevisiae)	0.07	0.85
	ILMN_2627350	NM_010760.2	Magoh	Mago-Nashi Homolog, Proliferation-Associated	0.06	0.85
	ILMN_2975640	NM_026506.1	Snrpg	Small Nuclear Ribonucleoprotein Polypeptide G	0.04	0.85
	ILMN_2865822	NM_025898.1	Napa	N-Ethylmaleimide-Sensitive Factor Attachment Protein, Alpha	0.03	1.15
protein complex binding						
	ILMN_2628339	NM_001083334.1	Bin1	Bridging Integrator 1	0.07	1.14
	ILMN_2928320	NM_013477.2	Atp6v0d1	ATPase, H+ Transporting, Lysosomal 38kDa, V0 Subunit D1	0.02	1.17
protein C-terminus binding; protein homodimerization activity						
	ILMN_2453874	NM_001098227.1	Sdcbp	Syndecan Binding Protein (Syntenin)	0.03	1.15
protein homodimerization activity						
	ILMN_2700408	NM_011844.3	Mgll	Monoglyceride Lipase	0.09	1.12
protein kinase binding						
	ILMN_2830898	NM_023117.1	Cdc25b	Cell Division Cycle 25B	0.06	1.27
	ILMN_2944413	NM_018747.3	Akap7	A Kinase (PRKA) Anchor Protein 7	0.09	1.19
	ILMN_1217662	NM_009733.1	Axin1	Aliases	0.09	0.88
	ILMN_2614380	NM_011945.2	Map3k1	Mitogen-Activated Protein Kinase Kinase Kinase 1, E3 Ubiquitin Protein Ligase	0.10	0.94
	ILMN_2893077	NM_009096.2	Rps6	Ribosomal Protein S6	0.09	0.90
protein serine/threonine kinase activity						
	ILMN_2614212	NM_008551.1	Mapkapk2	Mitogen-Activated Protein Kinase-Activated Protein Kinase 2	0.06	1.15
	ILMN_2652181	NM_008641.2	Mast2	Microtubule Associated Serine/Threonine Kinase 2	0.10	1.19
	ILMN_2757150	NM_011049.4	Pctk1	Cyclin-Dependent Kinase 16	0.07	1.13
	ILMN_3124885	NM_001080773.1	Pdpk1	3-Phosphoinositide Dependent Protein Kinase-1	0.03	0.87
	ILMN_2842137	NM_010562.1	Ilk	Integrin-Linked Kinase	0.04	1.17
protein serine/threonine phosphatase activity						
	ILMN_1237696	NM_019674.3	Ppp4c	Protein Phosphatase 4, Catalytic Subunit	0.04	0.85
protein transmembrane transporter activity						
	ILMN_2499944	NM_025394.2	Tomm7	Translocase Of Outer Mitochondrial Membrane 7 Homolog (Yeast)	0.06	0.88
protein tyrosine phosphatase activity						
	ILMN_2830898	NM_023117.1	Cdc25b	Cell Division Cycle 25B	0.06	1.27
pyridoxal phosphate binding						
	ILMN_2628281	NM_016717.3	Scly	Selenocysteine Lyase	0.09	1.09
pyrophosphatase activity						
	ILMN_1214899	NM_153104.2	Phospho1	Phosphatase, Orphan 1	0.03	1.25
Rab GTPase binding						
	ILMN_2719507	BC019118	Rab6	ELKS/RAB6-Interacting/CAST Family Member 1	0.09	1.13
receptor activity						
	ILMN_2616792	NM_027212.2	Med30	Mediator Complex Subunit 30	0.04	0.87
	ILMN_3145814	NM_001081079.1	Ogfrl1	Opioid Growth Factor Receptor-Like 1	0.08	1.15
receptor binding						
	ILMN_2679456	NM_007760.3	Crat	Carnitine O-Acetyltransferase	0.09	1.16
	ILMN_1249691	NM_019966.2	Mlycd	Malonyl-CoA Decarboxylase	0.06	1.12
	ILMN_2755399	NM_138748	Ppp2r4	Protein Phosphatase 2A Activator, Regulatory Subunit 4	0.08	1.21
RES complex						
	ILMN_2593532	NM_146000.2	Bud13	BUD13 Homolog (S. Cerevisiae)	0.06	0.85
RNA binding						
	ILMN_1245733	NM_001024922.2	Ddx49	DEAD (Asp-Glu-Ala-Asp) Box Polypeptide 49	0.08	1.20
	ILMN_2735981	NM_013536.1	Emg1	EMG1 N1-Specific Pseudouridine Methyltransferase	0.07	0.86
	ILMN_2735615	NM_020583.4	Isg20	Interferon Stimulated Exonuclease Gene 20kDa	0.06	1.23
	ILMN_2971946	NM_025520.2	Lsm5	LSM5 Homolog, U6 Small Nuclear RNA Associated (S. Cerevisiae)	0.07	0.85
	ILMN_2627350	NM_010760.2	Magoh	Mago-Nashi Homolog, Proliferation-Associated	0.06	0.85
	ILMN_2975640	NM_026506.1	Snrpg	Small Nuclear Ribonucleoprotein Polypeptide G	0.04	0.85
	ILMN_2690460	NM_178394.3	Jakmip1	Janus Kinase And Microtubule Interacting Protein 1	0.05	0.86
	ILMN_1234759	NM_026623.3	Nudt21	Nudix (Nucleoside Diphosphate Linked Moiety X)-Type Motif 21	0.04	0.84
	ILMN_2970685	NM_019489.2	Ppie	Peptidylprolyl Isomerase E (Cyclophilin E)	0.05	0.86
	ILMN_2709456	NM_133693.1	Rbm42	RNA Binding Motif Protein 42	0.10	1.12
	ILMN_2851231	NM_011292.1	Rpl9	Ribosomal Protein L9	0.05	0.88

Functional classification (according to Gene Ontology GO)	PROBE_ID	REFSEQ_ID	SYMBOL	Gene Name	q-Value	Fold change
	ILMN_2881322	NM_009077.2	Rpl18	Ribosomal Protein L18	0.01	0.84
	ILMN_1259905	NM_001093753.1	Sfrs11	Serine/Arginine-Rich Splicing Factor 11	0.07	0.90
	ILMN_2650732	NM_027427.1	Taf15	TAF15 RNA Polymerase II, TATA Box Binding Protein (TBP)-Associated Factor, 68kDa	0.08	0.92
	ILMN_2747744	NM_011568.1	Thoc4	THO complex subunit 4	0.05	0.90
sequence-specific DNA binding ; sequence-specific DNA binding transcription factor activity						
	ILMN_2659380	NM_007920.3	Elf1	E74-Like Factor 1 (Ets Domain Transcription Factor	0.02	0.81
	ILMN_1252110	NM_021899.2	Foxj2	Forkhead Box J2	0.04	0.88
sequence-specific DNA binding transcription factor activity						
	ILMN_2624477	NM_183301.1	E2f2	E2F Transcription Factor 2	0.09	1.28
	ILMN_1259753	NM_009239.2	Sp4	Sp4 Transcription Factor	0.09	0.86
SH3 domain binding						
	ILMN_2783403	NM_011203.2	Ptpn12	Protein Tyrosine Phosphatase, Non-Receptor Type 12	0.08	1.12
single-stranded DNA binding						
	ILMN_2900827	NM_133772.1	Ssbp4	Single Stranded DNA Binding Protein 4	0.08	1.10
steroid hormone receptor activity; sequence-specific DNA binding						
	ILMN_2972292	NM_007953.2	Esrra	Estrogen-Related Receptor Alpha	0.03	0.87
structural constituent of nuclear pore						
	ILMN_2758695	NM_172410	Nup93	Nucleoporin 93kDa	0.03	0.86
structural constituent of ribosome						
	ILMN_2999797	NM_011289.1	Rpl27	Ribosomal Protein L27	0.09	0.89
	ILMN_2967528	NM_025589.1	Rpl36al	Ribosomal Protein L36a-Like	0.08	0.89
	ILMN_2881322	NM_009077.2	Rpl18	Ribosomal Protein L18	0.01	0.84
tetracycline transporter activity						
	ILMN_1252243	NM_026660.2	Mfsd10	Major Facilitator Superfamily Domain Containing 10	0.06	0.88
threonine-type endopeptidase activity						
	ILMN_1226683	NM_010724	Psmb8	Proteasome (Prosome, Macropain) Subunit, Beta Type, 8	0.09	0.87
transport						
	ILMN_2481182	NM_011671.3	Ucp2	Uncoupling Protein 2 (Mitochondrial, Proton Carrier)	0.03	1.18
transport vesicle						
	ILMN_1239874	NM_138303.1	Yipf2	Yip1 Domain Family, Member 2	0.05	1.17
transporter activity						
	ILMN_2683374	NM_019652.1	Asna1	ArsA Arsenite Transporter, ATP-Binding, Homolog 1	0.08	1.12
	ILMN_2598972	NM_016774.3	Atp5b	ATP Synthase, H+ Transporting, Mitochondrial F1 Complex, Beta Polypeptide	0.05	1.17
ubiquitin protein ligase binding						
	ILMN_2630459	NM_009911.2	Cxcr4	Chemokine (C-X-C Motif) Receptor 4	0.10	0.87
ubiquitin thiolesterase activity						
	ILMN_3151631	NM_027554.2	Usp38	Ubiquitin Specific Peptidase 38	0.08	0.87
ubiquitin-protein ligase activity						
	ILMN_2935032	NM_013909.1	Fbxl6	F-Box And Leucine-Rich Repeat Protein 6	0.01	0.84
	ILMN_2869312	NM_134099.1	Fbxo4	F-Box Protein 4	0.07	0.89
	ILMN_1239770	NM_023324.2	Peli1	Pellino E3 Ubiquitin Protein Ligase 1	0.09	0.90
	ILMN_2517041	NM_010931.2	Uhrf1	Ubiquitin-Like With PHD And Ring Finger Domains 1	0.08	1.14
unfolded protein binding						
	ILMN_2725428	NM_178055.3	Dnajb2	DnaJ (Hsp40) Homolog, Subfamily B, Member 2	0.09	1.22
	ILMN_3109989	NM_001013369.1	Pfdn4	Prefoldin Subunit 4	0.07	0.88
	ILMN_2839303	NM_026992.1	Dph4	DnaJ (Hsp40) Homolog, Subfamily C, Member 24	0.06	0.90
	ILMN_1245092	NM_011149.2	Ppib	Peptidylprolyl Isomerase B (Cyclophilin B)	0.03	0.88
water channel activity						
	ILMN_1214634	NM_022026.2	Aqp9	Aquaporin 9	0.06	1.22
zinc ion binding						
	ILMN_2734661	NM_024284.1	Hagh	Hydroxyacylglutathione Hydrolase	0.08	1.23
	ILMN_3124547	NM_001007465.1	Rffl	Ring Finger And FYVE-Like Domain Containing E3 Ubiquitin Protein Ligase	0.09	1.19
	ILMN_2477324	NM_011280.1	Trim10	Tripartite Motif Containing 10	0.08	1.30

Out of those 259 differentially regulated probes, 13 transcripts were chosen for qRT-PCR validation (Table 8). The selection of the candidates was based on literature research.

We were able to validate 2 candidates out of the preselected targets with two different housekeepers (Hprt and Rpl18a). Add1 was significantly down regulated in the good treatment responders compared to the poor treatment responders (Hprt: $T_{22} = 4.001$, $p < 0.005$; Rpl18a: $T_{22} = 2.762$, $p < 0.05$) (Figure 41A). The same expression pattern was

found for P2rx1. P2rx1 was significantly down regulated in the good treatment responders compared to the poor treatment responders (Hprt: $T_{21} = 4.199$, $p < 0.000$; Rpl18a: $T_{20} = 2.288$, $p < 0.05$) (Figure 41B).

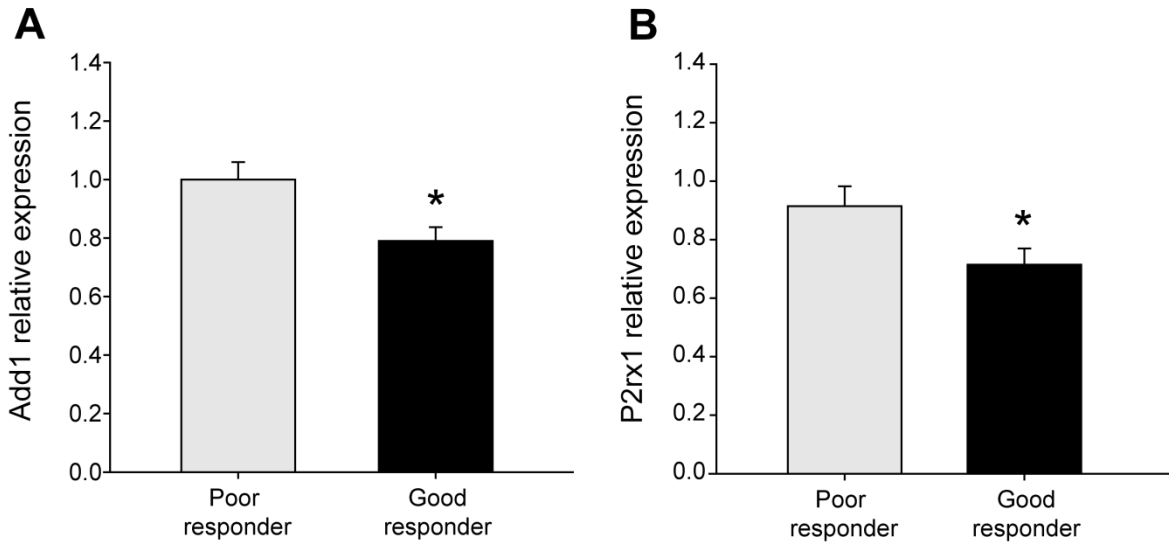

Figure 41: Validation of candidate genes from the microarray. (A) Add1 was significantly down regulated in good treatment responders compared to poor treatment responders. (B) P2rx1 was significantly down regulated in good treatment responders compared to poor treatment responders. * significant different to good treatment responders $p < 0.05$.

Table 8 shows the results for all preselected gene for both microarray and qRT-PCR results.

Table 8: Comparison of the microarray and the qRT-PCR data. Genes that were significantly regulated in the microarray and the qRT-PCR are printed in bold. Fold changes were normalized to poor responders.

		Microarray			qRT-PCR	
PROBE_ID	Gene Symbol	Fold Change	p-value	q-value	Fold Change	q-value
ILMN_2827535	Axol12	1.15	0.004	0.09	1.01	p = 0.96
ILMN_1228231	Chchd1	0.88	0.000	0.02	0.91	p = 0.46
ILMN_1239770	Peli	0.90	0.003	0.09	0.97	p = 0.73
ILMN_3033533	**Add1**	**1.12**	**0.001**	**0.06**	**0.79**	**p = 0.01**
ILMN_2499944	Tomm7	0.88	0.001	0.06	0.91	p = 0.47
ILMN_3124885	Pdpk1	0.87	0.0003	0.03	1.05	p = 0.77
ILMN_1259753	Sp4	0.86	0.005	0.09	0.92	p = 0.48
ILMN_2865822	Napa	1.15	0.000	0.03	0.91	p = 0.61
ILMN_2932453	**P2rx1**	**1.20**	**0.004**	**0.09**	**0.78**	**p = 0.03**
ILMN_2453874	Sdcbp1	1.15	0.000	0.03	0.81	p = 0.06
ILMN_2659380	Elf1	0.81	0.000	0.02	0.88	p = 0.25
ILMN_2715744	Mapk3	1.14	0.001	0.06	0.89	p = 0.198
ILMN_2546724	Ddrx12	0.83	0.000	0.02	0.89	p = 0.20

3.4.6 Predictive gene expression transcripts of antidepressant treatment response tested in a human sample

To assess the relevance of the gene expression transcripts for antidepressant response in humans, we tested their predictive ability to classify response status in a human sample. The sample (n=38), consisted of a subset of MDD patients treated with escitalopram for 12 weeks. These patients were recruited from two samples at Emory University School of Medicine (Department of Psychiatry and Behavioral Sciences). The first sample (n= 32) is a small subset of the PReDICT study (Dunlop et al., 2012), containing four hundred treatment-naive patients with MDD diagnosis. The second sample (n=6), also a subset of a previously published study (McGrath et al., 2013) consisted of patients with a primary diagnosis of MDD (assessed by the Structured Clinical Interview for *DSM-IV-TR* Axis I Disorders, Research Version, Patient Edition With Psychotic (Screen) (First MB, 2002) who were randomly assigned to 12 weeks of either escitalopram or cognitive behavioral therapy for 12 weeks. From both samples blood was drawn at baseline and after 12 weeks. Only patients from the drug groups (n=38) were included in the final analysis. From our full drug-treated sample, 27 patients were classified as responders and 11 as non-responders according to percent changes in HDRS-17 scores from baseline to week twelve (≥ 50% or < 50% change respectively).

Mouse gene expression transcripts (n=259) were mapped to its human orthologue genes present in the Illumina HT-12 arrays (n = 241). Gene expression repeated measures from the patients at baseline and week 12 were available, thus we computed the absolute difference between the expression levels of the transcripts between those time-points and tested whether these alterations were able to predict response to escitalopram treatment. Interestingly, we were able to detect differences in expression profiles from baseline to week 12 of the human-orthologues that allowed us to predict the response status (percent change in HDRS-17 from baseline to week 12) with an accuracy of 84% in the human sample. Prediction persisted after we permuted the response-status labels 1000 times ($p = 0.017$).

3.4.7 ENCODE ChIP-Seq enables us to detect common transcription factors, regulated by the gene set predicting antidepressant response in humans

Using the ENCODE ChIP-Seq Significance Tool (http://bioinformatics.oxfordjournals.org/content/early/2013/06/02/bioinformatics.btt316.full.pdf+html), we checked for transcription factor enrichment among our genes identified in

our analysis. Enrichment scores for this tool are calculated using a one-tailed hypergeometric test that is corrected for multiple testing using false discovery rate (Auerbach et al., 2013). For instance, the CCCTC-binding factor (CTCF) was one of the transcription factors enriched in our analysis. Out of the 183 mouse genes recognized in the database, 149 genes were regulated by CTCF within a 500 base pair radius of their respective transcription start sites (p = 3.845 * 10 ^ -77). The effect of this transcription factor was replicated in the human ortholog sample as 145 of the 236 genes recognized by the server were similarly regulated by CTCF (p = 2.44 * 10 ^ -6). Thus, the genes identified in our analysis are closely linked by CTCF transcription factor regulation, indicating a common mechanism.

4 Discussion

Depressive disorder is one of the most common mental diseases worldwide. However, when it comes to antidepressant treatment outcome, a significant number of patients do not show an adequate response to the treatment, relapse or continue to show remaining symptoms (Trivedi et al., 2006). The overarching aim of this thesis was to advance our current understanding of the neurobiology underlying individual antidepressant treatment response in major depression, and to furthermore identify predictors of treatment outcome. A number of studies have already aimed to identify valid biomarkers, which would allow the clinicians to predict antidepressant treatment outcome (Schmidt et al., 2011a; Cattaneo et al., 2013; Le-Niculescu et al., 2008a; Leuchter et al., 2010; Leuchter et al., 2009; Binder and Holsboer, 2006; Schwarz and Bahn, 2008). However, the results in such studies were rather disappointing. In search of confounding factors impairing the identification of response biomarkers in MDD, the following factors, amongst others, have been identified as being important. First, the unreliability of the diagnosis is a critical point for clinical studies, and is founded on the basis that depression is a complex syndrome, and not simply a disease entity (Rush, 2007). Different symptoms of the syndrome, such as sleep disturbances, lack of concentration and depressed mood may all have biologically distinct causes. Second, individual confounding environmental factors are likely to play a critical role in biomarker research. It is now generally accepted that susceptibility to major depression is determined by a combined effect of genes and environment, with heritability estimates ranging from 30% to 40%, complemented by a major impact of stressful or aversive life events (Villanueva, 2013; Malhi et al., 2000; Nestler et al., 2002a). Changes in epigenetic modifications during the lifespan as a consequence of a plethora of environmental influences, including previous disease episodes and treatment schedules, are also likely to hamper the identification of valuable predictive biosignatures for treatment response (Klengel et al., 2014; Dell'Osso et al., 2014; Pena et al., 2014; Nestler, 2014). Third, the heterogeneity of the patient's age in clinical studies is likely to be a critical point for the identification of biomarkers. To overcome these limitations, which are characteristics of any human experimental trail, we developed a novel experimental approach that mimics the heterogeneity of antidepressant treatment outcome in mice, which is already known from the clinical situation.

Using this novel experimental approach, we provide a large body of evidence that the here described animal model is a valid model, depicting the heterogeneity of

antidepressant treatment outcome in mice, and is therefore a good approach to investigate targets mediating individual antidepressant responses. After extensive validation of our experimental approach, we combined our model and findings from the clinical situation, in order to identify a subgroup of mice who responded well and poorly after a chronic and subchronic pharmacological treatment. Gene expression differences in the good responder and poor responder subgroups were extensively analyzed using an unbiased microarray approach, aiming to identify novel targets and gene networks mediating the antidepressant treatment outcome. After the chronic antidepressant treatment, we were not able to detect any significant differences in gene expression between good and poor treatment responders. However, after 14d of paroxetine treatment, we identified a gene expression signature in the peripheral blood that was able to predict the antidepressant response in our mouse model. Furthermore, these findings enabled us to predict the response status within a subset of human patients.

Additionally, we were able to identify and further characterize Sox11 as one of the most interesting candidate genes regulated during antidepressant treatment in the mouse brain. Specifically, chronic and subchronic antidepressant treatment induces Sox11 mRNA expression in the hippocampal DG, and moreover our data suggests that Sox11 is involved in modulating anxiety-related behavior.

4.1 Pharmacological studies

The commonly prescribed antidepressants are generally effective, although a subset of patients do not respond to any prescribed interventions. Paroxetine, a SSRI, is used regularly in the clinic to treat depression and its pharmacology is well described in humans. Preskorn and colleagues could show that all SSRIs are slowly and fully absorbed from the gut with a peak plasma concentration after 3 - 8 hours. They could also demonstrate that a minimum effective dosage of 20mg/day paroxetine is eliminated in the human with a half-life of 1 day (Preskorn, 1997). The pharmacokinetics and pharmacodynamics of paroxetine in the mouse have so far not been described in detail. This leaves the question about the correct and most importantly translatable dosage largely unanswered. As conclusive data are still not available from the literature, we conducted initial pharmacological studies.

4.1.1 Paroxetine - struggling for the right dosage

First, we were interested in identifying the minimum effective dosage for the DBA/2J mouse strain, as we wanted to avoid any possibility of animal overdosing. Thus, we performed two independent studies where we tested two different concentrations of paroxetine in various parameters.

In the beginning, we treated the animals chronically with a very low dose of paroxetine (1mg/kg BW twice a day) and detected a significant increase in body weight gain in the paroxetine treated animals compared to the vehicle treated control group. The same could be shown for the higher paroxetine concentration (5mg/kg BE twice a day) following chronic administration. These findings are in line with data from clinical studies, where an increase in body weight gain during antidepressant treatment is a common unwanted side effect (Flint and Kendler, 2014). Antidepressants not only influence body weight, but also have been consistently described to attenuate the HPA system (Holsboer, 2003; Holsboer and Barden, 1996). More than 30 years ago, Gibbons and colleague could demonstrate that plasma cortisol levels are elevated in depressed patients and are furthermore normalized after clinical remission (Holsboer and Barden, 1996; Gibbons, 1964). Other studies have demonstrated that untreated depressed patients show exaggerated cortisol release after Dex stimulation compared to healthy controls in a combined dexamethasone (Dex)/CRH-test, a common test to investigate changes in stress system function. Interestingly, after 1 week of amitriptyline treatment these abnormalities began to disappear and normalization of the HPA axis becomes even more pronounced after a longer antidepressant treatment period (Heuser et al., 1996). Furthermore, Ising and colleagues have demonstrated that patients presenting a significant reduction in stress hormone levels already after 2 weeks of antidepressant treatment, show a more pronounced reduction in the Hamilton Rating Scale for Depression (HDRS) after 5-6 weeks of treatment. Therefore, they found that an improvement in the Dex/CRH test after 2 weeks of antidepressant treatment was significantly associated with treatment response 5 weeks after a pharmacological intervention (Ising et al., 2007). Besides these clinical studies, there is also evidence from preclinical studies, in which a correlation between the dysregulation of the HPA system and the psychopathology of depression has been shown (reviewed in (Holsboer and Barden, 1996)). Reul and his coworkers also observed that chronic antidepressant treatment is able to reduce basal as well as stress-induced corticosterone (equivalent to cortisol in the human system) levels (Reul et al., 1993). Considering these findings all point to a central link between antidepressant treatment and

HPA axis regulation, we also examined corticosterone levels after chronic antidepressant treatment. When the low paroxetine dose was administered, we were not able to find a significant difference between paroxetine and vehicle treated animals. This low paroxetine dosage seems to influence physiological parameters, namely body weight gain, but is not able to evoke an attenuation of the HPA system in the DBA/2J mouse strain. However, the higher paroxetine concentration was able to attenuate the HPA axis reactivity, resulting in lower corticosterone levels in the paroxetine treated animals, which is in agreement with previous findings. Here, our novel animal model reproduced the same phenotype as numerous clinical studies including a reduction of stress hormone levels after antidepressant administration (Heuser et al., 1996; Ising et al., 2007; Shimoda et al., 1988).

Besides the physiological and neuroendocrine changes, antidepressant treatment should also provoke a robust behavioral phenotype, which has already been highlighted in various preclinical studies (Sillaber et al., 2008; Webhofer et al., 2011; Nestler and Hyman, 2010; Nestler et al., 2002b). At a concentration of 1mg/kg BW, paroxetine-treated animals tended to spend less time floating in the FST compared to vehicle-treated mice, but neither the time spent swimming or the time spent struggling was significantly different between the groups. These behavioral data indicate that at 1mg/kg BW, the concentration of paroxetine was too low to provoke robust behavioral and neuroendocrine phenotypes. By contrast, chronic paroxetine treatment administered at the higher dose was able to effectively provoke robust behavioral responses in the FST. Paroxetine-treated animals spent less time floating and more time engaged in active behaviors, namely swimming and struggling. These behavioral findings are in line with various other studies, which have demonstrated that antidepressant treatment leads to an increase in active behavior and a decrease in passive behavior in the FST (Sillaber et al., 2008; Webhofer et al., 2011).

In order to gain insight into the pharmacology of the two different antidepressant doses administered to the mice, paroxetine levels were measured in the brain and the plasma of the paroxetine-treated animals. At a concentration of 1mg/kg BW paroxetine, no significant difference was found in paroxetine plasma or paroxetine brain concentrations between the different responder groups, thereby ruling out that the individual differences in treatment efficacy was a consequence of different drug concentrations. Additionally, we could demonstrate that paroxetine brain and plasma concentrations are highly correlated. Nevertheless, it is important to acknowledge that the measured plasma paroxetine

concentrations, with an average of 50ng/ml, are relatively low compared to the human situation, showing average values of 180ng/ml (Heuser et al., 1996). Similarly, at the higher dose of paroxetine no significant difference was detected in paroxetine plasma and brain concentrations between the different responder groups. Plasma and brain paroxetine concentrations were significantly higher compared to the previously used 1mg/kg BW dose. We could show again a correlation of paroxetine brain and plasma concentrations.

In summary, we conclude that a concentration of 1mg/kg BW paroxetine is insufficient to evoke robust behavioral and neuroendocrine treatment effects in our experimental model. By contrast, chronic administration at 5mg/kg BW is sufficient to evoke robust behavioral and neuroendocrine treatment effects in our experimental model and was therefore selected for all further experimental investigations.

Does a subchronic paroxetine treatment evoke the same physiological profile as a chronic treatment?

Treatment duration is another important issue in any experimental design. We therefore addressed the question as to whether a subchronic (14d) treatment is sufficient to elicit the same behavioral and physiological phenotype compared to that resulting from chronic treatment. After 14d of paroxetine treatment we detected an increase in body weight gain, which is in line with our physiological data following chronic paroxetine treatment. However, it was not accompanied by a reduction in corticosterone levels. One can speculate that a treatment duration of 14d is too short to significantly modulate HPA axis activity, as has been shown by Reul and co-workers to occur following chronic treatment (Reul et al., 1993).

Antidepressants are known to alter the behavior of an animal in the FST. After subchronic paroxetine treatment we detected the same behavioral phenotype that manifested following chronic paroxetine treatment. Treated animals showed a reduction in the time spent floating and an increased time engaged in active behaviors. These behavioral data indicate that subchronic antidepressant treatment is sufficient to evoke robust behavioral phenotypes.

We next checked whether treatment response (good versus poor responders) correlates with plasma/brain paroxetine concentrations. Interestingly, plasma paroxetine

concentrations were significantly elevated in good responders compared to the intermediate responder group and the poor responder group. The same pattern was found for brain paroxetine concentrations. This significant difference in brain and plasma paroxetine concentrations could be a reasonable explanation, as to why some animals show a rapid and strong antidepressant response in the FST while others do not. However, in the subsequent microarray analyses on these animals, plasma paroxetine concentrations were considered as co-variate, and were excluded to play a significant role here (see chapter 3.4.4 - 3.4.7). There is evidence from clinical studies that polymorphisms in specific blood brain barrier transporters, such as ABCB1, are involved in a better and faster antidepressant response (Uhr et al., 2008). As we used an inbred mouse strain in our experiment, genetic polymorphisms are not likely to play a prominent role here. However, differences in gene expression regulation of specific blood brain barrier transporters, resulting from antidepressant treatment, may provide an explanation for the significant difference in brain paroxetine concentrations. Therefore, gene expression analysis for drug transporters at the blood-brain-barrier could be performed in future studies, in order to investigate their potential involvement in shaping the behavioral response. Nevertheless, further studies are need in order to elucidate the molecular mechanisms underlying the early response phenotype in these animals.

4.1.2 Elimination kinetics of paroxetine - can we really translate from men to mouse?

After we had identified the minimum effective dosage for the DBA/2J mouse strain, we aimed to gain a better understanding into the pharmacokinetics of paroxetine, especially with regards to the pharmacological half-life within the mouse organism. Therefore, male DBA/2J mice were treated chronically with 5mg/kg BW paroxetine twice daily and were subsequently killed at different time intervals after discontinuation of the paroxetine treatment. In a clinical study it has been shown, that a single dose of paroxetine administration (20mg) is eliminated with a half-life time of 10h in adult men. In the same study, multiple administrations of paroxetine (20mg/day) resulted in decreased elimination rates and a longer half-life time of 24h (Kaye et al., 1989). Here, we were able to show that the elimination rate following chronic paroxetine treatment in a mouse was similar to the elimination rate of multiple administrations of paroxetine in humans. One day after discontinuation of the antidepressant, the animals showed a 50% reduction in the paroxetine levels, which is in line with the human situation. Additionally, we could prove here that paroxetine plasma levels are no longer detectable 3 days after discontinuing

antidepressant treatment. As there is only limited access to the brain in human studies, we also investigated the paroxetine half-life in the mouse brain. We have shown that paroxetine brain and plasma concentrations are highly correlated, which has important clinical implications given the inability to assess human brain concentrations. We clearly demonstrated that paroxetine levels, which are measured in the blood, reflect the situation in the brain. Furthermore, we showed that paroxetine is detectable slightly longer in the brain, although there is nevertheless very little left 3 days after discontinuing paroxetine treatment.

Taken together, we have shown that paroxetine plasma and brain levels are highly correlated. Furthermore, we demonstrated that the elimination rate of paroxetine in the mouse is the same as what is observed in the human situation. These findings could serve as a basis to predict brain concentrations within clinical studies and enable us to really translate our pharmacological studies from the mouse to the human system.

4.1.3 Mouse pellets - one step closer to translational research

Gavaging, i.p. injection as well as oral administration via the drinking water are all common tools for drug application in preclinical sciences (Wagner et al., 2012; Santarelli et al., 2003; Ganea et al., 2012; Hodes et al., 2010; Qi et al., 2008). However, such routes of administrations are accompanied by certain limitations. For example, gavaging and i.p. injection are very time consuming techniques, especially when performed on a large number of animals. In addition, they are a very stressful for the animals and the animals need to be handled on a daily basis. Most of the time body weight loss accompanies these procedures (Atcha et al., 2010; Zhang, 2011; de Meijer et al., 2010), which is a reflection of the animal's discomfort, and can thus be interpreted as an additional stressful stimulus. Drug administration via drinking water also has its limitations. For examples, the researcher does not retain control of the exact amount of drug consumed by the experimental animal. Although the bottles are weighed on a regular basis, leakage cannot be completely prevented and thus calculation of the exact dose is not always accurate. Secondly, the concept of peak-trough, dosing as achieved by the administration of mouse pellets, cannot be achieved from continuous administration of the compound via the drinking water, as chosen in other rodent studies. However, the route of administration is an important consideration when designing a valid animal model that mimics the human situation. For example, there is good evidence to believe that pharmacokinetics play an important role when it comes to the regulation of gene expression (Schug et al., 2013).

This study is, to our knowledge, the first to use customized mouse pellets for drug administration. These pellets bring us one step closer to translational research, as nearly all patients receive their antidepressants via tablets. Besides the fact that this approach will bring us closer to clinical research, the mouse pellets have additional advantages. The use of pellets represents a non-invasive drug delivery system, as the pellets are simply dropped in the animal's home cage and the animals are totally free to consume these pellets. Moreover, the pellets are a highly palatable food for the animals, and they consume it within the first minutes, and therefore this type of administration represents a stress-free route of delivery. To ensure that administration of mouse pellets is comparable to the commonly used i.p. injection, 10 male mice were injected with one acute 5mg/kg BW dosage of paroxetine. Animals administered paroxetine via i.p. injections presented significantly higher plasma paroxetine levels and higher brain paroxetine levels compared to the animals treated with the mouse pellet. In addition, paroxetine brain and plasma levels after i.p. injection were also highly correlated. Clinical studies have shown that after chronic paroxetine administration the maximum plasma concentration is around 105µg/ml (Heydorn, 1999). Therefore, we conclude that although we detected a significant difference between the two application forms, the paroxetine plasma levels of the mouse pellets are still in a similar pharmacological range compared with the human situation.

4.2 Novel experimental approach - modeling individual antidepressant response in mice

The identification of novel biomarkers in depression has been relatively unsuccessful in clinical studies, so far (Schmidt et al., 2011a; Sim and Ingelman-Sundberg, 2011). The reasons for this are not yet clear. Human genetic studies are searching for chromosomal regions or candidate genes that play a role in mood regulation and/or other neuropsychiatric disorders. To-date, the clinical data is rather disappointing since the human data sets are very heterogeneous as they are influence by many co-factors, including different drugs, ages, disease history, and a variety of environmental influences that very likely impact gene expression (epigenetic factors) ((Le-Niculescu et al., 2008a) and reviewed in (Philibert et al., 2014)). In contrast, animal models are mainly performed with homogeneous inbred mouse strains in controlled environments. This overcomes some limitations associated the human studies. However, animal studies are often lacking in terms of relevance to the human condition (Le-Niculescu et al., 2008b). Depression is a very complex psychiatric disorder (Kessler et al., 2005; Nestler et al., 2002a), and it's diagnosis is already challenging enough in humans. Translating this complex human

disorder into an animal model approach is even more challenging. The ideal animal model should fulfill certain criteria: it should mimic the human conditions with regard to symptomatology, pharmacological treatment and the biological basis (McKinney et al., 1969). However, meeting all these criteria is very difficult, especially in depression where some key features (worthlessness, guilt and suicidal intention) are defined by a subjective verbal report, which can never be modeled in animals (Sillaber et al., 2009). Furthermore, the most commonly used animal models are non-primate, often rodents, and are based on exposing a healthy animal to a stressful environment. These models then only account for experienced-related behavioral changes in depression (Kalueff et al., 2007). Some aspects, such as the influence of genetic variations are completely ignored in these models and thus the development of the ideal homologous model seems out of reach (Sillaber et al., 2009). As depression is a very complex disease, only certain key symptoms, such as anhedonia, dysregulation of the HPA axis and altered brain morphology, can be mimicked (Sillaber et al., 2009). DBA/2J represent an inbred mouse strain with an high innate anxiety and a high responsiveness to antidepressant treatment under basal condition (Ohl et al., 2003; Yilmazer-Hanke et al., 2003), and was thus selected as the ideal mouse strain for our experimental approach. By using this mouse strain, we avoided the use of additional stressors, which would have been needed in other mouse strains to evoke an antidepressant treatment response. In this experimental design, we just focused on individual antidepressant treatment response in mice. Moreover, this novel attempt should not be seen as a novel model for depression-like symptoms but rather as a means for modeling the heterogeneity of antidepressant treatment outcome, an issue of supreme importance in psychiatric care. By using an inbred mouse strain housed under the same conditions, we tried to control for all the above mentioned factors, which may potentially disguise biomarkers in the clinical situation. Our hypothesis is that this completely controlled animal model may enable us to detect 'super-clean' biomarkers, which we could then translate to the clinic. Preclinical as well as clinical studies are thus highly relevant for this field, and more importantly, must be combined to detect potential strong candidates that would otherwise be missed in the independent models (Le-Niculescu et al., 2008a). These novel targets can be then extensively investigated in the animal model and thus may shed light on the field of biomarkers in antidepressant treatment outcome (Figure 42).

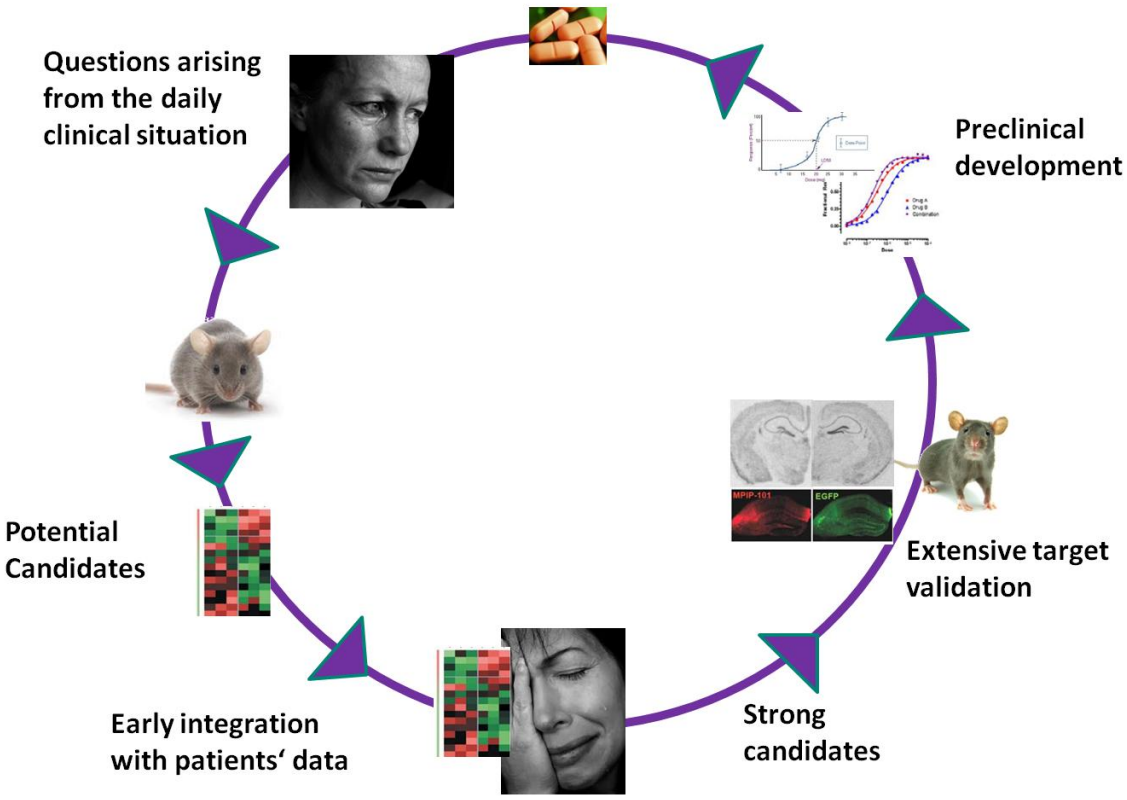

Figure 42: Need for novel experimental approaches: strategies for improving translational research in the field of depression. To detect novel candidate genes and biomarkers that are also relevant for the clinical situation, improved animal experimental approaches need to be established. To enable a translational approach, questions that are arising in the daily clinical situation need to be precisely formulated and then translated in an animal approach. With this animal approach we are able to detect novel targets, especially in the brain, which are mediating the individual antidepressant response. Furthermore, we need to integrate the mouse data at a very early stage with the human data, which would then enable us to detect really strong an promising candidates. These strong candidates can then be extensively investigated in the animal model and thus may lead to the development of potential novel compounds.

4.2.1 Heterogeneity in antidepressant treatment outcome can be modeled in mice

While many patients respond well to the currently available antidepressants, a significant number of patients do not show an adequate response to the treatment, show remaining symptoms or the patients relapse (Trivedi et al., 2006; Carter et al., 2012). Clinical studies, such as the STAR*D study have demonstrated that patients can be divided into remitters or 'good responders' and non-remitters or 'poor responders' to a prescribed therapy. Furthermore, it could be shown in clinical studies that most of the time, treatment strategies are based on a trial and error principle (Fabbri et al., 2013) and the longer the patients are treated the less chance they have to remit (Trivedi et al., 2006). These findings from clinical studies highlight the extensive variety in antidepressant treatment outcome. To-date, in preclinical research there is no available animal model able to

distinguish between good and poor treatment responders according to a behavioral readout. Our novel experimental design enables us to detect good and poor treatment responders, according to their performance in the FST. More importantly we are to establish a connection between clinical and preclinical findings.

The investigation of extreme groups has already been successfully performed in the field of stress research. Specifically, it has already been shown that not all animals respond in the same way to a stressful stimulus. Schmidt and colleagues subjected a large number of animals to a chronic social stress paradigm to demonstrate that some animals recover quickly from the stress procedure, whereas others do not. According to basal corticosterone levels measured 5 weeks after the stress procedure, stressed animals were classified either as 'vulnerable' or 'resilient'. With this experimental design, they could demonstrate that individual stress susceptibility can be detected when using a large animal cohort (Schmidt et al., 2010). However, with respect to antidepressant treatment response, nobody has yet followed such an experimental design. Our novel experimental approach is a promising, new attempt in order to shed light on treatment response and thus represents an innovative approach to investigate novel targets mediating individual responsiveness to antidepressant treatment.

4.2.2 Is the FST a suitable readout parameter for antidepressant response?

The FST is one of the most commonly used behavioral tests to screen antidepressant activity in rodents (Cryan et al., 2002). Thus, we postulated that the FST, is a valid tool to detect individual antidepressant treatment responses within a large group of animals. Porsolt introduced the FST in rats in the late 1970s to assess antidepressant activity in preclinical animal models (Porsolt et al., 1977a). Since that time the FST is widely used to investigate antidepressant activity for novel and already known compounds, in order to detect depressive-like behavior and stress coping strategies in rodents (Cryan et al., 2002; Lucki, 1997). The test is based on establishing an inescapable situation for the rodent. The initial escapable-orientated motivation develops into an immobile posture (Cryan et al., 2002). This immobile posture is considered on the one hand, as a failure to pursue escape-directed behavior, and on the other hand, is seen as passive behavior that disengages the animal from active forms of coping with stressful stimuli (Lucki, 1997). In general, antidepressants increase escape-directed behavior and prolong the onset of immobility behavior (Cryan et al., 2002). However, the FST is debated controversially in the literature. Some studies criticize that acute antidepressant treatment evokes

behavioral effects in the FST, although acute antidepressant treatment has no effect in clinical studies (Cryan et al., 2002). The FST should be seen more as a reliable behavioral tool, which is not necessarily a model for depression but rather for antidepressant treatment outcome (Petit-Demouliere et al., 2005). Considering the identification of individual antidepressant treatment outcomes was one of the main aims of this thesis, the FST was the most suitable tool. Furthermore, to ensure that the behavioral readout describes real antidepressant response, we performed two FSTs, one before and one after the antidepressant treatment. This repeated testing enabled us to investigate whether differences in the treatment response of animals could be due to preexisting, inherent characteristics or due to a real pharmacological treatment effect. With this test, we were able to show that the preexisting inherent characteristics do not correlate with those arising after antidepressant treatment.

4.3 Genes and gene networks mediating an early onset of antidepressant response

According to findings from clinical studies, there is a subset of patients that respond to an antidepressant treatment at an early stage, i.e. after 2 weeks of treatment (Taylor et al., 2006; Nierenberg et al., 2000; Entsuah et al., 1998). Although all animals were treated and handled in the same way, we were also able to detect a large behavioral variation within the animals as indicated in the FST. After identifying good and poor responders, we investigated differences in their gene expression profile. Analysis of the brain microarray experiment revealed 87 differentially regulated genes between good responders and vehicle-treated animals, while there were no significant differences between good and poor treatment responders.

4.3.1 Subchronic paroxetine treatment enables the identification of an expression profile signature predicting antidepressant response in patients

In clinical studies, blood expression profiling has become a more frequently used technique to investigate genetic alterations following various treatment and/or environmental contexts in clinical studies. Therefore, we investigated the influence of subchronic paroxetine administration on gene expression alterations in peripheral blood in order to increase the translational value of our approach.

After statistical correction, we found a robust gene regulation effect of 259 transcripts when comparing RNA extracted from blood of good and poor treatment responders.

Interestingly, there was no overlap of significantly regulated genes in the periphery and the brain. This suggests that gene expression changes measured in the patients' blood are largely independent of gene expression alterations in the brain. To-date, there are few studies comparing the gene expression profile of the peripheral blood with that of the CNS. Sullivan and colleagues have shown in clinical studies, that whole blood share significant gene expression similarities with various human brain tissue, at least at the level of the transcriptome. Furthermore, when investigating candidate genes relevant to schizophrenia, they were able to show that approximately half of the genes were expressed in both whole blood as well as prefrontal cortex tissue (Sullivan et al., 2006). However, this study has its limitations: firstly, the human data set shows a high level of genetic heterogeneity, which makes it even harder to detect common genes. Secondly, there is always a general methodological problem when it comes to post-mortem tissue (Sullivan et al., 2006; Witt et al., 2013). Witt and colleague also compared the gene expression profiles of blood, hippocampus and prefrontal cortex in genetically identical rats under baseline conditions. Here, they could show that, nearly all genes expressed in the blood tissue are also expressed in at least one brain tissue. However, the authors clearly state that it would be desirable to investigate the co-expression of genes in blood and brain tissue after a certain form of challenge or treatment (Witt et al., 2013). The current findings reported here, are not in line with the afore mentioned studies. We were unable to detect any overlap between genes regulated in blood and hippocampal tissue in subchronically-treated male DBA/2J mice challenged to a FST. Given the importance of the comparability of gene expression profiles in blood and brain tissue in neuropsychiatric research (Witt et al., 2013), the need for more studies is inevitable.

In order to assess the relevance of the mouse gene expression transcripts for antidepressant response differences in humans, we tested their predictive ability to classify response status in a human sample. Repeated gene expression measures from the patients at baseline at 2 and 12 weeks after the treatment onset was available. Therefore we were interested as to whether differences in gene expression are able to predict antidepressant response. Interestingly, we detected differences in expression profiles from baseline to week 12 of the human-orthologues that allowed us to predict the response status (percent change in HDRS-17 from baseline to week 12) with an accuracy of 84% in the human sample. To our knowledge, this is the first study that has been able to show such a prediction rate in a translational approach. These findings bring us a step closer to predict antidepressant treatment response at an early stage during antidepressant treatment. In order to better understand, how the detected genes are

connected to each other, we performed further analyses to detect common transcription factors. Using the ENCODE ChIP-Seq Significance Tool, we identified the CTCF one of the candidates that was enriched in our data set. The effect of this transcription factor was replicated in the human ortholog sample. Specifically, 145 of the 236 genes were similarly regulated by CTCF in the human data set. Thus, the genes identified in our analysis are closely linked by CTCF transcription factor regulation, indicating a common mechanism (Figure 43). While CTCF hosts many cellular roles, one study implicated its role in the regulation of serotonin receptors, thereby linking this transcription factor to a predisposition to affective disorders (Phillips and Corces, 2009). The strong enrichment of our gene set for this transcription factor supports the role for possible activity of this factor in treatment response for major depression. According to the literature, CTCF seems to be a very promising candidate, playing an important regulatory role for numerous genes. However one has to keep in mind that approximately 14000 - 40000 binding sites for CTCF have already been identified genome-wide (Phillips and Corces, 2009). By identifying this common transcription factor, further studies should be performed in order to investigate how this transcription factor is mediating antidepressant responsiveness in our mouse model and more importantly, investigate how relevant CTFC is as a key modulator to the gene set detected in our translational approach.

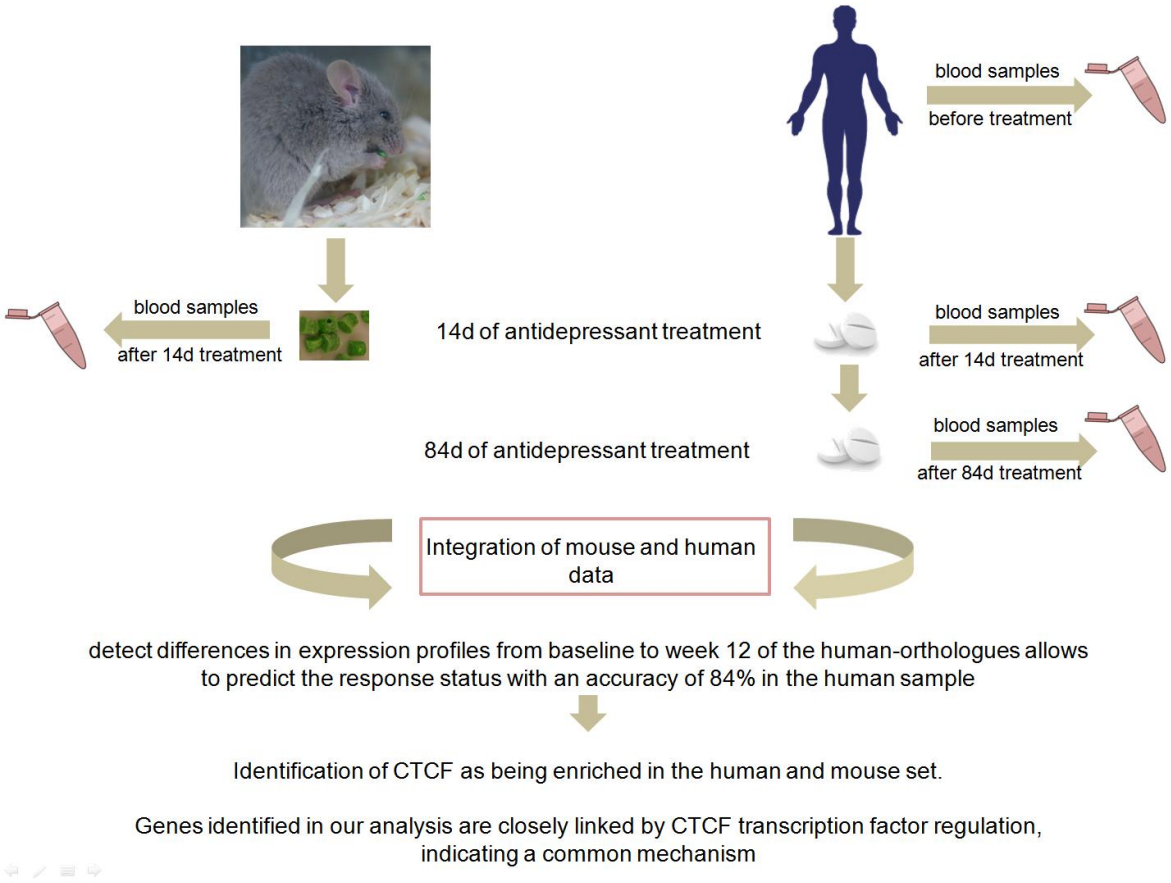

Figure 43: Translational approach enables us to detect common transcription factors. By using this translational approach we were able to detect a gene set, which is regulated in the mouse peripheral blood after 14d of paroxetine treatment. After the integration of the mouse data in the human dataset, we were able to detect differences in gene expression profiles in the human samples from baseline to week 12 that allow us to predict the response status with an accuracy of 84% in the human samples. Further investigations also identified CTCF, a transcription factor, as being enriched in both the human and mouse data set.

4.3.2 Subchronic paroxetine treatment regulates a distinct gene network in the brain

In order to gain a better understanding of the biological connections amongst the various detected genes in the brain, a pathway analysis was performed, based on information derived from literature-based interactions between proteins, small molecules and cellular processes (Webhofer et al., 2011). Interestingly, we were able to detect a gene network comprising 15 of the 87 differentially regulated genes. At present, there is little known about this gene network in the literature. Interestingly, immune-related genes such as Cxcl12 or Il-16, and structural genes such as Gfap and Vim, are highly represented in the detected network. There is growing evidence that an altered immune response is an important aspect of mood disorders (Friedrich, 2014). Cytokines as well as chemokines are hormonal mediators of the immune response and play a crucial role in the neuroendocrine system. Cytokines are small signaling molecules, which are secreted by various cell types, including astrocytes, microglia, lymphocytes (Arisi, 2014). It has been demonstrated that an elevation of circulating proinflammatory cytokines, namely IL-6 and tumor necrosis factor alpha, is a characteristic feature in a subset of depressed patients (Villanueva, 2013; Dunn, 2006). Proinflammatory cytokines do not only contribute to the innate immune response and inflammation, but they also have relevant neuroendocrine and metabolic effects, specifically affecting neurotransmitter metabolism and neural plasticity (Villanueva, 2013). We could show that subchronic antidepressant treatment regulates the proinflammatory cytokines. More specifically, we found that subchronic paroxetine exposure significantly downregulated Il-16 mRNA levels. This finding is in line with previous findings, showing that administration of cytokine Il-6 induces depressive-like behavior in rodents and fluoxetine treatment is able to neutralize this effect (Sukoff Rizzo et al., 2012). Besides Il-16, we also detected the chemokine Cxcl12. Chemokines are small secreted proteins with chemoattractant properties, meaning that they can attract and activate immune and non-immune cells (Réaux-Le Goazigo et al., 2013) and are thus acting as neuromodulators (Adler et al., 2005). Currently, the well-established roles of Cxcl12 all converge on immune functions, however, more and more reports also identify Cxcl12 as an important player in the CNS (Réaux-Le Goazigo et al., 2013). A potential role of Cxcl12 in mood disorders is strengthened by the fact that Cxcl12 is also involved in neuroprotection, neurogenesis, regeneration and axon guidance. Interestingly, Cxcl12 seems to interact with Stat3, a gene also detected in the gene network. It has been demonstrated that higher expression of Cxcl12 leads to higher Stat3 phosphorylation (Shen et al., 2013). Shen and colleagues were able to show that pharmacological

blockade of Stat3 activity inhibited Cxcl12-triggered Stat3 phosphorylation (Shen et al., 2013). Furthermore, studies could show that Stat3 is activated in various cell types by a number of cytokines, such as IL-6 and TGFα (Takeda et al., 1997). These cytokines are in turn implicated in triggering reactive astrogliosis (Balasingam et al., 1994; Klein et al., 1997; Levison et al., 2000; Rabchevsky et al., 1998). Herrmann and coworkers have shown that Stat3 is a critical factor for certain aspects of reactive astrogliosis (Herrmann et al., 2008) and thus is also a very interesting candidate for future investigation.

Besides immune-related genes, structural proteins namely glial fibrillary acidic protein (Gfap) and vimentine (Vim) were also regulated after subchronic antidepressant treatment. There is growing evidence in the field of depression that structural molecules play an important role in the pathology of depression as well as in antidepressant treatment response. In 2008, Sillaber and colleagues had already shown a significant upregulation of Gfap and Vim following chronic paroxetine treatment in male DBA mice, which is in line with our findings (Sillaber et al., 2008). Human post mortem studies have furthermore shown that GFAP proteins are significantly reduced in depressed patients, which strengthens the involvement of glial (dys)-function in mood disorders (Fatemi et al., 2004). Gfap is nearly exclusively expressed in astroytes and is involved in gliosis, neurodegeneration, neuroregeneration and neurogenesis (Fatemi et al., 2004; Sillaber et al., 2008). Astrocytes are structural and trophic supporters of neurons and play a key role in the CNS immune response, as well as a role in the clearance of ions and neurotransmitters (Allen and Barres, 2005; Araque, 2006). Some studies have demonstrated that astrocytes play a role in neural progenitor cells during development as well as in the mature CNS and promote neurogenesis (Goldman, 2003; Song et al., 2002). Additionally, it could be shown that 28d of antidepressant treatment is able to prevent stress-induced decreases in astrocyte number. This finding supports the hypothesis that dysregulation of glial cells may be involved in the pathophysiology of mood disorders (Sillaber et al., 2008; Czéh et al., 2005; Manev et al., 2003).

In summary, although selected connections between antidepressant-regulated genes have been identified, the complete picture of this antidepressant-induced gene network is still not clear. To advance the current understanding in regards to the individual role of different genes in antidepressant response, further investigations are required.

4.4 Gene expression profiling in the hippocampus following chronic antidepressant treatment

In a second study, we were interested in examining the differences between good and poor responder after chronic paroxetine treatment, as most depressed patients start responding to pharmacological treatment after at least 4 weeks of antidepressant administration (Wisniewski et al., 2009; Trivedi et al., 2006; Rojo et al., 2005; Nemeroff and Owens, 2002). Here, we aimed to identify novel genes differently regulated between good and poor responders. After the identification of the various responder subgroups, an unbiased microarray approach was conducted with the tissue derived from the chronically treated animals. After statistical analysis of the Illumina microarray chip, 30 genes were found to be differently regulated between vehicle treated animals and good responders. Although we did not detect a significant difference between good and poor treatment responders, a clear treatment effect was evident. Out of the 30 differently regulated genes, 12 genes were selected for further validation. With a validation rate of 75% we were able to validate a significant number of the selected candidates confirming the validity of our results. In the following section, select candidates are discussed in more detail:

ActivinA receptor type 1c, also known as Acvr1c or Alk-7, represents one of the genes that was significantly upregulated in the hippocampus of good responders. Activins belong to the transforming growth factor-β (TGFβ) superfamily which are now well-known as multifunctional regulatory proteins (Werner and Alzheimer, 2006). Besides their role in development and hormonal regulation, previous studies have also demonstrated that Activins play an important functional role in tissue repair and have been identified as an important target in various inflammatory diseases, including brain-related inflammatory diseases (Werner and Alzheimer, 2006). Acvr1c, as a member of the Activins, is a growth factor-associated gene involved in the survival and differentiation of adult neuronal cells (Miller et al., 2007). Furthermore, it is part of the Activin/Inhibin signaling cascade, which was previously found to be involved in antidepressant-like properties (Ganea et al., 2012). In the study conducted by Ganea and colleagues, Activinβ A exerted acute antidepressant-like effects when directly administered to the hippocampal dentate gyrus. Collectively, these findings support a potential role of Acvr1c in antidepressant treatment outcome and thus make it as a suitable candidate for further studies.

In addition to its effects of Acvr1c receptor activity, we found that chronic antidepressant treatment also affects other genes involved in the inflammatory system, which already

came up as a key system following subchronic treatment. One of these genes was the complement component 1, q subcomponent-like 2 (C1ql2). C1ql2 is a protein-coding gene and is part of the complement pathway, which is involved in the immune response system. C1q is a target recognition protein of the classical complement pathway. It's crucial role involves the clearance of pathogens and apoptotic cells (Kishore et al., 2004). C1q is also involved in a number of immunological processes such as phagocytosis of bacteria, neutralization of retroviruses, cell adhesion as well as modulation of dendritic cells (Kishore et al., 2004). Complement proteins are localized in the developing central nervous system synapses. They are present during a period of active synapse elimination and are crucial for normal brain wiring. It has been shown that their role in the brain is similar to their function in the immune system: the clearance of cellular material. C1q can be divided into two subfamilies: C1q-like proteins and cerebellin-like proteins. While it is known that cerebellin-like proteins are essential trans-neuronal regulators of synaptic integrity in the cerebellum (Iijima et al., 2010), not much is known about the role and function of C1q-like proteins and C1ql2 in particular. During adulthood, C1ql2 is only expressed in the dentate gyrus formation of the hippocampus (Iijima et al., 2010). Furthermore, there is evidence that C1ql2 is mainly expressed in neurons and to a lesser extent in glia cells during adulthood (Iijima et al., 2010). At present, there are no reports for an involvement of C1ql2 in depression. However, the link between depression and inflammation is highly recognized in the field of depression (Dantzer et al., 2008). Furthermore, the hippocampus is a main target region in depression research and thus the unique expression pattern of C1ql2 during adulthood strengthens its potential as a candidate gene in mental disorders.

Serpinf1 marks another gene that was detected in the microarray analysis. Serpinf1 belongs to the serpine family of peptidase inhibitors and is also known by the name pigment epithelium-derived factor (PEDF). During development, Serpinf1 is essential for the development of the neural retina (Steele et al., 1993). Bilak and colleagues could show that Serpinf1 is a neurotrophic factor, which is broadly distributed in the central nervous system. It has been suggested, that this factor could have pleiotrophic, neurotrophic and neuroprotective effects on non-retinal neurons (Bilak et al., 1999). Serpinf1 is a 50kDa, secreted glycoprotein, expressed in a variety of tissue types. For instance, adipocytes also secrete Serpinf1 and it thus showed promise as a candidate gene in obesity-induced insulin resistance (Böhm et al., 2012; Crowe et al., 2009). Furthermore, it was shown that Serpinf1 promotes neuronal survival, differentiation and potent inhibition of angiogenesis (Tombran-Tink et al., 1991; Tombran-Tink and

Barnstable, 2003). In 2008, Miller and colleagues were one of the first to show a potential link between Serpinf1 and antidepressant treatment. They could demonstrate that Serpinf1 is upregulated after chronic fluoxetine treatment, which is in line with our current finding. The fact that Serpinf1 is responsive to antidepressant treatment and is furthermore known to promote proliferation of neuronal progenitor cells, makes it to a very promising candidate in antidepressant treatment outcome (Miller et al., 2007).

Taken together, after chronic paroxetine treatment, we were not able to find significant differences, at least on mRNA level, between good and poor treatment responders. Our main gene expression differences were detectable between vehicle treated animals and good responders. However, to our knowledge, we were the first to examine individual antidepressant response after chronic treatment in DBA/2J mice. Thus our study provides novel, interesting and promising targets for further antidepressant studies.

4.5 Time course of gene expression regulation during antidepressant treatment in the mouse hippocampus

Interestingly, more genes were regulated by subchronic paroxetine treatment compared to chronic treatment, indicating that at the beginning of the treatment period a large cluster of genes are regulated. Our data suggest that following a 4-weeks treatment period, certain genes return to baseline expression levels, whereas others remain responsive to the ongoing treatment either through direct effects of antidepressant activity or rather indirectly as a result of activation of previous cascades. As the number of regulated genes significantly varies between the two different time points, the question arises as to whether there is an overlap between subchronic and chronic treatment. When comparing the gene expression profile of the two treatment time points, we can identify an overlap of 15 genes (Table 6) representing genes that were differently regulated following both treatment intervals.

Genes integral to immune function (C1ql2), neurogenesis (Sox11) and receptor activity (Acvr1c, Adra2c, Drd1a) are among the regulated genes.

Sox11 was identified as one of the genes regulated after both treatment durations, potentially signaling an important role for Sox11 in mediating antidepressants' mechanism of action. This finding encouraged us to consider Sox11as an interesting candidate gene for further investigations. Sox11 is a member of the Sox gene family that has been well characterized regarding its expression pattern in the developmental nervous system and

its role in neurogenesis, neural cell survival and neurite outgrowth (Bergsland et al., 2006). During development, Sox11 is highly expressed in developing sensory neurons (Jankowski et al., 2009) and in brain areas that are important for neuron differentiation (Kuhlbrodt et al., 1998). Importantly, Sox11 gene expression is regulated both spatially and temporally (Wilson and Koopman, 2002), meaning that its expression is reduced in late stages of gestation and remains low in adult neurons (Jankowski et al., 2009). Developmental studies have shown that Sox11 plays a crucial role in embryo development. This is further demonstrated in Sox11 knockout studies, which have revealed that total Sox11 knockout mice are embryonically lethal, whereas its partial depletion results in various craniofacial and skeletal malformations, asplenia and hypoplasia of the lung and stomach, altogether suggesting an important role of Sox11 in tissue remodeling. These findings are in line with the human situation (Sock et al., 2004). Jankowski and coworkers provide evidences that Sox11 plays a central role in regulating processes, which in turn promote neurite growth as well as neuron survival (Jankowski et al., 2006). Studies could show that the basal level of Sox11 expression is lower during adult hood compared to the developmental stage. However, it was found to be upregulated after nerve injury and was associated with injury-induced neuritogenesis (Elliott et al., 2003; Tanabe et al., 2003).

4.6 Sox11- a transcription factor and its putative role in emotional behavior

Only very little is known about a putative role of Sox11 in modulating emotional behavior.

4.6.1 Paroxetine is leading to a robust regulation of Sox11

We, therefore, continued to dissect the role of Sox11 in the neurobiology underlying antidepressants' mechanism of action in detail. We were able to show a significant upregulation of Sox11 mRNA levels, especially in the hippocampal DG, after subchronic and chronic paroxetine treatment. These findings are in line with previous findings, where chronic paroxetine treatment lead to a upregulation of Sox11 mRNA levels in DBA mice (Sillaber et al., 2008). We found Sox11 mRNA levels already upregulated as early as 14d (i.e. after subchronic) of treatment. Interestingly, we did not see any changes in Sox11 expression following an acute antidepressant administration, indicating that the paroxetine-induced time course of Sox11 induction corresponds with the delayed onset of action of antidepressant effects in the clinical setting. Sox11 has been well characterized regarding its expression pattern in the neurogenic niche and its role in neurogenesis, neural cell survival and neurite outgrowth (Bergsland et al., 2006). In the adult mouse

Sox11 is mainly expressed in the DG formation of the hippocampus (Haslinger et al., 2009). There is a large body of literature supporting the idea that stimulation of neurogenesis in the adult brain could be a crucial step in the successful treatment of depressive disorders. For example, various studies have shown an interplay between antidepressants and neurogenesis (Braun and Jessberger, 2014; D'Sa and Duman, 2002; Sahay and Hen, 2007). However the effect of antidepressant treatment on neurogenesis are mainly detected after a chronic administration (Malberg et al., 2000).

We were also interested as to whether the induction of Sox11 is a general antidepressant-induced phenomenon, or whether it is rather exclusively triggered by SSRIs. Therefore, we performed a chronic treatment with reboxetine, a NERI. In this experiment, we did not find a significant difference in Sox11 gene expression levels between vehicle-treated animals and reboxetine-treated animals. These findings suggest that Sox11 upregulation is specific for SSRIs in general and paroxetine in particular. It is hypothesized that the antidepressant effect on neurogenesis is mediated by serotonergic regulation of intracellular signaling mechanisms that consequently upregulate transcription and growth factors and are thus involved in neuron proliferation (Duman et al., 2001). In support of this hypothesis, Santarelli and colleagues treated mice for three weeks with fluoxetine and found a significant upregulation of cell proliferation (70%) in the dentate gyrus. In a follow-up experiment they used 5-HT_{1A}receptor knockout mice and the effect was gone (Santarelli et al., 2003). These results further support our findings that serotonergic modulations especially lead to changes in cell proliferation and thus neurogenesis. Hence, it is not surprising that transcription factors or genes that are involved in cell proliferation are more responsive to serotonergic antidepressants compared to antidepressants based on noradrenergic transmission.

4.6.2 Sox11 overexpression reduces anxiety-related behavior, but is not influencing neurogenesis

Considering that Sox11 was upregulated after chronic SSRI treatment and chronic antidepressant treatment lead to a less depressive-like phenotype in the FST, we hypothesized that viral overexpression of Sox11 may also lead to a less depressive-like phenotype, as reflected in the FST. However, we did not detect any behavioral alteration in the FST following a viral overexpression of Sox11.

David and colleagues demonstrated that a fluoxetine-induced FST phenotype is independent of hippocampal neurogenesis (David et al., 2009). Thus, if the predominant

function of Sox11 in the DG is neurogenesis-related (Haslinger et al., 2009; Haslinger et al., 2009), an effect of Sox11 OE on the FST phenotype would be unlikely.

However, we could clearly show that overexpression of Sox11 significantly reduced anxiety-related behavior compared to the vehicle-treated empty control animals. Besides its cognitive function, the hippocampus is also involved in regulating emotional behavior, including anxiety. Various studies have demonstrated a link between the hippocampus, neurogenesis and anxiety. For instance, Revest and colleagues could show that a decrease in adult-born neurons increases anxiety-related behavior (Revest et al., 2009). More specifically, they demonstrated that an impairment in neurogenesis is associated with an increased avoidance of novel and potentially threatening environments. Two other studies are in line with Revest et al., however they directly manipulated various target genes like Activin and TrkB receptor (Ageta et al., 2008; Bergami et al., 2008). As Sox11 is involved in cell proliferation (Haslinger et al., 2009; Wegner, 2011) and thus directly and/or indirectly involved in neurogenesis, our results are fitting well to the previous findings. We were able to induce a less anxious phenotype by increasing Sox11 expression. As we do not see any changes in the FST, we can ensure that the effect is selective for anxiety-related behavior. As reboxetine treatment modulated neither anxiety-related behavior nor the expression of Sox11 mRNA, these findings support our hypothesis that Sox11 could be involved in shaping anxiety-related behavior.

To further investigate whether the reduction in anxiety-like behavior might be accompanied by changes in cell proliferation, we performed a cell proliferation study. Therefore, we artificially overexpressed Sox11 via an AAV virus injection and investigated neurogenesis and cell proliferation in these animals. Animals were injected for three consecutive days with a 100mg/kg pulse of BrdU. This timeline was chosen, as it has been shown in previous studies, that DBA/2J mice show very little baseline neurogenesis. The rare of neurogenesis rate is highly heritable but also highly variable among the different inbred mouse strains (Kempermann et al., 2006). For example, it has been shown in a previous study, comparing four inbred mouse strains, that DBA/2J mice show a cell survival rate of 19% 4 weeks after the BrdU administration. In the same study, they additionally demonstrated that DBA/2J mice produce significantly fewer neurons compared to the other mouse strains under examination but significantly more astrocytes (Kempermann and Gage, 2002). To investigate cell proliferation, select animals were killed 2h or 28d after the last BrdU injection. When investigating differences in BrdU-positive cells we did not find any differences between the two groups. Despite the known

role of Sox11 in neurogenesis, we did not observe an effect of Sox11 OE on cell proliferation or maturation. It has been shown that chronic stress reduces neurogenesis by modulating cell proliferation and maturation rate, whereas antidepressants are able to reverse such stress-induced effect (Braun and Jessberger, 2014; David et al., 2009; Duman and Monteggia, 2006; Santarelli et al., 2003). The lack of this effect in our study could be due to the stage-specific expression of Sox11 in cells of the adult neurogenic lineage (Haslinger et al., 2009). This means that Sox11 expression is associated with a downregulation of Sox2 and with the onset of DCX expression, an early neuronal lineage marker (Brown et al., 2003). The stage-specific restriction of Sox11 corresponds with the transient expression during embryonic development and more specifically embryonic neurogenesis (Bergsland et al., 2006; Hargrave et al., 1997), which suggests that Sox11 controls similar stage-specific processes during embryonic development and adult neurogenesis (Haslinger et al., 2009). At present, Sox11 regulation in the adult neurogenic lineage remains unknown (Haslinger et al., 2009) and it is still unclear whether Sox11 itself is directly responsible for neurogenesis. Some studies suggest that Sox11 plays an important role in adult neurogenesis (Sha et al., 2012; Jankowski et al., 2006; Haslinger et al., 2009), yet to our knowledge nobody has performed a BrdU experiment with Sox11 OE mice. Our experiment thus sheds light on this topic. We have shown that the viral overexpression of Sox11 itself is not sufficient to increase cell proliferation and cell maturation rates although we were able to detect behavioral phenotypes similar to those ascribed to alterations in neurogenesis. Although the overexpression of Sox11 leads to an altered behavioral phenotype, the cellular explanation for this behavioral phenotype is not as obvious as first speculated. One explanation is founded on the stage-specific expression of Sox11 in neurogenic lineage. We performed viral overexpression of Sox11 and then waited for 4 weeks in order to achieve robust overexpression of Sox11. As Sox11 expression is associated with the downregulation of Sox2 and with the onset of DCX expression (Brown et al., 2003), it is possible that we targeted the wrong time window to detect differences in neurogenesis due to viral Sox11 OE. Alternatively, the involvement of Sox11 in neurogenesis is not directly regulated via Sox11. If this would be the case, manipulation of Sox11 upstream targets are needed to potentially evoke robust neurogenesis effects on a cellular level. Nonetheless, further investigations are indeed necessary in order to find a cellular explanation for the anxiety-like phenotype.

4.6.3 Sox11 knockdown does not influence antidepressant response but leads to a higher mortality rate

As Sox11 OE decreases anxiety-related behavior, we were also interested as to whether a knockdown of Sox11 is able to produce a more anxious phenotype and whether or not paroxetine would be able to reverse this effect. Surprisingly, hippocampal knockdown of Sox11 in adulthood, resulted in higher mortality rates in DBA/2J mice compared to the control group. It is known that Sox11 plays a crucial role during development and is essential for normal organ development (Sock et al., 2004). However, to-date there is nothing known about the role of a partial knockdown or knockout of Sox11 during adulthood. In our experimental animals we observed convulsive poses in the homecage in the late afternoon (n=3) and while weighing the animals (n=2). These observations led us to speculate that the high mortality rate in the Sox11 KD animals might be due to epileptic seizures. There is growing evidence in the literature that genes, which are involved in neurogenesis, may also play a significant role in epilepsy (Elliott et al., 2003). Therefore, further investigations are needed to investigate the role of Sox11 KD in adult DBA/2J mice in terms of epileptic seizures. Moreover, the mortality rate should be kept in mind when interpreting the behavioral parameters. In contrast to our previous experiments, we observed a paroxetine-induced hyperactivity. Hyperactivity resulting from antidepressant treatment is controversial with mixed findings in the literature. Some studies have shown a significant increase in basal locomotor activity following antidepressant treatment whereas others have shown no effect (Dulawa et al., 2004; Prut and Belzung, 2003). In the current experiment, the previous surgery may have confounded the results, and may possibly underlie the animals' hypersensitivity to paroxetine-induced hyperactivity. Interestingly, we did not observe an effect of Sox11 manipulation on the FST behavior. By contrast Sox11 manipulation has a clear, directional effect on anxiety-like behavior. Specifically hippocampal overexpression of Sox11 promotes a reduced anxiety-like phenotype, whereas hippocampal knockdown of Sox11 suitably increased anxiety-related behavior in the DaLi, an effect that was independent of the treatment. These findings support a pivotal role of Sox11 in modulating anxiety-related behavior. To deliver a plausible explanation for this is not possible at the moment. Further investigations, at a cellular and behavioral level, are needed in order to advance our current understanding of the function and signaling cascades of Sox11.

At present, we can conclude that Sox11 plays an essential role during adulthood and is a potential novel target for modulating anxiety-related behavior.

4.7 Summary

Major depressive disorder is one of the most common mental disorders. It is a very complex and multifactorial psychiatric disease, which affects up to 20% of the general population (Kessler et al., 2005). Furthermore, unipolar depressive disorders pose an immense burden on society and the WHO ranked depression as the fourth leading cause of disability (Murray and Lopez, 1996; Rubinow, 2006). Additionally, bipolar disorders (episodes of major depression and mania) and anxiety are two diseases that most frequently overlap diagnostically with depression (Flint and Kendler, 2014). Despite the immense research that has been ongoing over the past decades, the pathophysiology of depression as well as the neurobiology underlying the surprisingly high heterogeneity in antidepressant treatment response are still largely unknown.

The present study therefore aimed to identify novel targets mediating an individual antidepressant response in mice. Furthermore, we attempted to translate these findings to the clinical situation in order to detect novel biomarkers for antidepressant treatment outcome. As a first step, we investigated the pharmacological profile of paroxetine in order to define the minimum effective dose for DBA/2J mice. To our knowledge, this is the first study to extensively investigate the pharmacological profile of paroxetine in mice. Furthermore, the current thesis provides a compelling basis for the involvement of Sox11 in anxiety-related behavior. We extensively investigated the function of Sox11 under various antidepressant substances, different treatment durations as well as after genetic manipulation to provide strong evidence that Sox11 is a promising target for anxiety-related disorders. Previous studies have ascribed a potential role for Sox11 in neurogenesis (Haslinger et al., 2009; Mu et al., 2012a). Nevertheless, by genetically manipulating Sox11, we have shown that Sox11 alone is not sufficient to directly influence the neurogenesis rate in DBA/2J mice. Regardless, Sox11 is a very interesting candidate when investigating anxiety-related behavior.

To address the problems of the delayed onset of antidepressant action, we aimed to identify novel targets mediating an early antidepressant response. Therefore, we performed a subchronic paroxetine treatment and investigated alterations in gene expression profiles in the periphery and the brain. In a next step, we integrated our findings with human data in order to assess whether such gene expression profiles are able to predict antidepressant response status in the human sample population. To our knowledge, this is the first study that was able to show such a prediction in antidepressant

response using a translational approach. These findings allow us to predict at an early stage, i.e. two weeks after treatment onset, whether the patient will show an appropriate response after 12 weeks of antidepressant treatment (Figure 44). Moreover, we were able to identify common transcription factors that seems to play a role in antidepressant treatment response.

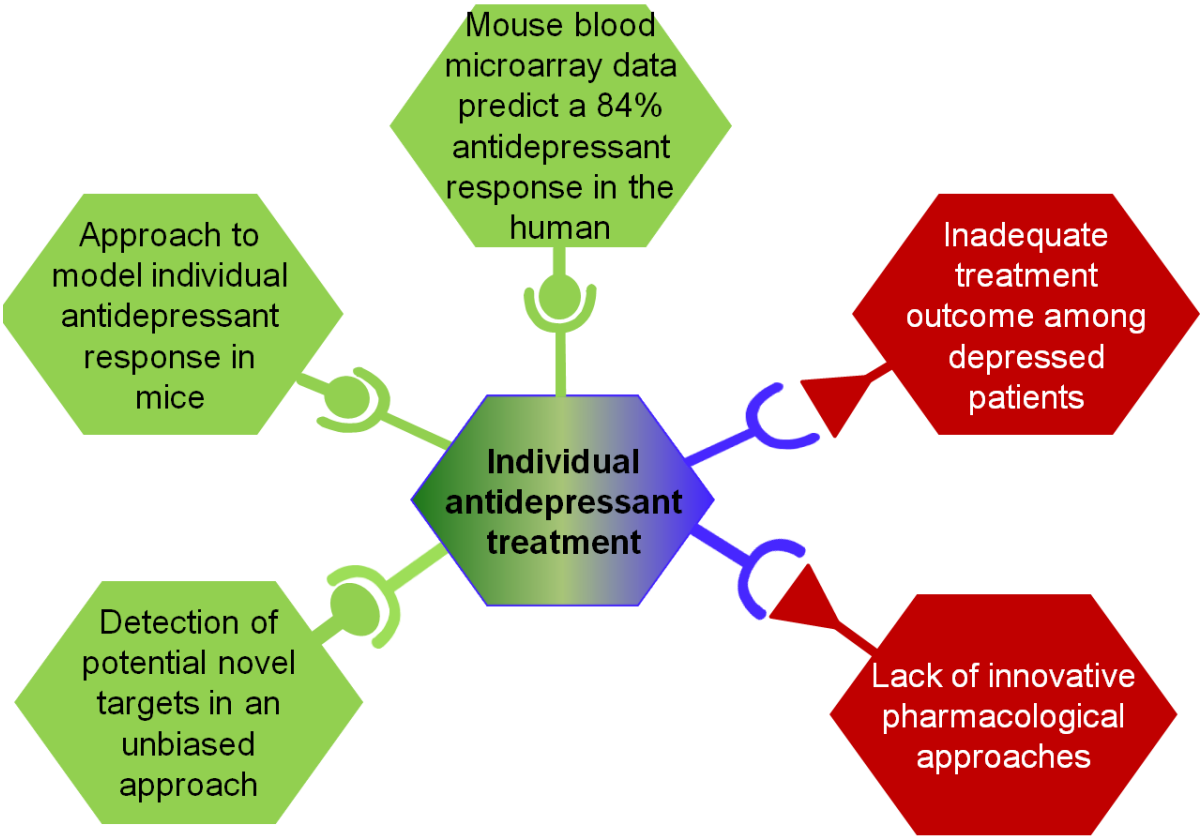

Figure 44: Achievements of this thesis. This experiment approach was able to solve some basic but important questions in depression research. However these data needs further investigations and some questions still need to be addressed.

This study provides essential, novel information regarding gene regulation by antidepressant treatment and is therefore a good starting point for the identification of novel biomarkers mediating individual antidepressant response. We were able to shed new light on the field of antidepressant treatment outcome and more specifically, on early antidepressant response. Furthermore, our translational approach enabled us to translate our findings from mice to men and thus provides a good basis for further research.

References

Adler M, Geller E, Chen X, Rogers T (2005) Viewing chemokines as a third major system of communication in the brain. AAPS J 7:E865-E870.

Ageta H, Murayama A, Migishima R, Kida S, Tsuchida K, Yokoyama M, Inokuchi K (2008) Activin in the brain modulates anxiety-related behavior and adult neurogenesis. PLoS One 3:e1869.

Allen NJ, Barres BA (2005) Signaling between glia and neurons: focus on synaptic plasticity. Current Opinion in Neurobiology 15:542-548.

Altamura C, Maes M, Dai J, Meltzer HY (1995) Plasma concentrations of excitatory amino acids, serine, glycine, taurine and histidine in major depression. European Neuropsychopharmacology 5, Supplement 1:71-75.

Araque A (2006) Astrocyte-neuron signaling in the brain--implications for disease. Curr Opin Investig Drugs 7:619-624.

Arisi GM (2014) Nervous and immune systems signals and connections: Cytokines in hippocampus physiology and pathology. Epilepsy & Behavior.

Atcha Z, Rourke C, Neo AH, Goh CW, Lim JS, Aw CC, Browne ER, Pemberton DJ (2010) Alternative Method of Oral Dosing for Rats. pp 335-343.

Auerbach RK, Chen B, Butte AJ (2013) Relating Genes to Function: Identifying Enriched Transcription Factors using the ENCODE ChIP-Seq Significance Tool. Bioinformatics.

Baghai TC, Volz HP, Moller HJ (2006) Drug treatment of depression in the 2000s: An overview of achievements in the last 10 years and future possibilities. World J Biol Psychiatry 7:198-222.

Balasingam V, Tejada-Berges T, Wright E, Bouckova R, Yong VW (1994) Reactive astrogliosis in the neonatal mouse brain and its modulation by cytokines. J Neurosci 14:846-856.

Barriga C, Martín MI, Tabla R, Ortega E, Rodríguez AB (2001) Circadian rhythm of melatonin, corticosterone and phagocytosis: effect of stress. Journal of Pineal Research 30:180-187.

Bergami M, Rimondini R, Santi S, Blum R, Götz M, Canossa M (2008) Deletion of TrkB in adult progenitors alters newborn neuron integration into hippocampal circuits and increases anxiety-like behavior. Proceedings of the National Academy of Sciences 105:15570-15575.

Bergsland M, Werme M, Malewicz M, Perlmann T, Muhr J (2006) The establishment of neuronal properties is controlled by Sox4 and Sox11. Genes & Development 20:3475-3486.

Beyer CE, Stahl SM (2010) Next Generation Antidepressants Moving Beyond Monoamines to Discover Novel Treatment Strategies for Mood Disorders. Cambridge University Press.

Bilak MM, Corse AM, Bilak SR, Lehar M, Tombran-Tink J, Kuncl RW (1999) Pigment epithelium-derived factor (PEDF) protects motor neurons from chronic glutamate-mediated neurodegeneration. J Neuropathol Exp Neurol 58:719-728.

Binder EB, Nemeroff CB (2010) The CRF system, stress, depression and anxiety-insights from human genetic studies. Mol Psychiatry 15:574-588.

Binder EB, Holsboer F (2006) Pharmacogenomics and antidepressant drugs. Ann Med 38:82-94.

Böhm A, Ordelheide AM, Machann J, Heni M, Ketterer C, Machicao F, Schick F, Stefan N, Fritsche A, Haring HU, Staiger H (2012) Common genetic variation in the SERPINF1 locus determines overall adiposity, obesity-related insulin resistance, and circulating leptin levels. PLoS One 7:e34035.

Bortolato M, Chen K, Shih JC (2008) Monoamine oxidase inactivation: From pathophysiology to therapeutics. Advanced Drug Delivery Reviews 60:1527-1533.

Bradley RG, Binder EB, Epstein MP, Tang Y, Nair HP, Liu W, Gillespie CF, Berg T, Evces M, Newport DJ, Stowe ZN, Heim CM, Nemeroff CB, Schwartz A, Cubells JF, Ressler KJ (2008) Influence of child abuse on adult depression: moderation by the corticotropin-releasing hormone receptor gene. Arch Gen Psychiatry 65:190-200.

Braun SMG, Jessberger S (2014) Review: Adult neurogenesis and its role in neuropsychiatric disease, brain repair and normal brain function. Neuropathol Appl Neurobiol 40:3-12.

Brown JP, Couillard-Despres S, Cooper-Kuhn CM, Winkler J, Aigner L, Kuhn HG (2003) Transient expression of doublecortin during adult neurogenesis. J Comp Neurol 467:1-10.

Burmeister M (1999) Basic concepts in the study of diseases with complex genetics. Biological Psychiatry 45:522-532.

Bush WS, Moore JH (2012) Chapter 11: Genome-Wide Association Studies. PLoS Comput Biol 8:e1002822.

Carter GC, Cantrell RA, Victoria Z, Haynes VS, Phillips G, Alatorre CI, Goetz I, Paczkowski R, Marangell LB (2012) Comprehensive review of factors implicated in the heterogeneity of response in depression. Depress Anxiety 29:340-354.

Cattaneo A, Gennarelli M, Uher R, Breen G, Farmer A, Aitchison KJ, Craig IW, Anacker C, Zunsztain PA, McGuffin P, Pariante CM (2013) Candidate Genes Expression Profile Associated with Antidepressants Response in the GENDEP Study: Differentiating between Baseline `Predictors' and Longitudinal `Targets'. Neuropsychopharmacology 38:377-385.

Chadman KK, Yang M, Crawley JN (2009) Criteria for validating mouse models of psychiatric diseases. Am J Med Genet 150B:1-11.

Checkley S (1996) The neuroendocrinology of depression and chronic stress. Br Med Bull 52:597-617.

Crane GE (1956) The psychiatric side-effects of iproniazid. Am J Psychiatry 112:494-501.

Crawley JN (1985) Exploratory behavior models of anxiety in mice. Neurosci Biobehav Rev 9:37-44.

Crowe S, Wu LE, Economou C, Turpin SM, Matzaris M, Hoehn KL, Hevener AL, James DE, Duh EJ, Watt MJ (2009) Pigment Epithelium-Derived Factor Contributes to Insulin Resistance in Obesity. Cell Metabolism 10:40-47.

Cryan JF, Markou A, Lucki I (2002) Assessing antidepressant activity in rodents: recent developments and future needs. Trends in Pharmacological Sciences 23:238-245.

Cryan JF, Valentino RJ, Lucki I (2005) Assessing substrates underlying the behavioral effects of antidepressants using the modified rat forced swimming test. Neuroscience & Biobehavioral Reviews 29:547-569.

Czéh B, Michaelis T, Watanabe T, Frahm J, Biurrun Gd, Kampen Mv, Bartolomucci A, Fuchs E (2001) Stress-Induced Changes in Cerebral Metabolites, Hippocampal Volume, and Cell Proliferation are Prevented by Antidepressant Treatment with Tianeptine. Proceedings of the National Academy of Sciences of the United States of America 98:12796-12801.

Czéh B, Simon M, Schmelting B, Hiemke C, Fuchs E (2005) Astroglial Plasticity in the Hippocampus is Affected by Chronic Psychosocial Stress and Concomitant Fluoxetine Treatment. Neuropsychopharmacology 31:1616-1626.

D'Sa C, Duman RS (2002) Antidepressants and neuroplasticity. Bipolar Disorders 4:183-194.

Dantzer R, O'Connor JC, Freund GG, Johnson RW, Kelley KW (2008) From inflammation to sickness and depression: when the immune system subjugates the brain. Nat Rev Neurosci 9:46-56.

David DJ, Samuels BA, Rainer Q, Wang JW, Marsteller D, Mendez I, Drew M, Craig DA, Guiard BP, Guilloux JP, Artymyshyn RP, Gardier AM, Gerald C, Antonijevic IA, Leonardo ED, Hen R (2009) Neurogenesis-Dependent and -Independent Effects of Fluoxetine in an Animal Model of Anxiety/Depression. Neuron 62:479-493.

de Foubert G, Carney SL, Robinson CS, Destexhe EJ, Tomlinson R, Hicks CA, Murray TK, Gaillard JP, Deville C, Xhenseval V, Thomas CE, O'Neill MJ, Zetterström TSC (2004) Fluoxetine-induced change in rat brain expression of brain-derived neurotrophic factor varies depending on length of treatment. Neuroscience 128:597-604.

de Kloet ER, Joels M, Holsboer F (2005) Stress and the brain: from adaptation to disease. Nat Rev Neurosci 6:463-475.

de Meijer VE, Le HD, Meisel JA, Puder M (2010) Repetitive orogastric gavage affects the phenotype of diet-induced obese mice. Physiology & Behavior 100:387-393.

de Montigny C, Aghajanian GK (1978) Tricyclic antidepressants: long-term treatment increases responsivity of rat forebrain neurons to serotonin. Science 202:1303-1306.

Delgado PL (2004) How antidepressants help depression: mechanisms of action and clinical response. J Clin Psychiatry 65 Suppl 4:25-30.:25-30.

Dell'Osso B, D'Addario C, Carlotta Palazzo M, Benatti B, Camuri G, Galimberti D, Fenoglio C, Scarpini E, Di Francesco A, Maccarrone M, Carlo Altamura A (2014) Epigenetic modulation of BDNF gene: Differences in DNA methylation between unipolar and bipolar patients. Journal of Affective Disorders 166:330-333.

Dellu F, Contarino A, Simon H, Koob GF, Gold LH (2000) Genetic Differences in Response to Novelty and Spatial Memory Using a Two-Trial Recognition Task in Mice. Neurobiology of Learning and Memory 73:31-48.

Dellu F, Mayo W, Cherkaoui J, Le Moal M, Simon H (1992) A two-trial memory task with automated recording: study in young and aged rats. Brain Research 588:132-139.

Drevets WC (2000) Neuroimaging studies of mood disorders. Biological Psychiatry 48:813-829.

Dulawa SC, Hen R (2005) Recent advances in animal models of chronic antidepressant effects: The novelty-induced hypophagia test. Neuroscience & Biobehavioral Reviews 29:771-783.

Dulawa SC, Holick KA, Gundersen B, Hen R (2004) Effects of Chronic Fluoxetine in Animal Models of Anxiety and Depression. Neuropsychopharmacology 29:1321-1330.

Duman RS (2004) Depression: a case of neuronal life and death? Biological Psychiatry 56:140-145.

Duman RS, Monteggia LM (2006) A Neurotrophic Model for Stress-Related Mood Disorders. Biological Psychiatry 59:1116-1127.

Duman RS, Nakagawa S, Malberg J (2001) Regulation of Adult Neurogenesis by Antidepressant Treatment. Neuropsychopharmacology 25:836-844.

Duman RS, Voleti B (2012) Signaling pathways underlying the pathophysiology and treatment of depression: novel mechanisms for rapid-acting agents. Trends in Neurosciences 35:47-56.

Dunlop BW, Binder EB, Cubells JF, Goodman MM, Kelley ME, Kinkead B, Kutner M, Nemeroff CB, Newport DJ, Owens MJ, Pace TW, Ritchie JC, Rivera VA, Westen D, Craighead WE, Mayberg HS (2012) Predictors of remission in depression to individual and combined treatments (PReDICT): study protocol for a randomized controlled trial. Trials 13:106. doi: 10.1186/1745-6215-13-106.:106-113.

Dunn AJ (2000) Cytokine Activation of the HPA Axis. Annals of the New York Academy of Sciences 917:608-617.

Dunn AJ (2006) Effects of cytokines and infections on brain neurochemistry. Clin Neurosci Res 6:52-68.

Elliott RC, Miles MF, Lowenstein DH (2003) Overlapping microarray profiles of dentate gyrus gene expression during development- and epilepsy-associated neurogenesis and axon outgrowth. J Neurosci 23:2218-2227.

Entsuah R, Derivan A, Kikta D (1998) Early onset of antidepressant action of venlafaxine: pattern analysis in intent-to-treat patients. Clinical Therapeutics 20:517-526.

Fabbri C, Di Girolamo G, Serretti A (2013) Pharmacogenetics of antidepressant drugs: An update after almost 20 years of research. Am J Med Genet 162:487-520.

Fanselow MS (2000) Contextual fear, gestalt memories, and the hippocampus. Behavioural Brain Research 110:73-81.

Fatemi SH, Laurence JA, Araghi-Niknam M, Stary JM, Schulz SC, Lee S, Gottesman II (2004) Glial fibrillary acidic protein is reduced in cerebellum of subjects with major depression, but not schizophrenia. Schizophr Res 69:317-323.

Fava M, Judge R, Hoog SL, Nilsson ME, Koke SC (2000) Fluoxetine versus sertraline and paroxetine in major depressive disorder: changes in weight with long-term treatment. J Clin Psychiatry 61:863-867.

First MB SRGMWJ (2002) Structured Clinical Interview for DSM-IV-TR Axis I Disorders, Research Version, Patient Edition With Psychotic Screen (SCID-I/P W/PSY SCREEN). New York, New York State Psychiatric Institute: Biometrics Research.

Flint J, Kendler KS (2014) The Genetics of Major Depression. Neuron 81:484-503.

Foust KD, Nurre E, Montgomery CL, Hernandez A, Chan CM, Kaspar BK (2009) Intravascular AAV9 preferentially targets neonatal neurons and adult astrocytes. Nat Biotech 27:59-65.

Freimer NB, Sabatti C (2007) Human genetics: Variants in common diseases. Nature 445:828-830.

Freund TF, Buzsaki G (1996) Interneurons of the hippocampus. Hippocampus 6:347-470.

Frey R, Schreinzer D, Heiden A, Kasper S (2001) Use of electroconvulsive therapy in psychiatry. Nervenarzt 72:661-676.

Friedrich MJ (2014) Research on psychiatric disorders targets inflammation. JAMA.

Frye MA, Tsai GE, Huggins T, Coyle JT, Post RM (2007) Low Cerebrospinal Fluid Glutamate and Glycine in Refractory Affective Disorder. Biological Psychiatry 61:162-166.

Ganea K, Menke A, Schmidt MV, Lucae S, Rammes G, Liebl C, Harbich D, Sterlemann V, Storch C, Uhr M, Holsboer F, Binder EB, Sillaber I, Müller MB (2012) Convergent animal and human evidence suggests the activin/inhibin pathway to be involved in antidepressant response. Transl Psychiatry 2:e177.

Garrett L, Lie D, Hrabe de Angelis M, Wurst W, Holter S (2012) Voluntary wheel running in mice increases the rate of neurogenesis without affecting anxiety-related behaviour in single tests. BMC Neuroscience 13:61.

GENDEP Investigators, MARS Investigators, STAR*D Investigators (2013) Common genetic variation and antidepressant efficacy in major depressive disorder: a meta-analysis of three genome-wide pharmacogenetic studies. Am J Psychiatry 170:207-217.

Gibbons JL (1964) Cortisol secretion rate in depressive illness. Archives of General Psychiatry 10:572-575.

Goldman S (2003) Glia as neural progenitor cells. Trends in Neurosciences 26:590-596.

Gould E, Cameron HA, Daniels DC, Woolley CS, McEwen BS (1992) Adrenal hormones suppress cell division in the adult rat dentate gyrus. J Neurosci 12:3642-3650.

Guth SIE, Wegner M (2008) Having it both ways: Sox protein function between conservation and innovation. Cell Mol Life Sci 65:3000-3018.

Hargrave M, Wright E, Kun J, Emery J, Cooper L, Koopman P (1997) Expression of the Sox11 gene in mouse embryos suggests roles in neuronal maturation and epithelio-mesenchymal induction. Dev Dyn 210:79-86.

Hascoet M, Bourin M, Nic Dhonnchadha Bd (2001) The mouse ligth-dark paradigm: A review. Progress in Neuro-Psychopharmacology and Biological Psychiatry 25:141-166.

Hashimoto K, Sawa A, Iyo M (2007) Increased Levels of Glutamate in Brains from Patients with Mood Disorders. Biological Psychiatry 62:1310-1316.

Haslinger A, Schwarz TJ, Covic M, Chichung Lie D (2009) Expression of Sox11 in adult neurogenic niches suggests a stage-specific role in adult neurogenesis. European Journal of Neuroscience 29:2103-2114.

Heim C, Mletzko T, Purselle D, Musselman DL, Nemeroff CB (2008) The dexamethasone/corticotropin-releasing factor test in men with major depression: role of childhood trauma. Biol Psychiatry 63:398-405.

Heim C, Nemeroff CB (2001) The role of childhood trauma in the neurobiology of mood and anxiety disorders: preclinical and clinical studies. Biological Psychiatry 49:1023-1039.

Herrmann JE, Imura T, Song B, Qi J, Ao Y, Nguyen TK, Korsak RA, Takeda K, Akira S, Sofroniew MV (2008) STAT3 is a critical regulator of astrogliosis and scar formation after spinal cord injury. J Neurosci 28:7231-7243.

Heuser IJ, Schweiger U, Gotthardt U, Schmider J, Lammers CH, Dettling M, Yassouridis A, Holsboer F (1996) Pituitary-adrenal-system regulation and psychopathology during amitriptyline treatment in elderly depressed patients and normal comparison subjects. Am J Psychiatry 153:93-99.

Heydorn WE (1999) Paroxetine: a review of its pharmacology, pharmacokinetics and utility in the treatment of a variety of psychiatric disorders. Expert Opin Investig Drugs 8:417-441.

Hirschhorn JN, Daly MJ (2005) Genome-wide association studies for common diseases and complex traits. Nat Rev Genet 6:95-108.

Hodes GE, Hill-Smith TE, Lucki I (2010) Fluoxetine treatment induces dose dependent alterations in depression associated behavior and neural plasticity in female mice. Neuroscience Letters 484:12-16.

Holick KA, Lee DC, Hen R, Dulawa SC (2007) Behavioral Effects of Chronic Fluoxetine in BALB/cJ Mice Do Not Require Adult Hippocampal Neurogenesis or the Serotonin 1A Receptor. Neuropsychopharmacology 33:406-417.

Holsboer F (2003) High-Quality Antidepressant Discovery by Understanding Stress Hormone Physiology. Annals of the New York Academy of Sciences 1007:394-404.

Holsboer F (2000) The corticosteroid receptor hypothesis of depression. Neuropsychopharmacology 23:477-501.

Holsboer F (2001) CRHR1 antagonists as novel treatment strategies. CNS Spectr 6:590-594.

Holsboer F (2014) Redesigning antidepressant drug discovery. Dialogues Clin Neurosci 16:5-7.

Holsboer F, Barden N (1996) Antidepressants and hypothalamic-pituitary-adrenocortical regulation. Endocr Rev 17:187-205.

Iijima T, Miura E, Watanabe M, Yuzaki M (2010) Distinct expression of C1q-like family mRNAs in mouse brain and biochemical characterization of their encoded proteins. European Journal of Neuroscience 31:1606-1615.

Ising M, Holsboer F (2006) Genetics of stress response and stress-related disorders. Dialogues Clin Neurosci 8:433-444.

Ising M, Lucae S, Binder EB (2009) A genomewide association study points to multiple loci that predict antidepressant drug treatment outcome in depression. Archives of General Psychiatry 66:966-975.

Ising M, Horstmann S, Kloiber S, Lucae S, Binder EB, Kern N, Künzel HE, Pfennig A, Uhr M, Holsboer F (2007) Combined Dexamethasone/Corticotropin Releasing Hormone Test Predicts Treatment Response in Major Depression-A Potential Biomarker? Biological Psychiatry 62:47-54.

Jankowski MP, Cornuet PK, McIlwrath S, Koerber HR, Albers KM (2006) SRY-box containing gene 11 (Sox11) transcription factor is required for neuron survival and neurite growth. Neuroscience 143:501-514.

Jankowski MP, McIlwrath SL, Jing X, Cornuet PK, Salerno KM, Koerber HR, Albers KM (2009) Sox11 transcription factor modulates peripheral nerve regeneration in adult mice. Brain Research 1256:43-54.

Jay P, Goze C, Marsollier C, Taviaux S, Hardelin JP, Koopman P, Berta P (1995) The Human SOX11 Gene: Cloning, Chromosomal Assignment and Tissue Expression. Genomics 29:541-545.

Kalueff AV, Wheaton M, Murphy DL (2007) What's wrong with my mouse model?: Advances and strategies in animal modeling of anxiety and depression. Behavioural Brain Research 179:1-18.

Kaye CM, Haddock RE, Langley PF, Mellows G, Tasker TC, Zussman BD, Greb WH (1989) A review of the metabolism and pharmacokinetics of paroxetine in man. Acta Psychiatr Scand Suppl 350:60-75.:60-75.

Keeney A, Jessop DS, Harbuz MS, Marsden CA, Hogg S, Blackburn-Munro RE (2006) Differential effects of acute and chronic social defeat stress on hypothalamic-pituitary-adrenal axis function and hippocampal serotonin release in mice. J Neuroendocrinol 18:330-338.

Kempermann G, Chesler EJ, Lu L, Williams RW, Gage FH (2006) Natural variation and genetic covariance in adult hippocampal neurogenesis. Proceedings of the National Academy of Sciences of the United States of America 103:780-785.

Kempermann G, Gage FH (2002) Genetic influence on phenotypic differentiation in adult hippocampal neurogenesis. Developmental Brain Research 134:1-12.

Kendler KS, Gatz M, Gardner CO, Pedersen NL (2006) A Swedish national twin study of lifetime major depression. Am J Psychiatry 163:109-114.

Kessler RC, Berglund P, Demler O, Jin R, Merikangas KR, Walters EE (2005) Lifetime prevalence and age-of-onset distributions of dsm-iv disorders in the national comorbidity survey replication. Archives of General Psychiatry 62:593-602.

Kiefer JC (2007) Back to basics: Sox genes. Dev Dyn 236:2356-2366.

Kishore U, Gaboriaud C, Waters P, Shrive AK, Greenhough TJ, Reid KBM, Sim RB, Arlaud GJ (2004) C1q and tumor necrosis factor superfamily: modularity and versatility. Trends in Immunology 25:551-561.

Klein MA, Möller JC, Jones LL, Bluethmann H, Kreutzberg GW, Raivich G (1997) Impaired neuroglial activation in interleukin-6 deficient mice. Glia 19:227-233.

Klengel T, Pape J, Binder EB, Mehta D (2014) The role of DNA methylation in stress-related psychiatric disorders. Neuropharmacology 80:115-132.

Kohli MA, et al. (2011) The Neuronal Transporter Gene SLC6A15 Confers Risk to Major Depression. Neuron 70:252-265.

Krawiec JA, Chen H, Alom-Ruiz S, Jaye M (2009) Modified PAXgene method allows for isolation of high-integrity total RNA from microlitre volumes of mouse whole blood. Lab Anim 43:394-398.

Krishnan V, Nestler EJ (2008) The molecular neurobiology of depression. Nature 455:894-902.

Kuhlbrodt K, Herbarth B, Sock E, Enderich J, Hermans-Borgmeyer I, Wegner M (1998) Cooperative function of POU proteins and SOX proteins in glial cells. J Biol Chem 273:16050-16057.

Kuhn R (1957) Treatment of depressive states with an iminodibenzyl derivative (G 22355). Schweiz Med Wochenschr 87:1135-1140.

Kuhn R (1989) The discovery of modern antidepressants. Psychiatr J Univ Ott 14:249-252.

Le-Niculescu H, Kurian SM, Yehyawi N, Dike C, Patel SD, Edenberg HJ, Tsuang MT, Salomon DR, Nurnberger JI, Jr., Niculescu AB (2008a) Identifying blood biomarkers for mood disorders using convergent functional genomics. Mol Psychiatry 14:156-174.

Le-Niculescu H, Kurian SM, Yehyawi N, Dike C, Patel SD, Edenberg HJ, Tsuang MT, Salomon DR, Nurnberger JI, Jr., Niculescu AB (2008b) Identifying blood biomarkers for mood disorders using convergent functional genomics. Mol Psychiatry 14:156-174.

Leonard B (2000) Stress, depression and the activation of the immune system. World J Biol Psychiatry 1:17-25.

Lesch KP (2004) Gene-environment interaction and the genetics of depression. J Psychiatry Neurosci 29:174-184.

Leuchter AF, Cook IA, Marangell LB, Gilmer WS, Burgoyne KS, Howland RH, Trivedi MH, Zisook S, Jain R, McCracken JT, Fava M, Iosifescu D, Greenwald S (2009) Comparative effectiveness of biomarkers and clinical indicators for predicting outcomes of SSRI treatment in Major Depressive Disorder: Results of the BRITE-MD study. Psychiatry Research 169:124-131.

Leuchter A, Cook I, Hamilton S, Narr K, Toga A, Hunter A, Faull K, Whitelegge J, Andrews A, Loo J, Way B, Nelson S, Horvath S, Lebowitz B (2010) Biomarkers to Predict Antidepressant Response. Curr Psychiatry Rep 12:553-562.

Levison SW, Jiang FJ, Stoltzfus OK, Ducceschi MH (2000) IL-6-type cytokines enhance epidermal growth factor-stimulated astrocyte proliferation. Glia 32:328-337.

Li N, Lee B, Liu RJ, Banasr M, Dwyer JM, Iwata M, Li XY, Aghajanian G, Duman RS (2010) mTOR-Dependent Synapse Formation Underlies the Rapid Antidepressant Effects of NMDA Antagonists. Science 329:959-964.

Livak KJ, Schmittgen TD (2001) Analysis of Relative Gene Expression Data Using Real-Time Quantitative PCR and the 2(T)(Delta Delta C) Method. Methods 25:402-408.

Lucas BG, Strangeways DH (1963) The nature of the nerve cell chenges in the hippocampus following anoxia. J Pathol Bacteriol 86:283-91.:283-291.

Lucki I (1997) The forced swimming test as a model for core and component behavioral effects of antidepressant drugs. Behav Pharmacol 8:523-532.

Lucki I, O'Leary OF (2004) Distinguishing roles for norepinephrine and serotonin in the behavioral effects of antidepressant drugs. J Clin Psychiatry 65 Suppl 4:11-24.:11-24.

Maes M, Verkerk R, Vandoolaeghe E, Lin A, Scharpe S (1998) Serum levels of excitatory amino acids, serine, glycine, histidine, threonine, taurine, alanine and arginine in treatment-resistant depression: modulation by treatment with antidepressants and prediction of clinical responsivity. Acta Psychiatr Scand 97:302-308.

Malberg JE, Eisch AJ, Nestler EJ, Duman RS (2000) Chronic antidepressant treatment increases neurogenesis in adult rat hippocampus. J Neurosci 20:9104-9110.

Malhi G, Moore J, McGuffin P (2000) The genetics of major depressive disorder. Curr Psychiatry Rep 2:165-169.

Manev H, Uz T, Manev R (2003) Glia as a putative target for antidepressant treatments. Journal of Affective Disorders 75:59-64.

McGrath CL, Kelley ME, Holtzheimer PE, Dunlop BW, Craighead WE, Franco AR, Craddock RC, Mayberg HS (2013) Toward a neuroimaging treatment selection biomarker for major depressive disorder. JAMA Psychiatry 70:821-829.

McKinney WT, Jr., Bunney WE, Jr. (1969) Animal model of depression: I. review of evidence: implications for research. Archives of General Psychiatry 21:240-248.

Miller AH, Maletic V, Raison CL (2009) Inflammation and Its Discontents: The Role of Cytokines in the Pathophysiology of Major Depression. Biological Psychiatry 65:732-741.

Miller BH, Schultz LE, Gulati A, Cameron MD, Pletcher MT (2007) Genetic Regulation of Behavioral and Neuronal Responses to Fluoxetine. Neuropsychopharmacology 33:1312-1322.

Mirescu C, Gould E (2006) Stress and adult neurogenesis. Hippocampus 16:233-238.

Monory K, et al. (2006) The Endocannabinoid System Controls Key Epileptogenic Circuits in the Hippocampus. Neuron 51:455-466.

Mu L, Berti L, Masserdotti G, Covic M, Michaelidis TM, Doberauer K, Merz K, Rehfeld F, Haslinger A, Wegner M, Sock E, Lefebvre V, Couillard-Despres S, Aigner L, Berninger B, Lie DC (2012a) SoxC transcription factors are required for neuronal differentiation in adult hippocampal neurogenesis. J Neurosci 32:3067-3080.

Mu L, Berti L, Masserdotti G, Covic M, Michaelidis TM, Doberauer K, Merz K, Rehfeld F, Haslinger A, Wegner M, Sock E, Lefebvre V, Couillard-Despres S, Aigner L, Berninger B, Lie DC (2012b) SoxC Transcription Factors Are Required for Neuronal Differentiation in Adult Hippocampal Neurogenesis. The Journal of Neuroscience 32:3067-3080.

Müller MB, Holsboer F (2006) Mice with Mutations in the HPA-System as Models for Symptoms of Depression. Biological Psychiatry 59:1104-1115.

Murray CJ, Lopez AD (1996) Evidence-based health policy--lessons from the Global Burden of Disease Study. Science 274:740-743.

Nemeroff CB (2007) Prevalence and management of treatment-resistant depression. J Clin Psychiatry 68 Suppl 8:17-25.:17-25.

Nemeroff CB, Owens MJ (2002) Treatment of mood disorders. Nat Neurosci 5 Suppl:1068-1070.

Nestler EJ (2014) Epigenetic mechanisms of depression. JAMA Psychiatry 71:454-456.

Nestler EJ, Barrot M, DiLeone RJ, Eisch AJ, Gold SJ, Monteggia LM (2002a) Neurobiology of Depression. Neuron 34:13-25.

Nestler EJ, Gould E, Manji H (2002b) Preclinical models: status of basic research in depression. Biological Psychiatry 52:503-528.

Nestler EJ, Hyman SE (2010) Animal models of neuropsychiatric disorders. Nat Neurosci 13:1161-1169.

Nierenberg AA, Farabaugh AH, Alpert JE, Gordon J, Worthington JJ, Rosenbaum JF, Fava M (2000) Timing of onset of antidepressant response with fluoxetine treatment. Am J Psychiatry 157:1423-1428.

Nisticò L, et al. (1996) The CTLA-4 Gene Region of Chromosome 2q33 Is Linked to, and Associated with, Type 1 Diabetes. Human Molecular Genetics 5:1075-1080.

Ohl F, Roedel A, Binder E, Holsboer F (2003) Impact of high and low anxiety on cognitive performance in a modified hole board test in C57BL/6 and DBA/2 mice. European Journal of Neuroscience 17:128-136.

Öngür D, Ferry AT, Price JL (2003) Architectonic subdivision of the human orbital and medial prefrontal cortex. J Comp Neurol 460:425-449.

Orrego F, Villanueva S (1993) The chemical nature of the main central excitatory transmitter: A critical appraisal based upon release studies and synaptic vesicle localization. Neuroscience 56:539-555.

Pae CU, Patkar A (2013) Clinical Issues in Use of Atypical Antipsychotics for Depressed Patients. CNS Drugs 27:39-45.

Papakostas GI, Perlis RH, Scalia MJ, Petersen TJ, Fava M (2006) A meta-analysis of early sustained response rates between antidepressants and placebo for the treatment of major depressive disorder. J Clin Psychopharmacol 26:56-60.

Papakostas GI, Shelton RC, Smith J, Fava M (2007) Augmentation of antidepressants with atypical antipsychotic medications for treatment-resistant major depressive disorder: a meta-analysis. J Clin Psychiatry 68:826-831.

Pena CJ, Bagot RC, Labonté B, Nestler EJ (2014) Epigenetic Signaling in Psychiatric Disorders. Journal of Molecular Biology.

Pessoa L (2008) On the relationship between emotion and cognition. Nat Rev Neurosci 9:148-158.

Petit-Demouliere B, Chenu F, Bourin M (2005) Forced swimming test in mice: a review of antidepressant activity. Psychopharmacology 177:245-255.

Philibert R, Gunter HM, Kolassa IT (2014) The search for peripheral biomarkers for major depression: Benefiting from successes in the biology of smoking. Am J Med Genet 165:230-234.

Phillips JE, Corces VG (2009) CTCF: master weaver of the genome. Cell 137:1194-1211.

Phillips ML, Drevets WC, Rauch SL, Lane R (2003) Neurobiology of emotion perception II: implications for major psychiatric disorders. Biological Psychiatry 54:515-528.

Pijl H, Meinders AE (1996) Bodyweight Change as an Adverse Effect of Drug Treatment. Drug-Safety 14:329-342.

Porsolt RD, Bertin A, Jalfre M (1977a) Behavioral despair in mice: a primary screening test for antidepressants. Arch Int Pharmacodyn Ther 229:327-336.

Porsolt RD, LE PICHON M, Jalfre M (1977b) Depression: a new animal model sensitive to antidepressant treatments. Nature 266:730-732.

Preskorn SH (1997) Clinically relevant pharmacology of selective serotonin reuptake inhibitors. An overview with emphasis on pharmacokinetics and effects on oxidative drug metabolism. Clin Pharmacokinet 32 Suppl 1:1-21.:1-21.

Prut L, Belzung C (2003) The open field as a paradigm to measure the effects of drugs on anxiety-like behaviors: a review. European Journal of Pharmacology 463:3-33.

Qi X, Lin W, Li J, Li H, Wang W, Wang D, Sun M (2008) Fluoxetine increases the activity of the ERK-CREB signal system and alleviates the depressive-like behavior in rats exposed to chronic forced swim stress. Neurobiology of Disease 31:278-285.

Rabchevsky AG, Weinitz JM, Coulpier M, Fages C, Tinel M, Junier MP (1998) A role for transforming growth factor alpha as an inducer of astrogliosis. J Neurosci 18:10541-10552.

Rainen L, Oelmueller U, Jurgensen S, Wyrich R, Ballas C, Schram J, Herdman C, Bankaitis-Davis D, Nicholls N, Trollinger D, Tryon V (2002) Stabilization of mRNA expression in whole blood samples. Clin Chem 48:1883-1890.

Raison CL, Capuron L, Miller AH (2006) Cytokines sing the blues: inflammation and the pathogenesis of depression. Trends in Immunology 27:24-31.

Réaux-Le Goazigo A, Van Steenwinckel J, Rostène W, Mélik Parsadaniantz S (2013) Current status of chemokines in the adult CNS. Progress in Neurobiology 104:67-92.

Ressler KJ, Bradley B, Mercer KB, Deveau TC, Smith AK, Gillespie CF, Nemeroff CB, Cubells JF, Binder EB (2010) Polymorphisms in CRHR1 and the serotonin transporter loci: gene x gene x environment interactions on depressive symptoms. Am J Med Genet B Neuropsychiatr Genet 153B:812-824.

Reul JM, Stec I, Soder M, Holsboer F (1993) Chronic treatment of rats with the antidepressant amitriptyline attenuates the activity of the hypothalamic-pituitary-adrenocortical system. Endocrinology 133:312-320.

Revest JM, Dupret D, Koehl M, Funk-Reiter C, Grosjean N, Piazza PV, Abrous DN (2009) Adult hippocampal neurogenesis is involved in anxiety-related behaviors. Mol Psychiatry 14:959-967.

Rojo JE, Gibert K, Cobo J, Rodriguez-Cano E, Vallejo J (2005) Onset of antidepressant action: a pharmacological question? Hum Psychopharmacol Clin Exp 20:425-433.

Rosene DL, Van Hoesen GW (1977) Hippocampal efferents reach widespread areas of cerebral cortex and amygdala in the rhesus monkey. Science 198:315-317.

Rozen S, Skaletsky H (2000) Primer3 on the WWW for general users and for biologist programmers. Methods Mol Biol 132:365-86.:365-386.

Rubinow DR (2006) Treatment Strategies after SSRI Failure – Good News and Bad News. N Engl J Med 354:1305-1307.

Rush AJ (2007) The varied clinical presentations of major depressive disorder. J Clin Psychiatry 68 Suppl 8:4-10.

Sahay A, Hen R (2007) Adult hippocampal neurogenesis in depression. Nat Neurosci 10:1110-1115.

Sanacora G, Treccani G, Popoli M (2012) Towards a glutamate hypothesis of depression: An emerging frontier of neuropsychopharmacology for mood disorders. Neuropharmacology 62:63-77.

Santarelli L, Saxe M, Gross C, Surget A, Battaglia F, Dulawa S, Weisstaub N, Lee J, Duman R, Arancio O, Belzung C, Hen R (2003) Requirement of Hippocampal Neurogenesis for the Behavioral Effects of Antidepressants. Science 301:805-809.

Scharf SH, Sterlemann V, Liebl C, Müller MB, Schmidt MV (2013) Chronic social stress during adolescence: Interplay of paroxetine treatment and ageing. Neuropharmacology 72:38-46.

Schiepers OJG, Wichers MC, Maes M (2005) Cytokines and major depression. Progress in Neuro-Psychopharmacology and Biological Psychiatry 29:201-217.

Schildkraut JJ (1965) The catecholamine hypothesis of affective disorders: a review of supporting evidence. Am J Psychiatry 122:509-522.

Schmidt HD, Shelton RC, Duman RS (2011a) Functional Biomarkers of Depression: Diagnosis, Treatment, and Pathophysiology. Neuropsychopharmacology 36:2375-2394.

Schmidt MV, Scharf SH, Sterlemann V, Ganea K, Liebl C, Holsboer F, Müller MB (2010) High susceptibility to chronic social stress is associated with a depression-like phenotype. Psychoneuroendocrinology 35:635-643.

Schmidt MV, Sterlemann V, Ganea K, Liebl C, Alam S, Harbich D, Greetfeld M, Uhr M, Holsboer F, Müller MB (2007) Persistent neuroendocrine and behavioral effects of a novel, etiologically relevant mouse paradigm for chronic social stress during adolescence. Psychoneuroendocrinology 32:417-429.

Schmidt MV, Schülke JP, Liebl C, Stiess M, Avrabos C, Bock J, Wochnik GM, Davies HA, Zimmermann N, Scharf SH, Trümbach D, Wurst W, Zieglgänsberger W, Turck C, Holsboer F, Stewart MG, Bradke F, Eder M, Müller MB, Rein T (2011b) Tumor suppressor down-regulated in renal cell carcinoma 1 (DRR1) is a stress-induced actin bundling factor that modulates synaptic efficacy and cognition. Proceedings of the National Academy of Sciences 108:17213-17218.

Schug M, Stöber R, Heise T, Mielke H, Gundert-Remy U, Godoy P, Reif R, Blaszkewicz M, Ellinger-Ziegelbauer H, Ahr HJ, Selinski S, Günther G, Marchan R, Blaszkewicz M, Sachinidis A, Nüssler A, Oberemm A, Hengstler J (2013) Pharmacokinetics explain in vivo/in vitro discrepancies of carcinogen-induced gene expression alterations in rat liver and cultivated hepatocytes. Arch Toxicol 87:337-345.

Schwarz E, Bahn S (2008) Biomarker discovery in psychiatric disorders. Electrophoresis 29:2884-2890.

Sha L, Kitchen R, Porteous D, Blackwood D, Muir W, Pickard B (2012) SOX11 target genes: implications for neurogenesis and neuropsychiatric illness. Acta Neuropsychiatrica 24:16-25.

Shelton RC, Claiborne J, Sidoryk-Wegrzynowicz M, Reddy R, Aschner M, Lewis DA, Mirnics K (2011) Altered expression of genes involved in inflammation and apoptosis in frontal cortex in major depression. Mol Psychiatry 16:751-762.

Shelton RC, Miller AH (2010) Eating ourselves to death (and despair): The contribution of adiposity and inflammation to depression. Progress in Neurobiology 91:275-299.

Shen Hb, Gu Zq, Jian K, Qi J (2013) CXCR4-mediated Stat3 activation is essential for CXCL12-induced cell invasion in bladder cancer. Tumor Biol 34:1839-1845.

Shimoda K, Yamada N, Ohi K, Tsujimoto T, Takahashi K, Takahashi S (1988) Chronic administration of tricyclic antidepressants suppresses hypothalamo-pituitary-adrenocortical activity in male rats. Psychoneuroendocrinology 13:431-440.

Sillaber I, Holsboer F., Wotjak CT (2009) Animal Models of Mood Disorders. In: Neurobiology of Mental Disorders (Dennis S.Charney, Eric J.Nestler, eds), pp 378-391. New York: Oxford University Press.

Sillaber I, Panhuysen M, Henniger M, Ohl F, Kühne C, Pütz B, Pohl T, Deussing J, Paez-Pereda M, Holsboer F (2008) Profiling of behavioral changes and hippocampal gene expression in mice chronically treated with the SSRI paroxetine. Psychopharmacology 200:557-572.

Sim SC, Ingelman-Sundberg M (2011) Pharmacogenomic biomarkers: new tools in current and future drug therapy. Trends in Pharmacological Sciences 32:72-81.

Slattery DA, Cryan JF (2012) Using the rat forced swim test to assess antidepressant-like activity in rodents. Nat Protocols 7:1009-1014.

Sock E, Rettig SD, Enderich J, Bosl MR, Tamm ER, Wegner M (2004) Gene targeting reveals a widespread role for the high-mobility-group transcription factor Sox11 in tissue remodeling. Mol Cell Biol 24:6635-6644.

Song H, Stevens CF, Gage FH (2002) Astroglia induce neurogenesis from adult neural stem cells. Nature 417:39-44.

Steele FR, Chader GJ, Johnson LV, Tombran-Tink J (1993) Pigment epithelium-derived factor: neurotrophic activity and identification as a member of the serine protease inhibitor gene family. Proc Natl Acad Sci U S A 90:1526-1530.

Steru L, Chermat R, Thierry B, Simon P (1985) The tail suspension test: A new method for screening antidepressants in mice. Psychopharmacology 85:367-370.

Stranger BE, Stahl EA, Raj T (2011) Progress and Promise of Genome-Wide Association Studies for Human Complex Trait Genetics. Genetics 187:367-383.

Sugimoto Y, Yamamoto M, Tagawa N, Kobayashi Y, Mitsui-Saitoh K, Hotta Y, Yamada J (2011) Differences between mice strains in response to paroxetine in the forced swimming test: Involvement of serotonergic or noradrenergic systems. European Journal of Pharmacology 672:121-125.

Sukoff Rizzo SJ, Neal SJ, Hughes ZA, Beyna M, Rosenzweig-Lipson S, Moss SJ, Brandon NJ (2012) Evidence for sustained elevation of IL-6 in the CNS as a key contributor of depressive-like phenotypes. Transl Psychiatry 2:e199.

Sullivan PF, Fan C, Perou CM (2006) Evaluating the comparability of gene expression in blood and brain. Am J Med Genet 141B:261-268.

Takeda K, Noguchi K, Shi W, Tanaka T, Matsumoto M, Yoshida N, Kishimoto T, Akira S (1997) Targeted disruption of the mouse Stat3 gene leads to early embryonic lethality. Proc Natl Acad Sci U S A 94:3801-3804.

Tanabe K, Bonilla I, Winkles JA, Strittmatter SM (2003) Fibroblast growth factor-inducible-14 is induced in axotomized neurons and promotes neurite outgrowth. J Neurosci 23:9675-9686.

Tansey KE, Guipponi M, Hu X, Domenici E, Lewis G, Malafosse A, Wendland JR, Lewis CM, McGuffin P, Uher R (2013) Contribution of Common Genetic Variants to Antidepressant Response. Biological Psychiatry 73:679-682.

Taylor MJ, Freemantle N, Geddes JR, Bhagwagar Z (2006) Early onset of selective serotonin reuptake inhibitor antidepressant action: systematic review and meta-analysis. Arch Gen Psychiatry 63:1217-1223.

Tombran-Tink J, Chader GG, Johnson LV (1991) PEDF: a pigment epithelium-derived factor with potent neuronal differentiative activity. Exp Eye Res 53:411-414.

Tombran-Tink J, Barnstable CJ (2003) PEDF: a multifaceted neurotrophic factor. Nat Rev Neurosci 4:628-636.

Trivedi MH, Rush AJ, Wisniewski SR, Nierenberg AA, Warden D, Ritz L, Norquist G, Howland RH, Lebowitz B, McGrath PJ, Shores-Wilson K, Biggs MM, Balasubramani GK, Fava M (2006) Evaluation of outcomes with citalopram for depression using measurement-based care in STAR*D: implications for clinical practice. Am J Psychiatry 163:28-40.

Trullas R, Skolnick P (1990) Functional antagonists at the NMDA receptor complex exhibit antidepressant actions. European Journal of Pharmacology 185:1-10.

Uhr M, Grauer MT, Holsboer F (2003) Differential enhancement of antidepressant penetration into the brain in mice with abcb1ab (mdr1ab) P-Glycoprotein gene disruption. Biological Psychiatry 54:840-846.

Uhr M, Tontsch A, Namendorf C, Ripke S, Lucae S, Ising M, Dose T, Ebinger M, Rosenhagen M, Kohli M, Kloiber S, Salyakina D, Bettecken T, Specht M, Pütz B, Binder EB, Müller-Myhsok B, Holsboer F (2008) Polymorphisms in the Drug Transporter Gene ABCB1 Predict Antidepressant Treatment Response in Depression. Neuron 57:203-209.

van der Sijde MR, Ng A, Fu J (2014) Systems genetics: From GWAS to disease pathways. Biochimica et Biophysica Acta (BBA) - Molecular Basis of Disease.

Van Gelder RN, von Zastrow ME, Yool A, Dement WC, Barchas JD, Eberwine JH (1990) Amplified RNA synthesized from limited quantities of heterogeneous cDNA. Proc Natl Acad Sci U S A 87:1663-1667.

Vanina Y, Podolskaya A, Sedky K, Shahab H, Siddiqui A, Munshi F, Lippmann S (2002) Body weight changes associated with psychopharmacology. Psychiatr Serv 53:842-847.

Vaugeois JM, Passera G, Zuccaro F, Costentin J (1997) Individual differences in response to imipramine in the mouse tail suspension test. Psychopharmacology 134:387-391.

Videbech P, Ravnkilde B (2004) Hippocampal volume and depression: a meta-analysis of MRI studies. Am J Psychiatry 161:1957-1966.

Villanueva R (2013) Neurobiology of major depressive disorder. Neural Plast 2013:873278. doi: 10.1155/2013/873278. Epub;%2013 Oct 9.:873278.

Wagner KV, Marinescu D, Hartmann J, Wang XD, Labermaier C, Scharf SH, Liebl C, Uhr M, Holsboer F, Müller MB, Schmidt MV (2012) Differences in FKBP51 Regulation Following Chronic Social Defeat Stress Correlate with Individual Stress Sensitivity: Influence of Paroxetine Treatment. Neuropsychopharmacology 37:2797-2808.

Wang XD, Su YA, Wagner KV, Avrabos C, Scharf SH, Hartmann J, Wolf M, Liebl C, Kühne C, Wurst W, Holsboer F, Eder M, Deussing JM, Müller MB, Schmidt MV (2013) Nectin-3 links CRHR1 signaling to stress-induced memory deficits and spine loss. Nat Neurosci 16:706-713.

Warner-Schmidt JL, Duman RS (2006) Hippocampal neurogenesis: Opposing effects of stress and antidepressant treatment. Hippocampus 16:239-249.

Webhofer C, Gormanns P, Tolstikov V, Zieglgänsberger W, Sillaber I, Holsboer F, Turck CW (2011) Metabolite profiling of antidepressant drug action reveals novel drug targets beyond monoamine elevation. Transl Psychiatry 1:e58.

Wegner M (2011) SOX after SOX: SOXession regulates neurogenesis. Genes Dev 25:2423-2428.

Werner S, Alzheimer C (2006) Roles of activin in tissue repair, fibrosis, and inflammatory disease. Cytokine & Growth Factor Reviews 17:157-171.

Willner P (1984) The validity of animal models of depression. Psychopharmacology 83:1-16.

Wilson M, Koopman P (2002) Matching SOX: partner proteins and co-factors of the SOX family of transcriptional regulators. Current Opinion in Genetics & Development 12:441-446.

Wisniewski SR, Rush AJ, Nierenberg AA, Gaynes BN, Warden D, Luther JF, McGrath PJ, Lavori PW, Thase ME, Fava M, Trivedi MH (2009) Can phase III trial results of antidepressant medications be generalized to clinical practice? A STAR*D report. Am J Psychiatry 166:599-607.

Witt S, Sommer W, Hansson A, Sticht C, Rietschel M, Witt C (2013) Comparison of gene expression profiles in the blood, hippocampus and prefrontal cortex of rats. In Silico Pharmacology 1:15.

Wong ML, Licinio J (2004) From monoamines to genomic targets: a paradigm shift for drug discovery in depression. Nat Rev Drug Discov 3:136-151.

Xu W, Li JY (2010) SOX11 expression in mantle cell lymphoma. Leuk Lymphoma 51:1962-1967.

Yadid G, Nakash R, Deri I, Tamar G, Kinor N, Gispan I, Zangen A (2000) Elucidation of the neurobiology of depression: insights from a novel genetic animal model. Progress in Neurobiology 62:353-378.

Yilmazer-Hanke DM, Roskoden T, Zilles K, Schwegler H (2003) Anxiety-related behavior and densities of glutamate, $GABA_A$, acetylcholine and serotonin receptors in the amygdala of seven inbred mouse strains. Behavioural Brain Research 145:145-159.

Zeng W, Fu K, Quintanilla-Fend L, Lim M, Ondrejka S, Hsi ED (2012) Cyclin D1-negative Blastoid Mantle Cell Lymphoma Identified by SOX11 Expression. The American Journal of Surgical Pathology 36.

Zhang L (2011) Voluntary oral administration of drugs in mice.

Zhao C, Deng W, Gage FH (2008) Mechanisms and Functional Implications of Adult Neurogenesis. Cell 132:645-660.

Zobel AW, Nickel T, Künzel HE, Ackl N, Sonntag A, Ising M, Holsboer F (2000) Effects of the high-affinity corticotropin-releasing hormone receptor 1 antagonist R121919 in major depression: the first 20 patients treated. Journal of Psychiatric Research 34:171-181.

List of Figures

List of Tables

5 Curriculum Vitae

Personal information

Name:	Christiana Labermaier
Date of birth:	August 29th, 1985
Place of birth:	Erding, Germany
Nationality:	German

Education

since 05/2011	PhD studies in the research group 'Molecular Stressphysiology' at the Max Planck Institute of Psychiatry, Munich
10/2006 – 03/2011	Studies of Biology (Diploma 1.3) at the Ludwig-Maximilians-University Munich Major: Neuroscience Minors: Ecology; Toxicology and pharmacology
05/2010 - 03/2011	Diploma thesis performed in the research group 'Neurobiology of stress' at the Max Planck Institute of Psychiatry, Munich

Awards and Scholarships

2013	EBBS-EWCBR Young Investigator Award, 34.EWCBR Meeting 2014, Brides-les-Bains, Frankreich
	Reisestipendium, GlaxoSmithKline Stiftung, 33. EWCBR Meeting2013, Brides-les-Bains, Frankreich
	DAAD Reisestipendium zum SfN Meeting 2013, San Diego, USA
2012	Mifek-Kirscher Award, Max-Planck-Institut für Psychiatrie, München, Deutschland

6 Publications

2014 **Labermaier C**, Kohl C, Hartmann J, Devigny C, Altmann A, Weber P, Arloth J, Quast C, Wagner KV, Scharf SH, Czibere L, Widner-Andrä R, Brenndörfer J, Hausch F, Müller MB, Uhr M, Holsboer F, Binder EB, Schmidt MV: A polymorphism in the Crhr1 gene determines stress vulnerability in male mice. *Endocrinology. 2014 Jul;155(7):2500-10*

Santarelli S, Lesuis SL, Wang XD, Wagner KV, Hartmann J, **Labermaier C**, Scharf SH, Müller MB, Holsboer F, Schmidt MV: Evidence supporting the match/mismatch hypothesis of psychiatric disorders. *Eur Neuropsychopharmacol. 2014 Jun;24(6):907-18*

Balsevich G, Uribe A, Wagner KV, Hartmann J, Santarelli S, **Labermaier C**, Schmidt MV: The interplay between diet-induced obesity and chronic stress in mice: potential role of FKBP51. *Journal of Endocrinology 2014 Jul;222(1):15-26*

Masana M, Su YA, Liebl C, Wang XD, Jansen L, Westerholz S, Wagner KV, **Labermaier C**, Scharf SH, Santarelli S, Hartmann J, Schmidt MV, Rein T, Müller MB: The stress-inducible actin-interacting protein DRR1 shapes social behavior. *Psychoneuroendocrinology. 2014 Jun 19;48C:98-110*

Wagner KV, Häusl AS, Pöhlmann ML, Hartmann J, **Labermaier C**, Müller MB, Schmidt MV: Hippocampal Homer1 levels influence motivational behavior in an operant conditioning task. *PLoS One. 2014 Jan 21;9(1):e85975*

Weckmann K, **Labermaier C**, Webhofer C, Asara JM, Müller-Sitz MB, Turck CW: Time-dependent metabolomic profiling of Ketamine drug action reveals hippocampal pathway alterations and biomarker candidates. *(submitted to Translational Psychiatry)*

2013 **Labermaier C**, Masana M, and Müller MB: Biomarkers predicting antidepressant treatment response – how can we advance the field?.
Dis Markers. 2013;35(1):23-31

Wagner KV, Hartmann J, Mangold K, Wang XD, **Labermaier C**, Liebl C, Wolf M, Gassen NC, Holsboer F, Rein T, Müller MB, Schmidt MV: Homer1 mediates acute stress-induced cognitive deficits in the dorsal hippocampus.
Journal of Neuroscience 2013 Feb 27;33(9):3857-64

2012 Wagner KV, Marinescu D, Hartmann J, Wang XD, **Labermaier C**, Scharf SH, Liebl C, Uhr M, Holsboer F, Müller MB, Schmidt MV: Differences in FKBP51 regulation following chronic social defeat stress correlate with individual stress sensitivity: Influence of paroxetine treatment.
Neuropsychopharmacology. 2012 Dec;37(13):2797-808

Wang XD, **Labermaier C**, Holsboer F, Wurst W, Deussing JM, Müller MB, Schmidt MV: Early-life stress-induced anxiety-related behavior in adult mice partially requires forebrain corticotropin-releasing hormone receptor.
European Journal of Neuroscience 2012 Aug;36(3):2360-7

7 Acknowledgements

First of all, I would like to thank Prof. Dr. Marianne Müller and PD Dr. Mathias Schmidt. Both of you were the basis for this thesis. Without your constant support, help and excellent supervision I would not have been able to finish this work. You taught me so much related to science but also to life. Thank you for cheering me up when I was down, for always believing in me, for the nice conferences we have been to together but also for the great moments beside work.

Furthermore, I would like to thank Prof. Dr. Grothe who willingly accepted to read and evaluate my thesis.

However, this thesis would not been possible without the nicest and best colleagues in the world. I would like to acknowledge them in no particular order.

Sara, without our *grande conversazione* life would have been less entertaining. Thanks for sharing the last three year with me. The best 'officemate' I could think of, especially in the nice office at the very end ☺. You brought bella italia (not only with the radio) in sometimes hard and exhausting working days. Non fare il vecchio!!

Jakob, former diploma thesis supervisor and one of the nicest guys in our group. I really enjoyed talking with you especially when it came to the passion we shared (travelling). I think I have to refill your third drawer before I leave.

Binci, you were the one in the beginning you taught me all lab techniques and never got tired when I was calling for the fifth time: *'I just wanted to double check! Is….the right solution?'*. Besides that I would like to thank you for the last four years and the great moments we shared: your wedding, the lamb barbeque in our fire department safety zone and the nice days at the Isar with you!

Dani, the person I could always go to when I had problems. I really enjoyed the last four years with you. The morning conversations, when the fourth floor was still empty, the wine tour, the unrestricted helpfulness in the lab (thanks for waiting next to me at the Bioanalyzer, nights in Alpha, injections at horrible time points) and the love for good wine that we share.

Chrissi, thanks for supporting me with all kind of information, especially at the end with guidelines for the PhD thesis. But more important, I really enjoyed the conferences (EBBS and SFN) with you. We had a lot of fun while playing Schafkopfen for a week.

Georgia, thank you for the nice RNA isolation time, the nice week in France and for improving my English!

Carine, Merce and Andres I would really like to thank you guys as well, for having a great time together (Paella, Skylounge Parties) and for the direct and indirect support (great discussions, interaction and ideas). It was very nice to work in such a nice end friendly environment.

Special thanks also go to my students that I was happy to supervise and who contributed to the success of this thesis: Marleen, Danica and Claire. It was great working with you!

Furthermore, I would also like to thank my collaborators from other research groups. Without their support, the thesis would have not been possible in the current form: Chichung Li and Julia Wittgenstein from the University of Erlangen, Elisabeth Binder and her group (especially Peter, Anne, Monika, Tania and Caleb), Theo Rein and Svenja, Manfred Uhr and his coworkers Christian and Tamara.

During the four years at the MPI I also saw some people leaving, therefore I would like to thank some of my former colleagues for training me and I have not forgotten the great times we had together: Klaus (so many things I have to thank you for but most important, thanks that we keep in touch!!), Claudia (encouraging me especially during my diploma thesis and early PhD thesis), Xiao-Dong Wang (you showed me how to use a cryostat), Sebastian (next to Sara best officemate).

Obviously, not only the MPI was supporting for me during the last four years but also my family.

Mama und Papa: Danke, dass Ihr mich mein ganzes Studium und meine Promotion lang unterstützt habt. Ohne euren unersättlichen Glauben in mich wäre das hier wahrscheinlich nicht möglich gewesen. Ihr seid mit das wichtigste in meinem Leben! Danke, dass ihr immer für mich da seid.

Uneingeschränkter Dank gebührt auch dir Norbi!! Man könnte dir wahrscheinlich fast unterstellen, dass du auch am Entstehen der Arbeit beteiligt warst. ☺ Du warst derjenige, der immer an mich geglaubt hat und es auch immer noch tut. Du bist derjenige von uns, der auch in stressigen Phasen ruhig und entspannt bleibt. Du warst es außerdem, der mich an so manchen Tagen den Alltag vergessen hat lassen. Danke für die Tage an denen wir, trotz *'Ich-muss-am-Wochenende-die-Pillen-geben'* einfach vom stressigen Alltag geflohen sind. So groß und bedeutend sich diese Arbeit momentan anfühlt, so größer und bedeutender ist das was uns beide verbindet.

8 Assertion (Erklärung)

Hiermit versichere ich eidesstattlich, dass ich die vorliegende Dissertation selbstständig und nur mit den angegebenen Quellen und Hilfsmitteln angefertigt habe. Alle Ausführungen, die wörtlich oder sinngemäß übernommen wurden, sind als solche gekennzeichnet.

Des Weiteren erkläre ich, dass ich nicht anderweitig ohne Erfolg versucht habe, eine Dissertation einzureichen oder mich der Doktorprüfung zu unterziehen. Die vorliegende Dissertation liegt weder ganz, noch in wesentlichen Teilen einer anderen Prüfungskommission vor.

München, den 15.09.2014